

Polyurea Grafted Organoclay Nanocomposites for Oil Spill Remediation



Syeda Farrah Naz

00000117060

A dissertation submitted in partial fulfillment of requirements for the
Degree of Master of Science in Chemistry

Supervised by

Dr. Faroha Liaqat

Department of Chemistry

School of Natural Sciences

National University of Sciences and Technology

Islamabad, Pakistan.

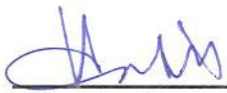
2017

National University of Sciences & Technology**MS THESIS WORK**

We hereby recommend that the dissertation prepared under our supervision by: Syeda Farrah Naz, Regn No. 00000117060 Titled: Polyurea Grafted Organocaly Nanocomposites for Oil Spill Remedation be accepted in partial fulfillment of the requirements for the award of **MS** degree.

Examination Committee Members

1. Name: PROF. HABIB NASIR Signature: 
2. Name: DR. FAHAD EHSAN Signature: 
3. Name: _____ Signature: _____
4. Name: DR. MUHAMMAD RIAZ Signature: 
- Supervisor's Name: DR. FAROHA LIAQAT Signature: 


Head of Department

31-08-2017
Date


COUNTERSIGNED


Date: 31/8/17



Dean/Principal

THESIS ACCEPTANCE CERTIFICATE

Certified that final copy of MS thesis written by Syeda Farrah Naz, (Registration No. 00000117060), of School of Natural Sciences has been vetted by undersigned, found complete in all respects as per NUST statutes/regulations, is free of plagiarism, errors, and mistakes and is accepted as partial fulfillment for award of MS/M.Phil degree. It is further certified that necessary amendments as pointed out by GEC members and external examiner of the scholar have also been incorporated in the said thesis.

Signature:  _____
Name of Supervisor: Dr. Faroha Liaqat
Date: 31/8/2017

Signature (HoD):  _____
Date: 31-08-2017

Signature (Dean/Principal):  _____
Date: 31/08/17



“And He has subjected for you, the night and the day, the sun and the moon, and the stars are subjected by His command. Indeed, in that are signs for people who understand.”

Al-Quran (Nahal: 12)

***Dedicated to
My Loving Parents & Siblings***

Contents

| | |
|-------------------------------------------------------------------------------------|----|
| Contents..... | 04 |
| List of Abbreviations..... | 07 |
| List of figures..... | 10 |
| List of Tables..... | 12 |
| Acknowledgements..... | 13 |
| Abstract..... | 14 |
| Chapter 1. Introduction | |
| 1.1 Polymers..... | 17 |
| 1.2 Composites..... | 25 |
| 1.3 Layered silicates..... | 35 |
| 1.3.1 Structure and Properties of Layered Silicates..... | 35 |
| 1.3.2 Classification of Clay Minerals..... | 36 |
| 1.3.3 Organic Modification of Clay Minerals..... | 39 |
| 1.3.4 Silylation of Clay Minerals..... | 41 |
| 1.4 Polymers- Layered Silicates Nanocomposites..... | 43 |
| 1.4.1 Properties of Polymer-Clay Nanocomposite..... | 44 |
| 1.4.2 Methods of Synthesis for Polymer-Clay Nanocomposites..... | 45 |
| 1.4.3 A Literature Review of Polymer-Clay Nanocomposites Using Montmorillonite..... | 48 |
| 1.5 Oil Spills..... | 54 |
| 1.5.1 Impact of oil spills..... | 55 |
| 1.5.2 Oil Spill Control Methods..... | 55 |
| 1.6 Overview of Various Materials Used in Oil Spill Cleanup..... | 58 |

| | | |
|-----|-----------------------------------------------------------------------------------|----|
| 1.7 | A Literature Review of the Implications of Organoclays for Oil Spill Removal..... | 62 |
| 1.8 | Motivation..... | 64 |

Chapter 2. Experimental and characterization Techniques

| | | |
|-------|-----------------------------------------------|----|
| 2.1 | Materials..... | 65 |
| 2.2 | Intercalation of Montmorillonite..... | 66 |
| 2.3 | Silane Functionalization of Organoclay..... | 69 |
| 2.4. | Synthesis of Polymer-Clay Nanocomposites..... | 71 |
| 2.5 | Characterization Techniques..... | 72 |
| 2.5.1 | X-ray Diffraction Spectroscopy (XRD)..... | 72 |
| 2.5.2 | Scanning Electron Microscopy (SEM)..... | 77 |
| 2.5.3 | Infrared Spectroscopy (IR)..... | 82 |
| 2.5.4 | UV-visible Spectroscopy..... | 83 |

Chapter 3. Results and Discussion

| | | |
|-------|--------------------------------------------------------------------|----|
| 3.1 | X-ray Diffraction Analysis..... | 85 |
| 3.1.1 | X-ray Diffraction Analysis of as Prepared Clays..... | 86 |
| 3.1.2 | X-ray Diffraction Analysis of Nanocomposites..... | 88 |
| 3.2 | FT-IR Spectroscopic Analysis..... | 89 |
| 3.2.1 | Pristine Montmorillonite..... | 89 |
| 3.2.2 | Organophilic Montmorillonite..... | 90 |
| 3.2.3 | Silylated Montmorillonite..... | 92 |
| 3.2.4 | Organo-Modified and Chemically Functionalized Montmorillonite..... | 93 |

| | |
|----------------------------------------------------------------------|------------|
| 3.2.5 FT-IR analysis for nanocomposites..... | 95 |
| 3.3 Performance Profile of Synthesized Material for Oil Removal..... | 98 |
| 3.3.1 Preparation of Synthetic Saline Oil-water..... | 98 |
| 3.3.2 Oil-Water Separation Test..... | 99 |
| 3.3.3 Adsorption Capacity Test..... | 106 |
| 3.3.4 Selectivity and Buoyancy Test..... | 107 |
| 3.4 Conclusion and Outlook..... | 110 |
| Bibliography..... | 112 |

List of Abbreviations

| | |
|------------------|----------------------------------|
| CS | Chemical structure |
| MMD | Molar mass distribution |
| -OH | Hydroxyl group |
| -COOH | Carboxyl group |
| -NH ₂ | Amine group |
| -NCO | Isocyanate group |
| HCl | Hydrochloric acid |
| CED | Cohesive Energy Density |
| MMCs | Metal matrix composites |
| CMCs | Ceramic matrix composites |
| CFRC | Ceramic fiber reinforced ceramic |
| SiC | Silicon carbide |
| PMCs | Polymer matrix composites |
| CCCs | Carbon-carbon composites |
| CTE | Coefficient of thermal expansion |
| TD | Thoria dispersed |
| PLS | Polymer-layered silicates |
| MMT | Montmorillonite |
| CEC | Cation exchange capacity |
| QACs | Quaternary ammonium cations |
| BTEA | Benzyl triethylammonium |
| TMA | Tetramethylammonium |

| | |
|--------------------------------|-----------------------------------------|
| TEPM | Trimethylphenylammonium |
| DODMA | Didodecyldimethylammonium |
| HDTMA | Hexadecyltrimethylammonium |
| OMMT | Organophilic montmorillonite |
| SBR | Styrene butadiene rubber |
| ODA | Octadecylamine |
| CTAC | Cetyltrimethylammonium chloride |
| ABS | Acrylonitrile-butadiene-styrene |
| APTES | 3-aminopropyltriethoxysilane |
| BP | British petroleum |
| NMR | Nuclear magnetic resonance |
| PS | Polystyrene |
| Fe ₃ O ₄ | Iron oxide |
| CNT | Carbon nanotubes |
| PPy | Polypyrrole |
| ADMBAC | Alkyl dimethyl benzyl ammonium chloride |
| DSDMAC | Distearyl dimethylammonium chloride |
| DDA | Dodecylamine |
| IPDI | Isophorone diisocyanate |
| wt% | Weight percent |
| XRD | X-ray diffraction |
| FWHM | Full width half maxima |
| kV | Kilo volt |
| SEM | Scanning electron microscopy |
| LaB ₆ | Lanthanum hexaboride |

| | |
|---------------|--------------------------------------|
| BSE | Back scattered electrons |
| SE | Secondary electrons |
| EDX | Energy dispersive X-ray spectroscopy |
| IR | Infrared |
| TGA | Thermogravimetric analysis |
| CAH | Contact angle hysteresis |
| UV | Ultra violet |
| SMMT | Silylated Montmorillonite |
| ppm | Parts per million |
| Ad | Adsorption capacity |
| PCN | Polymer/ clay nanocomposites |
| ε | Molar absorptivity coefficient |

List of Figures

| | |
|-----------------------------------------------------------------------------------------------------------------------------------------------------------------|----|
| Figure 1.1 Three main classes of materials with typical examples..... | 17 |
| Figure 1.2 Natural or biopolymers classified by source..... | 19 |
| Figure 1.3 Examples of semi-synthetic polymers..... | 20 |
| Figure 1.4 Amorphous polymer..... | 22 |
| Figure 1.5 Semi crystalline polymer..... | 22 |
| Figure 1.6 Examples of different types of copolymers..... | 24 |
| Figure 1.7 Matrix based classification of composites..... | 27 |
| Figure 1.8 Reinforcement based classification of composites..... | 32 |
| Figure 1.9 Crystal structure of 2:1 layer type minerals (Montmorillonite)..... | 38 |
| Figure 1.10 Configurations of exchanged organic cations between the layers of organoclays A) Monolayer B) Bi-layer C) Pseudotrimolecular and D) Paraffinic..... | 40 |
| Figure 1.11 Schematic representations of various microstructures of polymer/clay hybrids.. | 44 |
| Figure 1.12 Tortuous diffusion path in polymer/clay nanocomposites..... | 45 |
| Figure 1.13 Schematic view of in-situ intercalative polymerization..... | 47 |
| Figure 2.1 Scheme for organic modification of Montmorillonite..... | 67 |
| Figure 2.2 Scheme for synthesis of organically modified montmorillonite..... | 68 |
| Figure 2.3 Scheme for chemical functionalization of OMMT..... | 69 |
| Figure 2.4 Scheme for synthesis of organically modified and chemically functionalized montmorillonite..... | 70 |
| Figure 2.5 Scheme for possible interaction between polyurea matrix and organoclay reinforcement..... | 71 |
| Figure 2.6 Diffraction of X-rays by crystal..... | 74 |
| Figure 2.7 Graphical representation of an XRD pattern showing its basic features with their physical meanings..... | 76 |
| Figure 2.8 Main components and working principle of a typical SEM instrument..... | 78 |

| | |
|-----------------------------------------------------------------------------------------------------------------------------------------------------------------------------------------------------------------------------------------------|-----|
| Figure 2.9 Interaction of incident electron beam with the specimen..... | 81 |
| Figure 3.1 X-ray diffraction patterns for montmorillonite (MMT), silane functionalized montmorillonite (SMMT), chemically modified montmorillonite (OMMT) and organically modified and chemically functionalized montmorillonite (OSMMT)..... | 86 |
| Figure 3.2 X-ray diffraction patterns for polymer/clay nanocomposites..... | 88 |
| Figure 3.3 FT-IR spectrum of pristine montmorillonite..... | 90 |
| Figure 3.4 FT-IR spectrum for organically modified montmorillonite (OMMT)..... | 91 |
| Figure 3.5 FT-IR spectrum for silane functionalized montmorillonite (SMMT)..... | 92 |
| Figure 3.6 FT-IR spectrum of organically modified and silane functionalized montmorillonite..... | 93 |
| Figure 3.7 Merged FT-IR spectrums of nanocomposite systems..... | 96 |
| Figure 3.8 Calibration curve for estimation of unknown concentration of diesel oil in water..... | 100 |
| Figure 3.9 Calibration curve for estimation of unknown concentration of gasoline in water..... | 102 |
| Figure 3.10 Calibration curve for estimation of unknown concentration of kerosene in water..... | 103 |
| Figure 3.11A) Oil removal efficiency (% removal) B) removal capacity at equilibrium with synthesized sorbent materials using petroleum hydrocarbons..... | 105 |
| Figure 3.12 Adsorption capacities of nanocomposite sorbents in petroleum hydrocarbons.. | 107 |
| Figure 3.13 Evaluation of oil sorption capacity of 50wt% nanocomposites with different masses..... | 108 |
| Figure 3.14 Demonstration of oil-water separation process a) Oil-water emulsion b) addition of sorbent materials, c) and d) selectivity and buoyancy of sorbent materials..... | 109 |

List of Tables

| | |
|----------------------------------------------------------------------------------------------------|-----|
| Table 1.1 The basal spacing of OMMT intercalated with Quaternary onium salts..... | 41 |
| Table 2.1 List of chemicals and reagents used for synthesis of nanocomposites..... | 65 |
| Table 2.2 Compositions of Polyurea/organoclay nanocomposites..... | 72 |
| Table 3.1 XRD data for clays at 001 reflection..... | 87 |
| Table 3.2 Fourier Transform data for different clays..... | 95 |
| Table 3.3 A comparative analysis of FT-IR data for different composites..... | 98 |
| Table 3.4 Results of percent removal (% Rem) and removal capacity (Q_{eq}) for diesel oil..... | 101 |
| Table 3.5 Results of percent removal (%Rem) and removal capacity (Q_{eq}) for gasoline..... | 102 |
| Table 3.6 Results for percent removal (% Rem) and removal capacity (Q_{eq}) for kerosene..... | 103 |

Acknowledgements

If all the oceans turn into ink and all the woods become pens, even then the praise of Allah Almighty cannot be expressed. He, who created the universe and knows whether, is there in it hidden or evident. He bestowed His countless blessings and grace upon me. He gave me intellectual ability, knowledge, courage and wisdom to complete this work. Countless salutations are upon the Holy Prophet Hazrat Muhammad (S.A.W) the city of knowledge who has guided His "Ummah" to seek knowledge from cradle to grave.

*I feel sanguine to present my deep appreciation and thanks to my worthy supervisor **Dr. Faroha Liaqat** for her kind direction, inspiring guidance and invaluable discussion throughout the research work. Without her patience and encouragement this work would never be fulfilled. I am very grateful to have such a fulfilling and enriching experience of work under her kind consideration.*

*I am highly grateful to my GEC members, **Prof. Dr. Habib Nasir** and **Dr. M. Fahad Ehsan** for their kind suggestions, valuable time, guidance and unconditional support throughout my research phase. I am grateful to School of Natural Sciences, NUST, and NESCOM for giving me platform and financial support to complete this research work. I am also thankful to School of Chemical and Materials Engineering, Institute of Environmental Sciences & Engineering, NUST for providing me characterization equipment for sample analysis and their technical support.*

I would like acknowledge to all my class fellows, well-wishers and friends specially Zenab Qayyum, Fareaa Batool, Nazia Fakhar, Amna and many others for their kind assistance and guidance time by time. I owe much and pay my heartiest thanks to all of them.

Finally I reserve sincerest gratitude for my parents and brothers, Awais and Waqas, and my loving sister in law Wajeeha Awais as their endless prayers, love and care are source of encouragement and determination for me.

May Allah Almighty bestow His special blessings and gifts upon all of them (Ameen).

SYEDA FARRAH NAZ.

Abstract

Oil spill is a form of pollution that is currently becoming a major environmental concern in petroleum industry, as it not only results in significant loss of energy but also imparts hazardous and long lasting impacts on society, economy and environment. Different cleanup strategies have been in use to clean oil from water surface. Recently, much attention has been paid to develop high oil absorption materials with Superhydrophobic and superoleophilic properties. These materials ensure efficient and complete removal of oil from spill sites and help in environment.

Polymer-layered silicates nanocomposites (PLS) show incredible improvements in material as compared to virgin polymer and conventional micro and macro composites provided the silicate layers are homogenously dispersed in the polymer matrix. The lack of interfacial interaction between the two disparate phases, hinders the separation and dispersion of individual layers in the polymers. Functionalization of clay platelets or addition of swelling agent prior to use in nanocomposite formation offer a solution to avoid interfacial problems.

In present research work, for homogenous dispersion of clay into polyurea matrix, first its nature was changed from hydrophilic to organophilic by inserting the cation of dodecylamine between the silicate layers. After that surface modification of intercalated clay was carried out with silane coupling agent i.e. APTES. Hydroxyl groups present on the surface and edges of clay condensed with triethoxysilane groups of APTES, whereas the free amino group of silane coupling agents was exploited for the grafting of polyurea through its reaction with $-NCO$ group of diisocyanate. Polyurea/Organoclay nanocomposites with different concentration of

clay ranging from 10-90wt % were synthesized successfully and characterized with FT-IR and XRD. FT-IR analysis confirmed the formation of nanocomposites materials of choice. The results of x-ray diffraction analysis also provide strong evidence regarding the modification, functionalization of clay and ultimately formation of polyurea/clay nanocomposites. The capacity of synthesized materials to be used as sorbent materials for oil spill cleanup process was evaluated. The maximum percentage removal capacity of 90.41% was recorded for gasoline. These synthesized polymer/clay nanocomposites possessed excellent sorption capacities and have potential for use in oil spill cleanup process thus offer sustainable and practical competence for water treatment and environment protection.

Chapter 1

Introduction

Material is a form of matter, either raw or processed, with certain physical properties that can be used directly or indirectly for production and manufacturing processes. The interdisciplinary field of material sciences and engineering deals with the invention of new materials and improvement of already known materials. There exists a profound relationship between microstructure, composition, synthesis and processing of materials. By utilizing this relationship, material scientists and engineers design new materials and transform them into useful products [1, 2].

Depending on the nature, materials are divided into three main classes: metals, ceramics and polymers. The structure, properties and applications of each group is different from one another. Metals are inorganic materials with good thermal and electrical conductivity. There is large number of mobile electrons available in metals which facilitate the transport of heat and electric energy through the metal. They have high strength, high stiffness, ductility, high density and high melting points [3]. Inorganic crystalline materials composed of metallic and non-metallic elements with covalent and ionic bonds or combination of both are called ceramics. The word “ceramic” finds its basis from Greek word *Keramos* which means potter’s clay. Ceramics are metal oxides, carbides and nitrides such as aluminum, silicon dioxide, silicon carbide, silicon nitride, clay minerals, cement and glass etc. They are brittle, hard and possess good thermal and electrical insulating properties with extremely high melting temperatures. Advance ceramics are used in computer chips, sensors, capacitors, spark plugs,

electrical insulation and thermal barrier coatings. Certain consumer and industrial products also contain ceramic materials such as paints, tires, plastics and tiles etc [4-6].

The ease of processibility, low cost, durability and low density are some of the key reasons for substitution of polymers for other groups of materials. Polymers are inert; they are neither as stiff nor as strong as metals and ceramics. They are ductile and can easily be transformed into complex shapes.

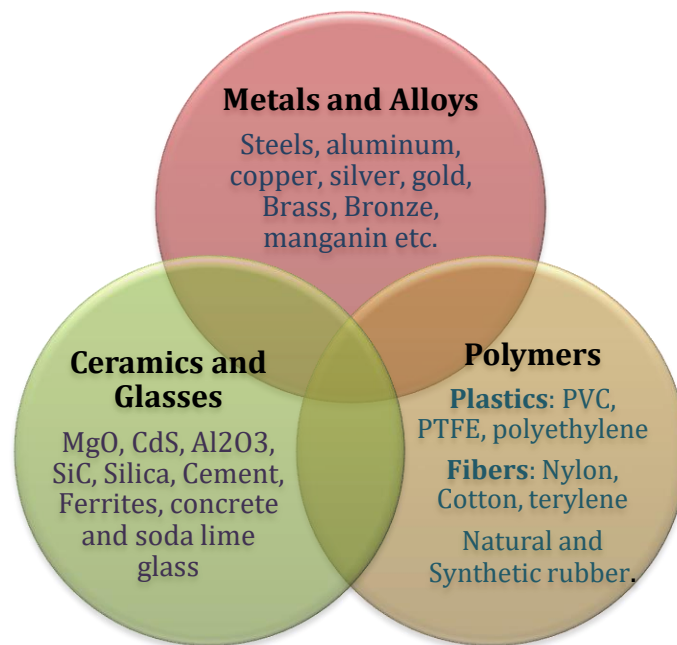


Figure 1.1: Three main classes of materials with typical examples.

1.1 Polymers

Macromolecules, consisting of regularly repeating chemical units joined together through covalent bonds to form long chain molecules, are called polymers. Diversity in molecular structures and properties of polymers allow them to be employed in a variety of applications, thus replacing traditional materials such as metals, ceramics, wood and natural fibers. Both synthetic and natural polymers play an essential role in everyday life ranging from familiar

synthetic plastics and elastomers to natural bio-polymers such as nucleic acid and proteins etc [4, 7].

In 1922, Hermann Staudinger coined the term *Makromolekul* for both natural and synthetic polymers. In a paper entitled "Über polymerization", he proposed several polymerization reactions in which a large number of small molecules (repeat units) were linked together through covalent bonds to form high molecular weight molecules. Initially the idea of macromolecules by Staudinger received criticism but ultimately he was awarded with the Nobel Prize in 1953. Wallace Carothers was the father of synthetic polymer science. He studied condensation polymerization and was able to prepare the two important groups of polymers that were polyester and polyamides [8]. In early 1940's, a new class of polymers was originated; these were silicon polymers that contained silicon atoms instead of carbon atoms in main chain. Silicon rubber was developed in 1945 which can withstand much higher temperature than carbon based rubber. The development of Ziegler- Natta catalyst by Italian chemist G. Natta and German K. Ziegler proved a milestone in the production of polyolefins. Polyethylene produce by this method has high density with greater stiffness and high heat resistance [7, 9]. Paul J. Flory worked in the area of kinetics for condensation and step-growth polymerization and was awarded with Nobel Prize in 1974 [10].

Chemical structure (CS) and molar mass distribution (MMD) of polymers are two fundamental characteristics that determine all the properties of polymers. The chemical structure includes the nature of repeating unit, nature of end groups, composition of branches and cross links and the defects present in structural sequences. Molar mass distribution gives information regarding the average molecular size, regularity or irregularity of molecular size. The cohesive

forces, packing density, crystallinity, and the molecular mobility can be determined directly by CS and MMD. In an indirect way, they control the morphology of the polymers [11].

Classification of Polymers

There are different ways of classifying polymeric materials depending upon their source, chemical linkages, structure and nature of monomer, physical properties, thermal response, strength, polymerization mechanism and preparative techniques. Based on their origin or source, polymers can be natural, synthetic or semi-synthetic. **Natural polymers** are those polymers that are produced by the plants, animals and other living organisms. They are also termed as biopolymers. Typical examples of natural polymers are proteins, nucleic acid, cellulose, starch, chitin, amber, and natural rubber etc.

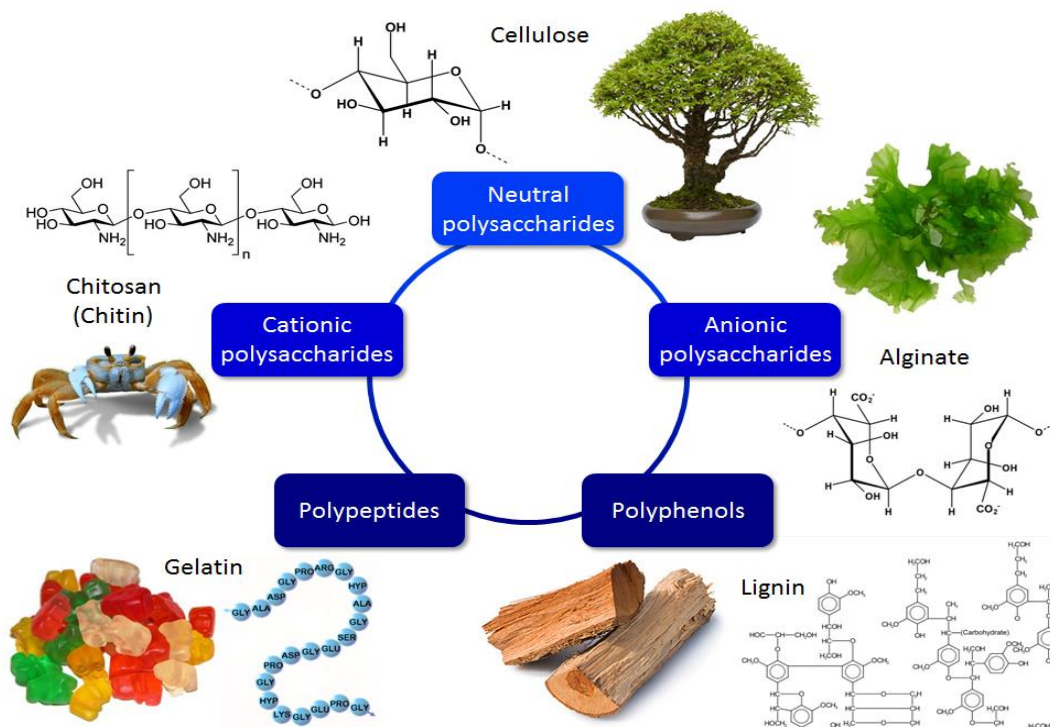


Figure 1.2: Natural or biopolymers classified by source

In order to improve the properties of natural polymers for different applications, these can be chemically modified. These synthetically modified natural polymers are called **Semi-synthetic polymers** [7]. Vulcanized rubber, cellulose diacetate, cellulose nitrate etc are some examples of semi-synthetic polymers, as shown in Fig 1.3.

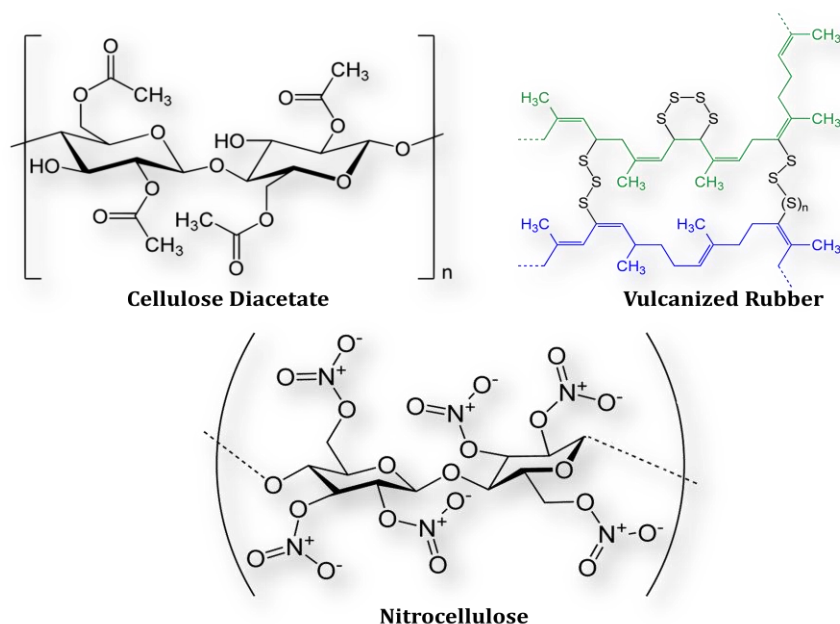


Figure 1.3: Examples of semi- synthetic Polymers

Synthetic polymers are manmade polymers that are synthesized in laboratory. Common examples of synthetic polymers are nylon, epoxy, polyethylene, polyester, polystyrene, polyvinylchloride, neoprene and Bakelite etc. Synthetic polymers are used in a wide range of applications such as films, fibers, food packaging, paper and pipes etc.

Depending on their nature, polymers are divided into two categories; organic and inorganic polymers. In **organic polymers**, carbon atoms constitute the main chain or backbone of polymer. **Inorganic polymers** do not contain carbon atoms in their main chain; instead, inorganic elements such as Si, S, N, and P etc are present. However, these polymers may

contain any carbon containing moiety in its side chain. Examples of inorganic polymer include glass, polysilane, polysiloxanes, silicon rubber and polyphosphazenes. Sometime **organometallic polymers** are also included in this classification scheme. These metal containing polymers are highly thermostable and possess both carbon and metallic elements in their main chain. Antimony and bismuth containing polymers are some examples of organometallic polymers [7].

The heat energy response of polymers i.e. thermal behavior of polymer is another criterion for classifying polymers into two important groups called thermosets and thermoplastics. Those polymers that can be repeatedly softened on heating and transformed into desirable hard materials after cooling without any significant change in their properties are called **Thermoplastic polymers**. These polymers have linear or light branched polymer molecules so they can be moulded even after attaining their final stage. Polyethylene, polystyrene, polyethers and polyesters are examples of thermoplastic polymers. Whereas **thermosetting polymers**, on exposure of heat or high energy radiation like UV, γ -rays and X-rays undergo irreversible chemical crosslinking reactions and transformed into infusible rigid material that can never come back to its original state. Bakelite, melamine, phenolic and epoxy resins are examples of thermosetting polymers [7, 12].

The degree of crystallinity in the structure of polymers i.e. presence of long range order also help to classify the polymeric materials as crystalline or non-crystalline (amorphous). Polymers containing bulkier molecular chains and large functional groups in their side chain are stiffer and do not fold properly to form crystals. Such polymers which lack high degree of crystallinity and ordering in their structure are called **amorphous or non- crystalline polymers**. Polystyrene, polycarbonate, butadiene rubber atactic polypropylene and

copolymer of styrene and butadiene are examples of amorphous polymers. Figure 1.4 shows the amorphous polymer.



Fig 1.4: Amorphous polymer

Crystalline polymers have a high degree of crystallinity in their structure. Polymers having linear structure and simple main chain without bulky side groups tend to be flexible and are able to form ordered crystalline areas. Polymers are not as crystalline as that of pure solid materials, but are semi crystalline. Both crystalline and amorphous regions can co-exist with crystalline phase being embedded in amorphous region, as shown in Fig 1.5 [9]. Polyethylene, Isotactic polypropylene, nylon-6, 6 and polyester constitute this class of polymers.

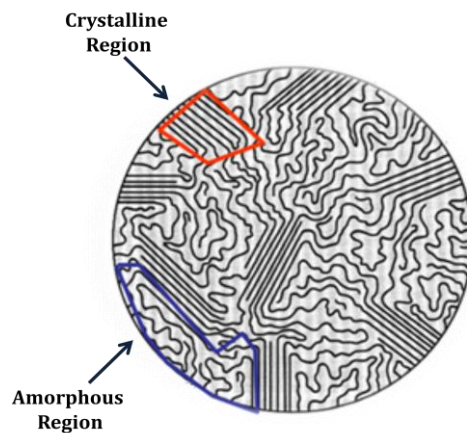


Figure 1.5: Semi Crystalline Polymer

The term “tacticity” comes from Greek word *taktikos* which refers to the spatial arrangement of substituents on main polymeric chain. On the basis of tacticity, polymers are divided into Isotactic, syndiotactic and atactic polymers. When all the substituent groups are on the same side of the macromolecular backbone i.e. each repeat unit has identical configuration. Such types of polymers are **Isotactic polymers**. They form very compact and well-ordered crystalline structure having high strength. The alternative substituents along the main chain represent the class of **syndiotactic polymers**. While in the case of **atactic polymers**, substituents are randomly located on the main chain. They possess lowest strength and highest solubility [7, 8].

Based on the nature of chemical reactions involve in the polymerization process, Carothers was the first to propose another classification for polymers in 1929. The two major groups of polymers are regarded as addition and condensation polymers. Condensation polymerization involves the formation of polymers by the reaction of polyfunctional monomers having reactive functional groups like -OH, -COOH, -NH₂, and -NCO etc. Small molecules such as water, HCl, methanol and ammonia are eliminated as by products in this process. The polymers formed by this mechanism are called **condensation polymers**. **Addition polymers** are formed by the addition of monomers to the growing chain without the loss of small molecules. Addition polymers are also called chain polymers. Polyethylene, polypropylene and polystyrene are addition polymers [7, 9].

The classification of polymers according to the types of repeating units present in the polymer chain, leads two categories of polymers called homopolymers and copolymers. A polymer containing only one type of monomer (repeat unit) in its structure is called **homopolymer**. Polyethylene, polyvinyl chloride and polybutadiene are homopolymers. **Copolymers** or

heteropolymers are formed when more than one type of monomers are present in the polymer structure. Depending upon the arrangement of monomers in copolymers, they are further classified as **alternating, random, graft and block copolymers** [13]. Example for each type of copolymer is given in the Fig. 1.6.

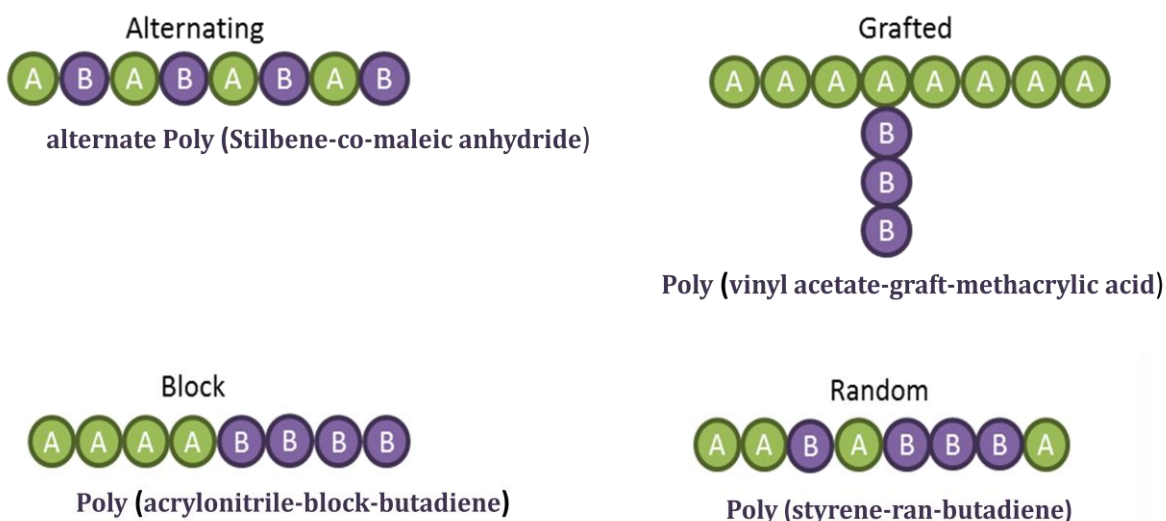


Figure 1.6: Examples of different types of copolymers.

Depending on the physical properties such as cohesive energy density (CED), modulus, extensibility and crystallinity polymers are of three types. **Elastomers** are polymers that can undergo very high and reversible elongation possessing high chain flexibility. Above their glass transition temperature, they have low modulus because of low intermolecular forces. CED value for elastomers is least among all types of polymers. **Plastics** are polymers that are formed in liquid state and then hardened to a rigid solid. CED value for plastics fall in between elastomers and fibers. They show better mechanical properties than elastomers. **Fibers** have low elasticity, high tensile strength and high modulus as compared to elastomers and plastics.

Strong intermolecular forces are present in their chain molecules which impart high crystallinity to fibers. Fibers possess maximum cohesive energy density [11].

1.2 Composites

“A structural material, fabricated or naturally occurring, resulting from the combination of two or more constituent materials with different physical and chemical properties is called a composite material or simply a composite”. The materials that constitute the composite impart unique properties but remain distinct at macro and microscopic levels within the finished product, as they do not dissolve or blend into each other [14, 15].

Wood is a natural composite composed of cellulose fibers that are held together by a weaker substance called lignin. Similarly, bones present in our body are also naturally occurring composite materials. A hard but brittle material termed as hydroxypatite (calcium phosphate) with a soft and flexible protein called collagen together constitute the bone and give it the properties required to support the body. In addition to these natural composites, there are many engineering composite materials in use since long. The examples of such materials include carbon black in rubber, straw bricks, Portland cement, asphalt mixed with sand and glass fiber in resin, etc [16].

There has been an increasing demand for stiffer and stronger but lighter material in fields of energy, aerospace and construction since 1960s. To satisfy the user requirements, this naturally led to re-emergence of the ancient concept of combining materials to yield a composite which results in better performance, unattainable by the individual constituents and offer great advantage of flexible design. The history of modern composite materials began with the development of glass fiber in 1940s. Advanced fibers with extremely high modulus

such as boron, carbon, silicon carbide and alumina emerged in the third quarter of 20th century and have been used for reinforcement of resin, metal and ceramics matrices [17].

Composites, as a class of materials, possess high modulus, high strength, low density, fatigue, corrosion and wear, low and tailorable coefficient of thermal expansion, thus making them versatile materials. High impact strength, design flexibility, durability, permeability, biodegradability, electrical and optical properties are also some of the important characteristics associated with composite materials. Composite materials exhibit resistance to chemical attack as well [18, 19].

The large scale use of composites in aerospace industry involves the development of helicopters, military fighter aircraft, civil transport aircraft, missiles, launch vehicles and satellites. The most famous example is Boeing 787 in which composite material constitute 50% (by weight) of the total material.

Medical applications of composites include bone and joint replacements, artificial hearts, dental implants, replacement of degenerated tissues or organs, pacemakers and biosensors etc. Sport goods such as sailing boats, rackets, ice hockey sticks, softball bats, planning boats bows and arrows etc are made up of composite materials. Composite materials also find their applications in civil and domestic construction including long span roof, bridge components or complete bridge structure, doors, windows, furniture, tanks etc [19].

Constituents in Composites

Individual materials that combine to form composites are called constituents. These are basically two or more chemically distinct phases, separated by an interface. The one phase which is continuous, often present in larger quantity and surrounds the other phase is called

matrix phase. The phase which is discontinuous, present in lesser amount, and is dispersed or embedded in the matrix phase is called **reinforcing phase.** Matrix phase supports the reinforcing phase by maintaining its relative proportion and transfers the load towards reinforcement. On the other hand, reinforcement imparts strength and stiffness thus improving the physical and mechanical properties of the matrix phase. The properties of composites depend on the properties of constituent phases, their relative proportion and geometry of the reinforcing phase; whereas geometry of the reinforcement include its shape, size, distribution, orientation, volume fraction and microstructure [17].

Polymers, ceramics and metals can act as reinforcement or matrix phase; hence the composite materials can be classified into different categories based on the constituent used.

Matrix based classification of composites

Depending on the type of material employed as matrix, the composites are divided into following four classes, as shown in Fig.1.7.

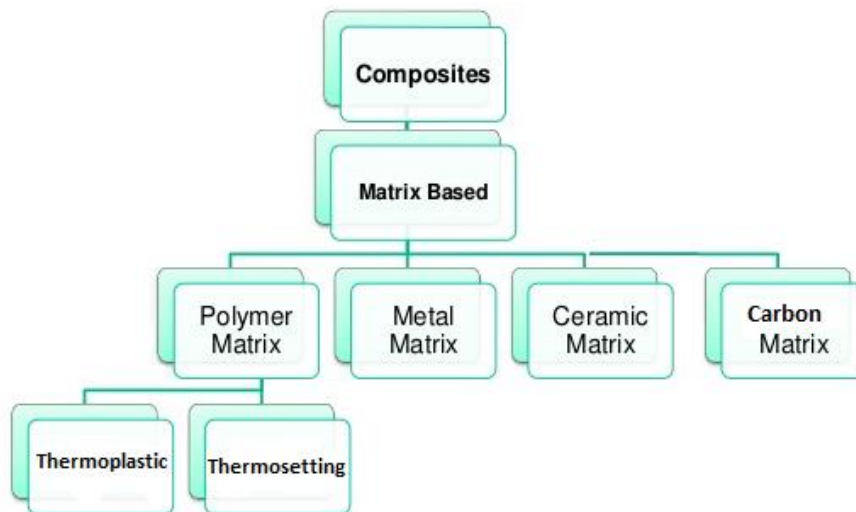


Figure 1.7: Matrix based classification of composites

(a) Metal matrix composites

Those composite materials in which a metal is employed as matrix either reinforced by another metal or any other material such as ceramic or organic compound are called metal matrix composites (MMCs). In metal matrix composites, usually a ductile metal is used for dispersion of reinforcing phase. Initially traditional alloys were used as matrix material for the synthesis of MMCs. Metallic materials that can be used as matrix include copper, lead, magnesium, cobalt, silver, as well as alloys of aluminum, titanium and iron [20].

These materials offer several advantages over the other types of composite materials such as high temperature operation, nonflammability and resistance to degradation by chemicals but they are more expensive and cannot be used at larger scale. By reinforcing the metallic materials with particles, continuous or discontinuous fibers, a new material with modified properties can be created, e.g. the compression strength of silicon carbide-reinforced titanium is four times greater than monolithic titanium.

With continuous fibers, the greatest increase in strength and modulus is achieved but their high cost limits the application of these materials. Continuous fibers used for reinforcing the metal matrix include carbon, silicon carbide, boron and alumina. Therefore, discontinuous fibers like silicon carbide whiskers, fibers of carbon and aluminum or particles of alumina and silicon carbide are most widely used to reinforce the metal matrix composites [21].

b) Ceramic matrix composites

For improving the fracture toughness of ceramics, a new generation of materials has been developed i.e. ceramic matrix composites (CMCs). Particles or fibers of one ceramic material are embedded in the matrix of another ceramic material resulting in a ceramic fiber

reinforced ceramic (CFRC). The fracture properties improvement is associated with the interactions of cracks and particles of dispersed phase. The initiation of cracks usually takes place in matrix phase whereas crack propagation is hindered by the particles, whiskers or fibers acting as reinforcing phase [21].

The most commonly used ceramics for CMCs matrices include silicon carbide, alumina, silicon nitride, mullite and various cements. Ceramic matrix composites are regarded as the least developed and most complex class among composite materials [23].

The most promising ceramic matrix composite is obtained by the addition of silicon carbide fibers to silicon carbide matrix (SiC/SiC). SiC/SiC has fracture toughness in the range of aluminum alloys, also possess excellent resistance to severe thermal shock. This all attributed to presence of continuous fiber reinforcement. CMCs are used in high temperatures gas turbines, disc brake system, as components for slide bearings and heat shield system for space vehicles [22].

c) Polymer matrix composites

The composite materials in which a polymeric substance is employed as matrix phase surrounding and supporting the reinforcement are called polymer matrix composites (PMCs). Unlike ceramic matrix composites, in which the reinforcement's function is to improve the fracture toughness, the reinforcement here imparts strength and stiffness to the polymers which are generally weak, less stiff and viscoelastic materials.

The resistance of PMCs towards Degradative processes is determined by the properties of matrix. Thermoplastics and thermosets are two major classes of polymers that are commonly used as matrix materials. Thermosetting resins used for composite formation are epoxies,

cyanate esters, thermosetting polyimides and polyester, benzoxazines, phenolics, vinyl esters and bismaleimides etc [21].

On account of this three dimensional crosslinked structure, thermosets tend to possess high dimensional stability, more resistant towards high temperature, solvents and corrosive environment as compared to thermoplastics. Among thermosetting epoxies produce composites with remarkable structural properties i.e. for aerospace applications [24].

In a general prospect, thermoplastics are inferior to thermosets but their high temperature strength and chemical stability shows more confrontation against cracking and impact damage. Secondly, from manufacturing point of view, the ability of a material to show easier and faster heating and cooling is more beneficial than to cure it, thus making the thermoplastic matrices more attractive to high volume industry like automotive industry. Amorphous, crystalline and liquid crystal thermoplastic polymers are used as matrix phase for composite formation. The degree of crystallinity has powerful impact on properties of matrix e.g. poor solvent resistance is exhibited by the amorphous thermoplastics while crystalline materials show better resistance [24, 25].

High performance filler materials including continuous or discontinuous fibers, ceramic or metallic particles are blended into polymer as reinforcement, which can boost up several properties like thermal and electrical conductivity, mechanical properties and gas separation performance etc. Most important fibers used for PMCs are glass, graphite, aramid, carbon and boron, organic fibers i.e. oriented polyethylene. Ceramic particles such as alumina, aluminum nitride, boron nitride and even diamonds are embedded into polymers for electrical insulation but also provide higher thermal conductivity. For improving thermal and electrically

conductivity, metallic particles of silver or aluminum are added. Ferrous or permanent magnetic particles are incorporated in various polymers for magnetic composites [26].

Another important feature of PMCs is interphase, as the properties of final composite product are also influenced by interphase along with reinforcement and matrix. "It is the region where mechanical load to which a material is subjected is transmitted between matrix and reinforcement is called interphase". Extent of interaction between the two phases can be customized as it varies from strong chemical bonds to weak frictional forces. This can be done by coating the reinforcing fibers etc [24, 27].

d) Carbon- Carbon composites

The most advanced and remarkable engineering composite material is carbon-carbon composite (CCCs) for example, carbon fiber reinforced carbon matrix has both phases as carbon based. Large fracture toughness values, high tensile moduli and high tensile strengths that can be retained to high temperatures are desirable properties exhibited by this class of composite materials. In addition, low coefficient of thermal expansion (CTE) and higher thermal conductivities are important characteristics shown by these composites. Carbon-carbon composites are employed as friction materials for aircrafts, turbine engine components, in rockets and high performance automobile etc. These materials are expensive and their tendency to high temperature oxidation limits their exercise at large scale [22, 28].

Reinforcement based classification of composites

For material fabrication as well as end application, the compatibility with matrix material, thermal stability, density and melting temperature are some characteristics that help in selecting an appropriate reinforcement incorporated into matrix to improve its physical and

metal glass properties. On the basis of reinforcing phase, composite materials consist of three main divisions, as shown in the Fig. 1.8

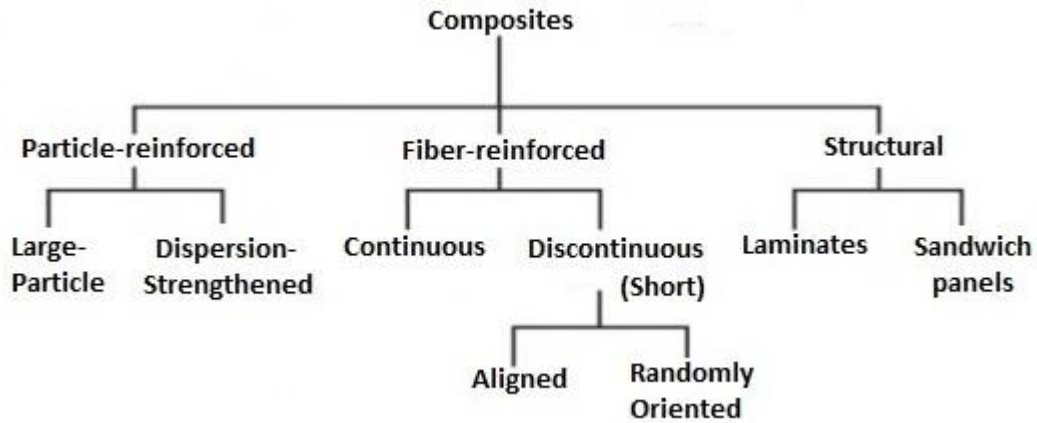


Figure 1.8: Reinforcement based classification of composites

(a) Particle reinforced composites

Particle reinforced composites, consist of particles of one material immersed in matrices of other materials such as alloys, ceramics and polymers etc. Particles have short dimensions, no preferred orientation and may have any size and shape like spherical, ellipsoidal, polyhedral or irregular in shape. To make them compatible with the matrix phase, particles may be chemically modified.

Two sub classifications of particulate composites include **large-particle composites** and **dispersion strengthened composites** based on strengthening mechanism. In large particle composites communication between particle and matrix cannot be considered at atomic or molecular level. In essence, the matrix transfers some of the applied stress to the particles, which bear a fraction of the load. Polymers containing fillers are also classified as large particle composites that replace some volume of more expensive polymers thus making it cost

effective. Materials that can be used as fillers include sawdust, silica flour and sand, glass, clay, talc, limestone and even some synthetic polymers may also used. Concrete is another familiar example of large particle composites where matrix phase is cement whereas sand and gravel (particulates) are used as reinforcement. All three types of materials: ceramics, polymers and metals can be utilized with large particle composites [21].

While in case of dispersion-strengthened composites, strengthening mechanism involves particle-matrix interactions at atomic or molecular level. Fine particles of inert and hard materials (Metallic or nonmetallic; oxide materials) are uniformly dispersed to several volume percent to strengthen and hardened the matrix phase. Major portion of an applied load is borne by the matrix while small dispersed particles prevent the motion of dislocations. Particles used in this type of particulate composites are normally much smaller having diameter between 10 and 100nm. An example of dispersed strengthened composites includes thoria-dispersed (TD) nickel used to significantly enhance the high temperature strength of nickel alloys.

b) Structural composites

The properties of structural composites depend on the properties of constituent materials as well as on the geometrical design of structural elements. There are two common forms of structural composites: laminates and sandwich panels.

A laminate structure is constructed by stacking a number of lamina together; a lamina (building block) is thin layer of composite material having a thickness in the order of 0.15mm. These are two dimensional sheets or panels preferred to have high strength direction. Laminae are stacked and paved together in such a way that with each successive layer the

direction of high strength varied. A laminar composite gains the advantage to combine the particular properties of each layer using different materials [21].

High structural rigidity, strength and lightness are the main features of **sandwich panels**, as a class of structural composites. Sandwich panels are made up of two outer sheets or faces separated and adhesively bonded to a low density core. A stiff and strong material such as aluminum alloys, fiber reinforced plastics, plywood, steel and titanium etc are employed as outer skin layer. These materials impart strength and stiffness so that the resultant material withstands tensile and compressive stresses. Sandwich panels are used where high mechanical performance with low weight is required such as in aerospace and aircrafts [21, 29].

c) Fiber reinforced composites

In fiber reinforced composites, high strength and high modulus fibers are embedded into matrix with distinct interface between them. Both the phases impart a useful combination of properties that cannot be achieved by individual constituent material; however each retains its physical and chemical identity in the end product. In these composites, matrix material can be polymer, metal or ceramics. Such composites offer various chemical compositions and microstructural arrangements. Fibers act as load carrying member while the matrix surrounding the fibers keeps them in proper location and orientation, behaves as load transferring medium and protects them from environmental damages caused by elevated temperature and humidity [21, 22].

1.3. Layered Silicates

It is believed that clay minerals came into existence from the hydrothermal exchange of basic volcanic ash and rocks of the Cretaceous (chalk, limestone) period. Many ideas about the mechanisms of ash-to-bushel transformation were proposed [30].

The term clay represents a class of geological materials, made up of layered silicates or clay minerals with organic matter and metal oxides as traces. Clay minerals are crystalline hydrous aluminum phyllosilicates, having variable amounts of iron, magnesium, alkali and alkaline earth metals and other cations. The regular stacks of aluminosilicates layers possess high aspect ratio and high surface area. The particle size of clay is less than 2 μm and the thickness of an individual clay platelet usually lies in the order of nanometers. As an economical inorganic material with large variability in chemical composition, morphology, chemical and thermal properties as well as the variations in their exchange behavior, clays find their application in industries, engineering and scientific field. Clays are used in many industries for instance, food, ceramics, oil drilling, chemical and paper industry. The scientific applications of clays include as catalysts, decoloration agents and adsorbents [31, 32].

1.3.1 Structure and properties of layered silicates

Layered silicates are natural or synthetic minerals used in the synthesis of nanocomposites are composed of very thin hydrous layered aluminosilicates or magnesium-aluminosilicates, bounded together through counter ions. The basic building blocks are tetrahedral and octahedral sheets which constitute each layer. In tetrahedral sheets each silicon atom is surrounded by four oxygen atoms, connected to one via covalent bonds. A basal plane is formed by these shared oxygen atoms while the remaining edge oxygen atoms are linked to

another layers of cation. The tetrahedral units are arranged in such a way that they form hexagonal network [33]. A tetrahedral sheet appeared to be composed of three parallel planes of atoms of oxygen, silicon and oxygen from a side view. A negative charge is created on the sheet when aluminum atom replaces the silicon atom in tetrahedral sheet. In an octahedral sheet a metal atom like aluminum or magnesium is coordinated with eight oxygen atoms. The thickness of the layer is 1nm whereas the lateral dimensions vary from 300Å to some microns, depending upon the type of silicate, source of clay and the method of clay preparation [34].

These layers structure themselves into stacks with a regular gap between them called interlayer or gallery. Isomorphic substitution within the layers can occur such as Al^{3+} is replaced by Mg^{2+} or Fe^{2+} and then Mg^{2+} is replaced by Li^{+} generating negative charges counterbalanced by alkali or alkaline earth cations located in interlayers [35].

1.3.2 Classification of clay minerals

Depending on the number and arrangement of octahedral and tetrahedral sheets in the structure of clay minerals, these are divided into three layer types.

(a) 1:1 layered structures

One tetrahedral and one octahedral sheet are present in structural unit of 1:1 layer minerals. Kaolin group represented this two sheet layered structure as having general formula $Al_2Si_2O_5(OH)_4$. The most common mineral of this group is kaolinite, a dioctahedral with Al^{3+} octahedral and Si^{4+} tetrahedral substitution. In case, if there is substitution in one sheet there will almost always compensating substitution in the other sheet thus maintaining the neutrality. 1:1 type minerals show low adsorption capacity of cations with low fertility [36, 37].

b) 2:1 layered structures

Two tetrahedral sheets join to one octahedral sheet to produce three sheet mineral structures. Illite (mica), smectite and vermiculite groups represent this class of clay minerals. The basic 2:1 structure with silicon atom in tetrahedral sheet and aluminum in the octahedral sheet with no substitution of atoms is called pyrophyllite [38]. As the layers of pyrophyllite are unable to expand in water, so these minerals have only an external surface area and no internal one, the adjacent layers are joined together by van der Waal bonds [35].

Smectite group represents the class of both dioctahedral and trioctahedral minerals. All minerals of this group show ability to expand and contract their structure but retaining their two dimensional crystallographic structure [39]. Significant amount of isomorphic substitutions take place in smectite resulting in the charge of 0.5-1.2 per unit cell. The overall negative charge is balanced by the calcium and sodium cations hydrated in the interlayer. As compared to mica, these ions are unable to fit in the tetrahedral layer, the layers are held together through relatively weak forces thus allowing the lattice to expand as water and other polar molecules can enter between the layers [40]. The most commonly used smectite clays are montmorillonite, hectorite, saponite, vermiculite, laponite, sepiolite and bentonite. They usually differ in chemical content and have the general formula $(Ca, Na, H) (Al, Mg, Fe, Zn)_2 (Si, Al)_4 O_{10} (OH)_2 .xH_2O$, X is the variable amount of water [35].

Montmorillonite

For the fabrication of polymer-layered silicates (PLS) nanocomposites most commonly used fillers belong to general family of 2:1 layers also called phyllosilicates i.e. smectite ,the most common of which is montmorillonite. Montmorillonite has been given several names:

smectite, Na-montmorillonite, sodium bentonite or swelling bentonite and sodium activated bentonite. The non-swelling bentonite is calcium MMT, bentonite or sub-bentonite. The crystal structure of MMT is shown in Fig. 1.9. In case of MMT, individual layers are 1nm thick whereas the lateral dimension is about 100nm [41-43]. Montmorillonite (MMT) has attracted a great deal of attention which due to its high surface area and swelling capacity, high cation exchange capacity (CEC) and strong adsorption capacity.

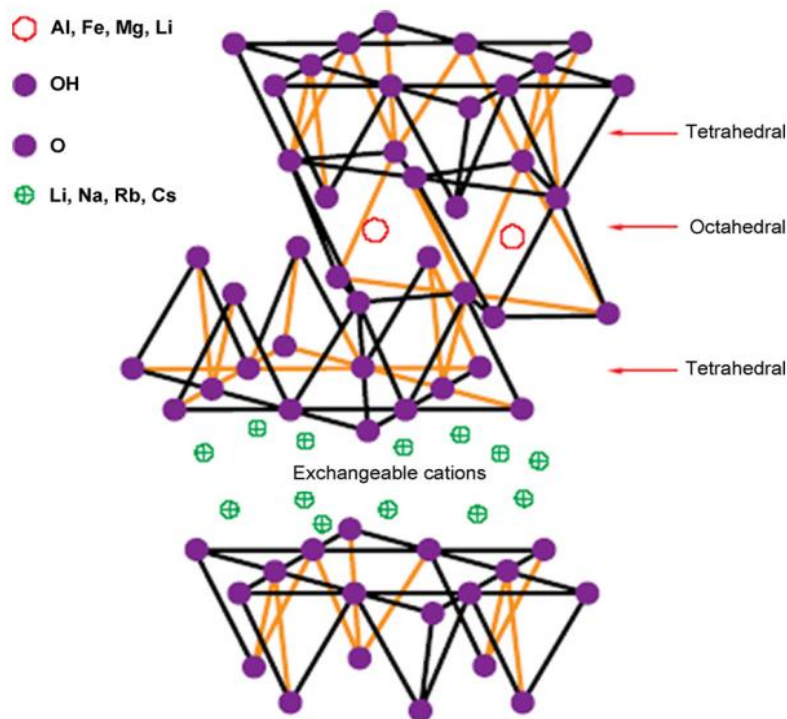


Figure 1.9: Crystal structure of 2:1 layer type minerals (Montmorillonite)

c) 2:1:1 layered silicates

This group is usually not considered as a part of clays but treated as a separate group within the phyllosilicates. The minerals of this group are called chlorites and have the basic structure as that of 2:1 layer structure. Isomorphous substitutions in hydroxide sheet created a net positive charge which is balance by the negative charge arising from the 2:1 layer.. Chlorites

are non-expansive minerals as there are no water molecules absorbed within the interlayer [37].

1.3.3 Organic modification of clay minerals

It is not possible to physically mix the polymer and clay particles to prepare polymer/clay nanocomposites with a good dispersion of clay layers in the polymer matrix. Other factors which lead to poor dispersion of clay nanolayers in most polymers are weak interfacial interactions, high face to face stacking of layers, hydrophilic nature of clay which makes it incompatible with hydrophobic polymers. There are some hydrophilic polymers e.g. polyethylene oxide, polyvinyl alcohol etc. that are miscible with clay. These problems can be overcome by the modification of clay layers with organic agents which reduces the surface energy of clay and makes it compatible with polymers. As a result polymer molecules are able to intercalate within the galleries of layered silicate [35, 44-45].

Quaternary alkyl ammonium salts and alkylphosphonium salts are cationic surfactants commonly used to prepare organophilic clay. The nature of quaternary alkyl ammonium salt influences the affinity between polymer and clay mineral. The cationic portion of these salts replaces the sodium and calcium cations present in the clay galleries [46]. The insertion of organic cation not only modifies the clay surface and changes its nature from hydrophilic to hydrophobic but also separates the layers in silicate minerals promoting high level of intercalation of polymer chains for nanocomposite formation. In addition, these organic cations can provide functional groups to interact with the polymer chains or can initiate polymerization. The interaction of clay minerals with ammonium ion was studied in early 1930s. The principal method for organic modification was based on cation exchange with

alkyl ammonium ions. These were quaternary ammonium compounds having alkyl, phenyl, benzyl and pyridyl groups in their structure [47]. Based on the structure of quaternary ammonium cations (QACs) and their mechanism of adsorption, organoclays are tabulated as adsorptive clays and organophilic clays. Quaternary ammonium salts with short chain alkyl groups or benzyl group are used to synthesize organoclays lead to adsorptive clay. The examples of such QACs include benzyltriethylammonium (BTEA), tetramethylammonium (TMA) and trimethylphenylammonium (TEPM) etc. In contrast, if the modification of clay is carried with QACs with long alkyl chains such as didodecyldimethylammonium (DODMA) or hexadecyltrimethylammonium (HDTMA), this class of organoclays is called as organophilic clays [48-50]. The size of alkyl chain also determines the arrangement of exchanged organic cations between the layers of organoclay. In adsorptive clay, organic cations due to their short chain length forms a monolayer, while bilayers, pseudo-trimolecular and paraffinic arrangement can be observed in organophilic clays because these are intercalated with long alkyl chain cations as shown in the Fig. 1.10[35, 44, 51-52].

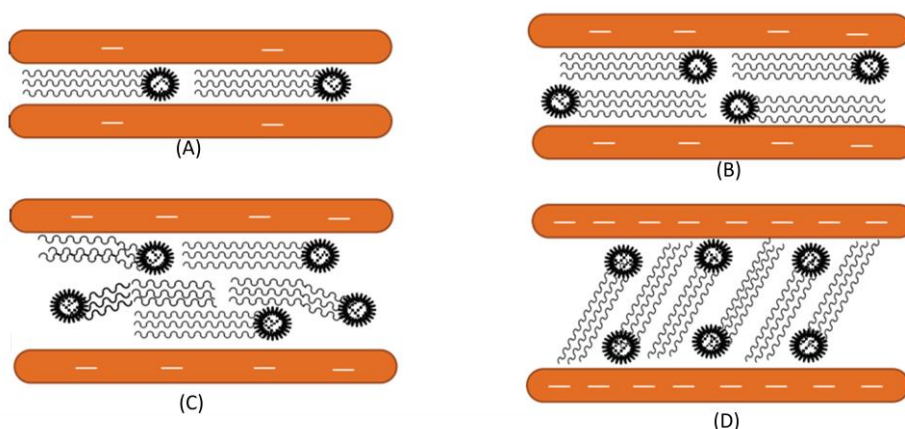


Figure 1.10: Configurations of exchanged organic cations between the layers of organoclays
 A) Monolayer, B) Bi-layer, C) Pseudotrimolecular and D) Paraffinic

These different configurations of organic cations result in increase of basal spacing to different extent. Table 1.1 shows the basal spacing of Organophilic montmorillonite (OMMT) prepared with different quaternary alkyl ammonium and alkylphosphonium cations [53].

Table 1.1: *The basal spacing of OMMT intercalated with Quaternary onium salts*

| Quaternary Onium Salt | d (nm) |
|------------------------------------------------------|--------|
| Tetrabutyl phosphonium bromide | 1.40 |
| Tributyl hexadecylphosphonium bromide | 2.32 |
| Tributyl tetradecylphosphonium chloride | 2.19 |
| Tetraphenyl phosphonium bromide | 1.76 |
| Ethyl triphenylphosphonium bromide | 1.76 |
| Propyl triphenylphosphonium bromide | 1.76 |
| (Butoxymethyl) dodecyl dimethylammonium chloride | 1.47 |
| Dodecyl dimethyl (hexyloxymethyl) ammonium chloride | 1.49 |
| Dodecyl dimethyl (octyloxymethyl) ammonium chloride | 1.53 |
| (Dodecyloxymethyl) dodecyl dimethylammonium chloride | 1.56 |
| (Benzyloxymethyl) dodecyl dimethylammonium chloride | 1.41 |
| Octadecylammonium chloride | 2.18 |

1.3.4 Silylation of clay minerals

The term “Silylation” refers to the introduction of substituted silyl group to a molecule. Silanes are renowned as competent coupling agents extensively used in composites and adhesive functionalization. By definition, coupling agents are synthetic hybrids which facilitate adhesion between dissimilar molecules. For improving mechanical strength of composites, adhesion, resin and surface modification, silane coupling agents are useful compounds [54].

Although, organic modification of clay minerals improves the dispersion and interaction of clay with polymer matrix, the effective clay/polymer matrix bonding cannot be achieved. Weak electrostatic interactions result in a distinct interface between hydrophilic clay mineral and polymer (organic matter) which negatively affects the mechanical properties of polymer clay nanocomposites. Secondly, the edges of modified clays show hydrophilicity, thus hindering the intercalation process by bulky hydrophobic groups resulting in poor dispersion of clay throughout the polymer matrix. During processing the quaternary ammonium salt may undergo degradation through the Hoffman degradation mechanism [55-57]. The functionalization of clay surface with silanes is a possibility of chemical modification. Silanes interact with the polymer matrix through reaction with hydroxyl groups of clay minerals located at the edges and at the structural defects situated at the external surfaces at the interlayers [57-58]. As a result of variations in structure and properties of phyllosilicates, silane grafting mechanism and sites differ significantly among different clay types. Silane readily intercalate into galleries of swelling clays such as montmorillonite. All external plus internal surfaces and broken edges are readily silylated under mild conditions without pre-intercalation. In case of non expanding clays such as kaolinite small polar molecules are used for pre-intercalation prior to inner surface silylation [59, 60].

The reactivity of clay surface also influences the silylation, which in turn depends on the density of surface hydroxyl group. Number of functional groups present in silanes and their configuration and reaction conditions such as temperature, time and nature of solvents are the major factors for successful silylation [61-64].

1.4. Polymer-layered silicates Nanocomposites

As engineering materials, polymer-layered silicates nanocomposites (PLS) show incredible improvement in material properties as compared to virgin polymer and conventional micro and macro composites. Depending upon the nature of layered silicate, polymer matrix, organic cation and method of preparation, there are three types of composite materials obtained as a result of association between layered clays and polymer [65, 66]. In **conventional or phase separated** polymer-clay composites, the organization of clay nanolayers remains undisturbed i.e. there will be no intercalation of polymer chains into clay layered structure. In such composites, clay acts mainly as filler and has little or no functional role in improving the properties of final composite. In addition, the degree of dispersion of clay platelets into polymer matrix determines the nanocomposite structure which results in two types of morphologies, namely intercalated and exfoliated [35].

The **intercalated** structure is obtained as a result of penetration of one or sometimes more than one extended polymer chains in the galleries of silicate layers thus leading to the formation of alternative polymer and inorganic layers structure. These polymers chain increase the interlayer space but the periodic assembly of clay layers remains intact. The separation between the clay platelets caused by the intercalation is less than 20-30Å [67].

Whereas an **exfoliated** nanostructure involves the complete separation of individual silicate layers by the insertion of polymer chains into galleries of clay minerals. These separated silicate layers are randomly dispersed within the polymer matrix. Generally, it is assumed that an exfoliated structure is obtained when the polymer chain increases the interlayer space greater than 80-100 Å. Exfoliated nanocomposites offer high aspect ratio, greater phase

homogeneity as well as require lower clay content due to well dispersion behavior of clay layers. As a result of larger surface interactions between polymer and clay, significant improvement in properties of polymers can be achieved [67-69]. Structural configurations of various clay/polymer interactions have been given in the fig. 1.11.

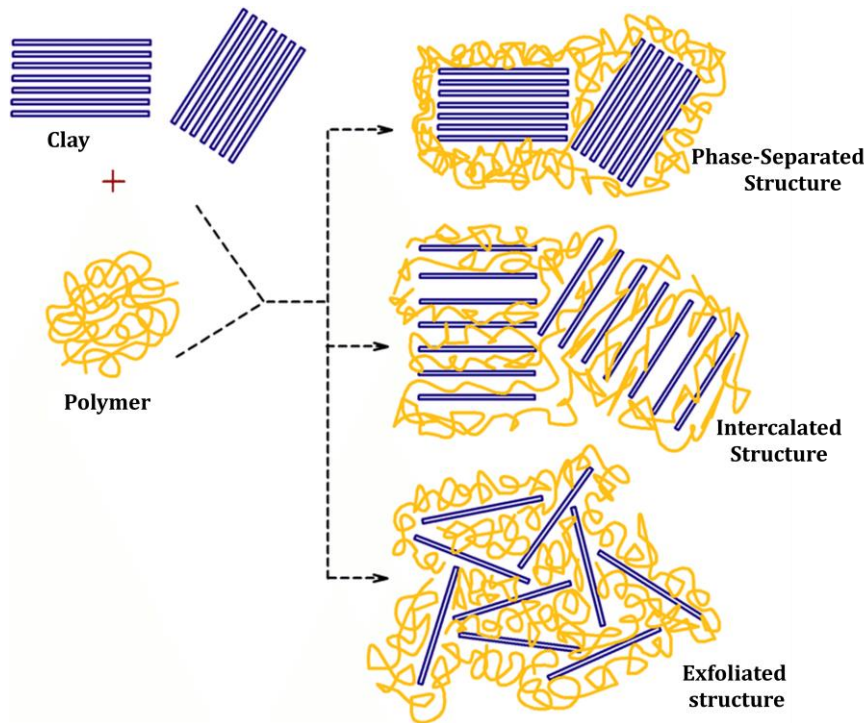


Figure 1.11: Schematic representation of various microstructures of polymer/clay hybrids

1.4.1 Properties of polymer-clay nanocomposites

Polymer-layered silicates exhibit several advantages as they are light in weight compared to those of conventionally filled polymers. They possess high stiffness and strength with low density. Polymer/clay nanocomposites exhibit excellent diffusion barrier properties and do not require multipolymer layered design. Their mechanical properties are superior to unidirectional fiber reinforced polymers, as the reinforcement by the layered silicates occurs in two dimensions. These composites show admirable flammability properties. During

combustion, a tough char layer is formed which act as mass transport barrier, thus slowing the escape of volatile by products [70].

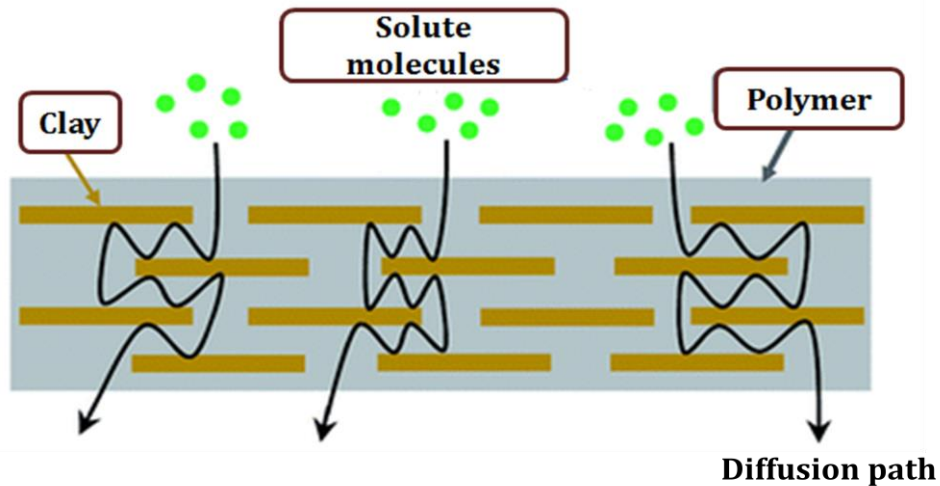


Figure 1.12: Tortuous diffusion path in polymer/clay nanocomposites

1.4.2 Methods of synthesis for polymer-clay nanocomposites

In order to prepare intercalated and exfoliated polymer-clay nanocomposite, various synthetic approaches have been developed. These methods differ from each other in term of starting materials and the processing techniques. Four principal synthesis methods are used for the preparation of polymer/clay nanocomposites.

a) In-situ template formation method

An aqueous solution or gel containing polymer and precursors of clay minerals is used for the in-situ synthesis of clay minerals within the polymer matrix. Magnesium hydroxide, silica and lithium fluoride are used as primary building blocks for clay formation. In this process, polymer assists the nucleation and growth of the inorganic crystals and gets confined within the layers as they grow up. This method involves the dispersion of clay layers within the

polymer matrix without onium cation modification of clay. This method offers several disadvantages for example high temperature is required for the synthesis of clay minerals that leads to polymer decomposition. However, this method can be employed for hectorite-type clay minerals that can be synthesized at lower temperatures. Secondly, synthesized silicate layers generated by self-assembly possess the high tendency to aggregate [35, 44, 71].

b) In-situ intercalative polymerization method

This method was first used by Toyota research group for the preparation of Nylon-6 /MMT nanocomposites using caprolactam monomers [68]. Organically modified layered silicate is allowed to swell in a liquid monomer or a monomer solution. As a result monomers get diffused into the galleries of the layered silicate where the polymerization occur between the intercalated layers. The polymer formation can be initiated either by heat or radiation, by diffusion of a suitable initiator, organic initiator or catalyst fixed inside the interlayer through cation exchange mechanism prior to swelling step by monomer. Intra as well as extra galleries polymerization occur, the clay layers are delaminated and a material with disordered structure is obtained. This method is suitable for preparation of thermoset/clay nanocomposites such as for epoxies and styrenic polymer nanocomposites. Studies showed that both modified and unmodified clay minerals can be used for preparation of polymer/clay nanocomposites using this method of synthesis [35, 72-73].

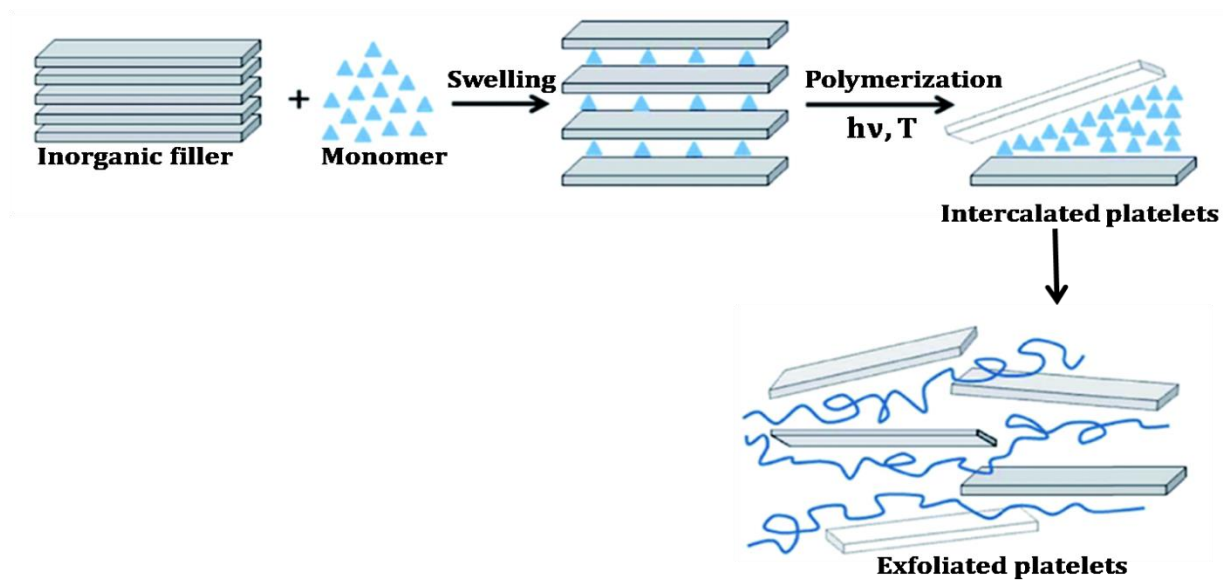


Figure 1.13: Schematic view of in-situ intercalative polymerization

c) Melt intercalation method

In this method, layered silicate is blended with the polymer in molten state. Above the softening point of polymer, this method involves annealing a mixture of polymer and organically modified layered silicate. Based on the compatibility between the chosen polymer and layer surface, the polymer can crawl into the interlayer space and either form intercalated or exfoliated nanocomposites. For thermoplastic nanocomposites this method is effective technique. Extrusion and injection molding are used for the dispersion of clay within the polymer matrix at its melting point. To achieve maximum compatibility between the two phases, clays are organically modified or surface of polymer chains are modified with polar functional group thus promoting the exfoliation. Among all the methods used for PLS synthesis, melt intercalation is industrially favorable because of its ease of execution and production. This method is environment friendly as it requires no organic solvent for processing [43, 45].

d) Solution intercalation method

Layered silicates have weak forces that stack the layers together and thus can be easily dispersed in an appropriate solvent. In this method, the layered silicate is dissolved in such a solvent in which the polymer or prepolymer is soluble. As a result of swelling, organo-clay is exfoliated to give single layers. The polymer is then added which intercalates between the layers of silicates. The final product is obtained by the removal of solvent either by drying under vacuum or by precipitation [35, 71].

The polymer chains absorbed on the surface of delaminated sheets diffuse into the layers as a result of entropy, gained by the exit of solvent molecules from the interlayers during solvent evaporation. After the solvent removal, sheets re-assemble thereby sandwiching the polymers and forming nanocomposite. One of the main disadvantages of this method is use of large quantity of solvents that make it impractical for industrial application [72].

e) Emulsion polymerization method

Emulsion polymerization involves the dispersion of clay in an aqueous solution in the presence of a surfactant that can be cationic, anionic or zwitter ionic. This method of nanocomposite preparation is also called solvent intercalation method. Monomers are added to the solution where they adsorb on the surface of clay. The polymerization and modification takes place simultaneously within the same solution as compared to in-situ polymerization in which clay functionalization is carried out in a separate step [74]. This technique was used by Toyota group for the synthesis of polyimide/clay nanocomposites [75].

1.4.3 Literature review of polymer-clay nanocomposites using modified montmorillonite

Montmorillonite was named after Montmorillon in central western France after its discovery there in 1847. It is very soft layered silicate with plate-shaped particles having cation exchange capacity of about 80-150_{meq}/100g. Natural montmorillonite modified with quaternary ammonium salts are called cloisites, used for the preparation of polymer clay nanocomposites.

S. Sadhu and A.K. Bhowmick (2004) prepared nanocomposites of styrene-butadiene rubber (SBR) and nitrile rubber reinforced with organically modified montmorillonite. Octadecylamine (ODA) was used as modifier; the increase in the gallery gap upon modification was confirmed by XRD studies. It was further concluded that the complete exfoliation of organoclays in case of SBR resulted in improved mechanical properties [76]. D.G. Lopez et al (2005) synthesized polyamide/layered silicate nanocomposites through melt intercalation method. For improving the dispersion of nanolayers in polymer matrix, MMT was modified with octadecylamine. The thermal and mechanical properties of corresponding nanocomposites showed enhancement in properties [77]. R. P. Moraes et al (2010) established the experimental investigation in which hybrid lattices of poly (styrene-co-butyl acrylate) and organically modified clay (3wt % and 6wt %) were prepared. Ammonium salts such as cetyltrimethylammonium chloride (CTAC), alkyl dimethyl benzyl ammonium and Distearyl dimethyl ammonium chloride were used for the intercalation of montmorillonite. These large alkyl chain and bulky group containing organic modifiers increased the basal spacing to larger extent which resulted in highly intercalated and exfoliated nanocomposites. The thermal stability of also showed increasing trend with the addition of 3 wt% OMMT

modified with Distearyl dimethyl ammonium chloride (18 carbons alkyl chains) [78]. A comparative study was carried out by J.W. Gilman (1998) which involved the use of two types of clay, modified with dioctadecyl substituted ammonium and monooctadecyl substituted ammonium. Nanocomposites of polystyrene and modified layered silicates were prepared through melt blending. An intercalated structure containing nanocomposites was obtained with the dioctadecyl substituted ammonium salt while the other one resulted in micro composite. They prepared the same nanocomposite system through in-situ polymerization method; the larger surfactant increased the d-spacing thus allowing the monomer to go through the gallery space, promoting polymerization [79].

Various chain lengths containing organic amines were used by S. Sadhu and A.K. Bhowmick (2003) for the preparation of styrene butadiene rubber (SBR)/MMT nanocomposites. Stearyl amine, hexadecyl amine, dodecyl amine and decylamine were used. The influence on the thermal and mechanical properties as a function of alkyl chain of organic modifier was investigated. MMT having ammonium salt with longer chain length gave better mechanical and thermal properties in nanocomposites than MMT modified with shorter chain length ammonium cation [80]. J. Morawiec et al. (2005) used ODA modified montmorillonite in low density polyethylene. The exfoliation of silicate layers was achieved through a compatible agent, maleic anhydride grafted polyethylene [81]. A. Ganguly et al. (2008) used both modified and unmodified Na⁺-Montmorillonite for the preparation of Poly (styrene(ethylene-co-butylene)-styrene) SEBS and fluoroelastomer/layered silicate nanocomposites. Stearyl amine and octadecylamine containing hydrophobic organo-MMT showed excellent improvement in mechanical properties of SEBS whereas fluoroelastomer showed best results with unmodified Na⁺-Montmorillonite [82]. M. Maiti et al. (2006) investigated the influence of

Octadecylamine treated clay on the mechanical properties of exfoliated ethylene-octene copolymer/MMT nanocomposites by solution blending. Improvement of 44% tensile strength, 63% modulus and 14% storage modulus was observed [83]. P. I. Xidas and K.S. Triantafyllidis et al. (2010) evaluated the thermal and mechanical properties of epoxy nanocomposites reinforced with organo-MMT. The organic modification of MMT was carried out with four different alkyl ammonium cations; primary and quaternary octadecylamine ammonium ions, quaternary dihydrogenated tallow ammonium and quaternary benzyl substituted tallow ammonium ions. They finally concluded that primary alkyl ammonium ions having reactive hydrogen atoms were effective for the preparation of epoxy nanocomposites as compared to others [84]. Dimethyl-hexadecyl-imidazolium was employed as organic modifier of MMT that was used to prepare nanocomposites with acrylonitrile-butadiene-styrene (ABS). The mechanical properties and thermal stability of these composites were compared with those alkyl ammonium treated MMT containing nanocomposites. Imidazolium treated MMT showed stability when processed at a temperature of 200°C while alkyl ammonium modified MMT showed degradation [85].

Y. Someya with coworkers (2005) synthesized poly (glycidylmethacrylate-co-methyl acrylate)/MMT. Four different surfactants including octadecylamine, 12-aminolauric acid (ALA), N-lauryldiethanolamine (LEA) and hexadecyl tributylphosphonium bromide (HBP) were used. Results showed enhancement in mechanical and thermal decomposition temperature as compared to pristine polymer [86]. M. Pramanik et al. (2003) changed the hydrophilicity of layered silicates to organophilicity through dodecylamine and used them for the preparation of ethylene vinyl acetate-45 rubber/clay nanocomposites. The increase in tensile properties, storage moduli and glass transition temperature was observed [87]. M.S.

Rama and S. Swaminathan (2010) applied MMT modified with quaternary phosphonium and imidazolium cation to synthesized polycarbonate (PC)/clay nanocomposites. It was inferred that organo MMT with reactive bisphenol group containing modifier gave exfoliated PC/MMT nanocomposite whereas nanocomposites obtained from O-MMT with non reactive functionality showed intercalated or phase separated morphology [98].

S. R. Ha and K. Y. Rhee (2008) modified Cloisite Na⁺ with 3-Aminopropyltriethoxysilane used for the preparation of polymer nanocomposites. The improved dispersion of modified MMT within the epoxy matrix as well as the adhesion with the epoxy was indicated by lower friction coefficient and specific wear rate [89]. Alvi et al. (2013) reported a method in which aminosilane grafted and diamine modified reactive montmorillonite was exploited to generate aromatic polyamide based nanocomposites. For better compatibility, the hydrophilic nature of MMT was changed into organophilic using 1, 4-phenylenediamine and the hydroxyl groups present on the clay surface and edges were used to graft 3-aminopropyltriethoxysilane (APTS) on clay sheets [90]. N-(2-aminoethyl)-3-aminopropyltrimethoxysilane was used for the silane functionalization of montmorillonite, further applied for epoxy nanocomposites preparation. Effective exfoliation of MMT with epoxy matrix was achieved. Increase in storage modulus and glass transition temperature was exhibited by the nanocomposites based on this clay [91]. Nylon-6/MMT nanocomposites were prepared by Toyota research group through in-situ polymerization method. Their studies showed that the thermal and mechanical properties had improved amazingly with very small loading of layered silicates. They first discovered the swelling of Na⁺-MMT modified with α , ω -amino acids in ϵ -caprolactam monomer at 100°C. N6/MMT nanocomposites were obtained by ring opening polymerization. For intercalation of ϵ -caprolactam, they used ammonium cation of ω -amino acids and

concluded that swelling behavior of MMT modified with ω -amino acids is affected by the number of carbon atoms in α , ω -amino acids. The extent of intercalation will be high if the number of carbon atoms is high. With continuation, this process was briefly described by Usuki et al, who also demonstrated the intercalative polymerization of ϵ -caprolactam without the organic modification of MMT [92].

S. R. Ha and K. Y. Rhee (2008) modified Cloisite Na⁺ with 3-Aminopropyltriethoxysilane used for the preparation of polymer nanocomposites. The improved dispersion of modified MMT within the epoxy matrix as well as the adhesion with the epoxy was indicated by lower friction coefficient and specific wear rate [89]. Alvi et al. (2013) reported a method in which aminosilane grafted and diamine modified reactive montmorillonite was exploited to generate aromatic polyamide based nanocomposites. For better compatibility, the hydrophilic nature of MMT was changed into organophilic using 1, 4-phenylenediamine and the hydroxyl groups present on the clay surface and edges were used to graft 3-aminopropyltriethoxysilane (APTS) on clay sheets [90]. N-(2-aminoethyl)-3-aminopropyltrimethoxysilane was used for the silane functionalization of montmorillonite, further applied for epoxy nanocomposites preparation. Effective exfoliation of MMT with epoxy matrix was achieved. Increase in storage modulus and glass transition temperature was exhibited by the nanocomposites based on this clay [91]. Nylon-6/MMT nanocomposites were prepared by Toyota research group through in-situ polymerization method. Their studies showed that the thermal and mechanical properties had improved amazingly with very small loading of layered silicates. They first discovered the swelling of Na⁺-MMT modified with α , ω -amino acids in ϵ -caprolactam monomer at 100°C. N6/MMT nanocomposites were obtained by ring opening polymerization. For intercalation of ϵ -caprolactam, they used ammonium cation of ω -amino acids and

concluded that swelling behavior of MMT modified with ω -amino acids is affected by the number of carbon atoms in α , ω -amino acids. The extent of intercalation will be high if the number of carbon atoms is high. With continuation, this process was briefly described by Usuki et al, who also demonstrated the intercalative polymerization of ϵ -caprolactam without the organic modification of MMT [92].

1.5 Oil Spills

As an important source of energy, petroleum and its derivatives are necessity for mankind. One of the environmental concerns with the continuing use of petroleum is oil pollution, regarded as a key issue in petroleum industry. The release of liquid petroleum hydrocarbons in environment during production, transportation and utilization is known as oil spill. Oil spills may also occur on land however the term is usually applied for oil accidents that happen in water bodies such as marine areas [93]. It is believed that about 5 million tons of petroleum products are transported around the globe through seas [94]. In addition to this, an oil spill may also arise from oil run-off from onshore rigs, oil blowout from off shore rigs or wells, inland pipelines and tanker trucks etc. As the oils spilled, they spread on the sea surface and form a thin layer termed as oil slick. Several physical and chemical processes act upon the oil slick and gradually start decaying it. These processes are collectively called oil weathering processes, for instance spreading, evaporation, emulsification, photolysis or photo-oxidation, tar ball formation, biodegradation, dissolution, dispersion, resurfacing and sedimentation etc. Sea conditions such as wind, movement of tides, temperature and other environmental conditions manipulate the kinetics of these processes [95].

1.5.1 Impact of oil spills

Oil spills are associated with severe and harmful impacts on economy, environment and public health along with sociocultural and psychological ones. The overall economic impacts of oil spills comprise energy losses, environmental damage, cost of cleanup practices etc. Again, there are number of factors which regulate the cleanup cost e.g. location, oil type and nature, sea conditions, oil weathering processes, spill size, methodology applied for cleanup process and proximity to shoreline [96,97]. One of the most recent and worst oil spills on sea water which drew the attention of world was in the Gulf of Mexico where British Petroleum (BP) Deep water Horizon oil rig blew out releasing 5million barrels of crude oil [98]. The spill lasted approximately for three months and brought about huge economical and environmental destruction as it threatened fishing and tourism industries costing 200,000 employment opportunities [99].

Spills affect marine life; due to presence of oily layer on water surface sunlight cannot pass through it which in turn makes the survival of sea plants and animals much difficult. The most vulnerable among the marine life include shell fishes and diving birds. The methods applied for cleanup process may act as secondary source of air and water pollution. Oil spills may cause serious issues to human health including neurological and acute toxic effects, nausea, throat infections, eye and nose irritation, migraines, headaches and the problems of respiratory system. Polycyclic aromatic hydrocarbons in oil products are cancer causing.

1.5.2 Oil spill control methods

The types of oil, its behavior in sea water and weathering, sea and weather conditions, location etc are some key factors which collectively determine the cleaning method for oil

spills. Sometimes, effective cleanup can be achieved with the combination of two or more methods. Some cleanup strategies are discussed below.

a) In-situ burning

In-situ burning technique involve ignition of oil slick on the sea water, thereby reducing the amount of oil in the water and subsequently reducing hazards to environment and ecosystem. 600-1800 barrels of oil in one hour can effectively be removed using this technique. Oil spill is initially put on the flames using Helitorch or by dropping diesel soaked rag. Then a fireproof boom is used to stabilize the oil and the combustion of oil is controlled. In-situ burning is effective in cold and ice water where conventional methods have limited efficiency.

However this technique has several disadvantages such as, it does not offer the complete removal of oil, constant monitoring is required and large quantity of smoke is generated which results in oily rain. Toxic compounds including carbon monoxide, sulfur dioxide and polycyclic aromatic hydrocarbons emit during burning of oil [100].

b) Mechanical techniques

In mechanical methods booms and skimmer are used to remove oil from water surface in the absence of harsh environmental conditions. Booms in the form of V-shaped barrier prevent the movement of oil and concentrate it in one place on the surface of water from where it is collected through skimmer boats and barges [101].

c) Bioremediation

Microorganisms like bacteria, yeasts and fungi are used for the biodegradation of oil in affected site. For this purpose, fertilizers and nutrients are introduced artificially to native

micro-organisms to stimulate them in the contaminated area. Sometimes, non-native microorganisms are also introduced to speed up the biodegradation process [101].

d) Dispersants

The use of dispersants is a chemical method and is capable of treating large areas as compared to other methods. Dispersants are basically surfactants which are partially soluble in oil as well as in water. Dispersants are sprayed on the surface of oil slick using spray equipment to reduce interfacial tension between oil and water which enhances the dispersion, dilution and biodegradation process [101].

Dispersants are expensive, contain toxic compounds and are not effective in calm water as sufficient mixing energy is not available to mix them with oil.

e) Sorbents

Among all the methods employed for oil removal during an oil spill process, the use of sorbents material has proved to be the cheapest and most effective method. Sorbent materials for oil spill cleanup are characterized with oleophilicity, hydrophobicity, good oil sorption capacity, selectivity and oil retention capability, recoverability of oil, buoyancy and strength. In addition to these properties, the efficiency of sorbent materials also depends on its density, wettability, recyclability as well as geometry. Based on their origin there are three categories of sorbent materials:

i) Natural organic sorbents

Agricultural products including straws, wood, sugarcane bagasse, cotton and cotton grass fiber, milkweed, silkworm cocoon, coconut shell and rice husks etc are used for removing oil

from water. They contain oils or wax due to which they possess affinity for oil greater than water. They are lightweight and able to float on water. They are cheap, eco-friendly and readily available. However these sorbents are difficult to remove from water as they sink after being soaked with oil [102].

ii) Synthetic organic sorbents

Synthetic organic sorbents include high molecular weight polymers e.g. polyurethanes and polypropylene with good oleophilic properties and high sorption capacity. Polymers in the form of foams, mats, fibers and powder (tire powder) are used for oil removal. Synthetic sorbents offer non-biodegradability which is major drawback [101].

iii) Inorganic mineral sorbents

Inorganic mineral sorbents are also called sinking sorbents. These are natural or processed highly dense, fine-grained minerals. Silica, silica gel, activated carbon, graphite, stearate treated chalk, zeolites and organoclays etc are all examples of sinking sorbents. As they are dense, they are used to sink floating oil thus offering non-recoverability and they are difficult to transport at the affected site [101].

1.6 Overview of various materials used in oil spill cleanup

The use of absorbent materials for oil spill cleanup has attracted the attention of many researchers. In this regard, a large number of adsorbents have been synthesized based on various natural, synthetic, organic and inorganic materials. A detailed overview of such materials is given below:

M. Zhang et al (2016) successfully fabricated hollow tubing polystyrene through co-axial electrospinning. The size of co-axial hollow tubing structure was tunable and had a great impact on the oil removal efficiency compared to porous polystyrene fibers without co-axial hollow tubing. The result showed the oil sorption capacity of 66g/g for diesel oil and 147g/g for motor oil. The oil-water separation property and oil retention capacity was also high. They concluded that hollow tubing structure polystyrene performed better than porous polystyrene fibers [103]. A. O. Ifelebuegu et al (2015) investigated the potential of human hair as oil spill sorbent using vegetable, crude and diesel oil. Based on origin, three types of human hairs were used. The adsorption capacities of 9300 (vegetable oil), 8100 (crude oil) and 7917 (diesel fuel) mg/g were achieved. Hair adsorbed oil up to three to nine times its weight. Desorption and reusability tests showed high reusability without any change in sorption capacity. As a low cost, environment friendly and effective biosorbent, human hairs have potential for oil spill cleanup [104]. S.A. Sayed and A.M. Zayed (2005) investigated the effectiveness of three adsorbent materials for oil spill cleanup. These materials include onion and garlic peel being agriculture waste and sludge composed of calcium aluminum silicate [105].

D. Wu and co-workers (2014) prepared a sorbent for oil removal based on polyurethane sponges. The final material was obtained by the treatment of polyurethane sponges with silica sol and gasoline. Different tests were carried out for the evaluation of material performance, indicated high sorption capacity and oil/water separation capability. They claimed that the one gram of synthesized sorbent indicated the possibility of absorbing 100 g of motor oil and extraordinary reusability, so it could be a better substitute for commercially available sorbents based on polypropylene [106]. G.O. Aydin and H.B. Sonmez synthesized reusable

hydrophobic polyalkoxysilane organogels. Thermal and structural properties were investigated through FTIR, solid state ^{13}C and ^{29}Si NMR and TGA. Results showed that the material possessed great oil absorbance capacity for different oil types as well as for organic solvents e.g. benzene, tetrahydrofuran, dichloromethane and toluene [107]. L. Yu et al. (2015) prepared $\text{Fe}_3\text{O}_4/\text{PS}$ nanocomposite through emulsion polymerization with excellent properties such as high hydrophobicity, superoleophilicity and non sinking ability. The absorption capacity test showed that these composites could absorb oil 2.5 times its weight [108]. S. Kizil et al. prepared Polyalkoxysilane organogels for oil and organic solvents removal. The organogels were prepared via the condensation polymerization of alkoxysilanes and 1, 3-benzenedimethanol. The material showed the quick absorption properties in petroleum derivatives such as gasoline and diesel fuel and could be applied several times without any loss in capacity of absorption [109]. M. Patowary and colleagues used palmitic acid for modification of hygroscopic magnesium carbonate and developed an oleophilic sorbent for removing oil from water. Scanning electron microscope (SEM), Fourier transform infrared spectroscopy and X-ray diffraction were used for the characterization of prepared material. The sorbent exhibited the contact angle of $154^\circ \pm 1$ indicating superhydrophobic character. Oil sorption studies demonstrated that the material was able to scavenge oil three times its weight. The adsorption capacity for different oils such as crude oil, diesel oil and kerosene oil was 3.593g/g, 3.017g/g and 3.350g/g respectively [110]. J. Lin et al. (2012) developed nanoporous polystyrene (PS) fibers as a sorbent material with high sorption capacity and high selectivity using one step electrospinning process. Results showed that the proposed material exhibited excellent sorption capacity for motor oil as well as for edible oils, which is 3-4 times greater than natural sorbents and polypropylene based mats already in use. Different surface morphologies of PS fibers exhibited different response towards oil sorption. For instance,

porous fibers with rough surface and small diameter showed larger sorption capability than PS fibers with smooth surface and large diameter. They concluded that the mechanism of oil sorption with porous PS fibers might be through capillary action, adsorption or the combination of both [111]. Experimental work by A. Siddiqa and co-workers (2015) demonstrated the synthesis of porous and low density carbon nanotubes (CNT) sponge decorated with silicon dioxide (SiO_2) via chemical vapor deposition. They reported the adsorption capacity of CNT sponges ranging from 128.3 to 185 wt % for oils and organic solvents. The recyclability of the adsorbent material was also examined [112]. M. Khosravi and S. Azizian (2015) reported the synthesis of oleophilic polypyrrole and palmitic acid (PPy-PA) sponge for oil spill cleanup. The prepared sponge exhibited the recoverability of sorbed oil when subjected to mechanical pressure. The results indicated that large amount of oil can easily be separated hence offering potential to be used at large scale to remove oil and organic contaminants in water bodies [113]. K.G. Raj and P.A. Joy prepared a magnetic composite using activated carbon based on coconut shell and iron oxide magnetic nanoparticles. The material showed excellent oil retention capability, recoverability as well as reusability which contributed to its cost effectiveness. The oil water separation process involving this material is fast and economical [114]. P.M. Reddy et al (2016) fabricated iron oxide (Fe_3O_4) nanospheres grafted with polystyrene and poly (butyl acrylate) polymers. The former showed oil removal efficiency greater than poly (butyl acrylate). The materials showed excellent oil-water separation process and reusability. The major advantage associated with these materials was its convenient removal from water after oil sorption i.e. separation by magnet [115].

1.7 Literature review on the implication of organoclays for oil spill removal

M.F. Mota et al (2014) presented an experimental study in which quaternary ammonium salts, alkyl dimethyl benzyl ammonium chloride (ADMBAC) and distearyl dimethyl ammonium chloride (DSDMAC) were used to modify clay for use as adsorbent for removing oil from oil-water emulsion. The performance of exchange reactions and affinity for oil products were examined using various characterization techniques involving XRD and IR and expansion tests such as Foster swelling and adsorption capacity measurements. The change in basal spacing from 1.56nm (unmodified clay) to 1.96nm (for DSDMAC) and 2.25nm (for ADMBAC) was observed for modified clay. IR results also confirmed the successful incorporation of organic cations between silicate layers. The expansion test revealed that organoclays possess high capacity for oil adsorption than unmodified one [116]. Rodrigues et al. (2010) examined the swelling capacity of Brazilian organoclay in various oil products of petroleum industry. The modification of clay was carried out by distearyl dimethyl ammonium chloride (DSDMAC). The increase in basal spacing was verified by XRD indicating the appropriate intercalation of organic modifier between the layers [117]. Queiroz et al. (2010) modified Bragel and gray clay with cetyltrimethyl ammonium bromide. Expansion tests demonstrated the compatibility and affinity of modified clays with petroleum products [118]. The performance of organophilic clay modified with alkyl dimethyl benzyl ammonium chloride for oil water separation process was evaluated by Mota et al (2011). The high potential of adsorbent for oil removal was given by its removal efficiency which was 95% whereas material showed 38mg/g removal capacity [119]. C. Bertagnolli and M.G.C. da Silva organophilized bentonite clay with cetyl pyridium chloride and Benzalkonium chloride for sorption of petroleum fuels

and organic solvents such as toluene, xylene and benzene [120]. Pereira et al (2005) prepared organophilic clay with cetyltrimethyl ammonium chloride and characterized using X-ray diffraction and infrared spectroscopy. The results deduced the compatibility of modified clay with petroleum fuels [121]. H. Moazed and T. Viraraghavan used powdered organoclay derived from bentonite for removing oil from water. Based on the tests for estimating oil removal efficiency they concluded that 100% removal of oil from oil-water system might be achieved [122]. O. Carmody et al modified Na⁺-MMT with octadecyltrimethylammonium bromide with one long C₁₈ chain, didecyldimethylammonium bromide (two long C₁₈ chain) and di (hydrogenated tallow) dimethylammonium chloride and was evaluated for adsorption of hydrocarbons. Burns et al. (2003) studied the retention and adsorption capacity for gasoline hydrocarbons with the application of bentonite clay. The hydrophilic nature of clay was changed to oleophilic via the intercalation of hexadecyltrimethylammonium and triethylbenzylammonium cations through cation exchange reaction. Another work presented by A.C. Gonzaga et al (2007) also involved the use of cetyltrimethylammonium as organic modifier. Bentonite clay after organic modification exhibited compatibility with petroleum hydrocarbons, alcohols and other organic solvents including toluene and acetone [123].

1.8 Motivation

As an important source of energy, petroleum oil and its derivatives are essential in the modern world. With the development of global economy, the demand for oil is growing day by day. The harmful and long term impacts of oil spill on environment as well as economy cannot be overemphasized. As a major environmental issue it grabs the attention of researchers, environmentalists and petroleum industry. Among various cleanup strategies, the use of sorbents materials is a fascinating alternative owing to its simplicity and cost effectiveness, reusability and high sorption capacity. In the present research work, a new composite system is synthesized as candidate sorbent for oil spill cleanup, combining the porosity and adsorption ability of clay-polymer composites. This study paved the way towards the development of a novel nanocomposite material which possesses maximum adsorption capacity for petroleum and its derivatives and low water affinity; therefore it can be used to selectively remove oil from water.

Chapter 2

Experimental and Characterization

Techniques

This study deals with the design and execution of experiments related to the preparation of polymer-clay nanocomposites for oil spill cleanup processes. The objective was to develop a novel material possessing maximum adsorption capacity for petroleum and its derivatives and low water affinity to selectively remove oil from water.

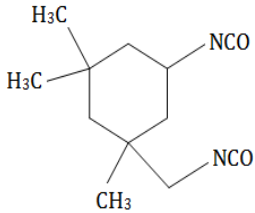

Montmorillonite was used as reinforced phase while polyurea was employed as the matrix phase. To avoid interfacial problems between the two phases, organic modification as well as chemical functionalization of clay was carried out, prior to use in nanocomposites formation.

2.1. Materials

Chemicals required for synthesis of organoclay, chemical functionalization and grafting of polyurea onto organoclays are given in table 2.1. All the chemicals were of analytical grades and used without further purification.

Table 2.1: List of chemicals and reagents used for synthesis of nanocomposites

| Chemical Name | Chemical Structure | Supplier | Purity (%) |
|-----------------------------------------|-----------------------------------------------------------------------------------------------|----------|------------|
| Dodecylamine (DDA) | $\text{CH}_3(\text{CH}_2)_{11}\text{NH}_2$ | Aldrich | 98.0 |
| Montmorillonite (MMT) (K-10 powder) | $\text{Na}_{0.33}((\text{Al}_{1.67}\text{Mg}_{0.33})(\text{OH})_2(\text{Si}_4\text{O}_{10}))$ | Aldrich | - |
| Hydrochloric acid | HCl | Aldrich | 37 |
| Distilled water | H_2O | - | - |

| | | | |
|--------------------------------------|--------------------------------------------------------------------------------------------------|-----------------|-------|
| Silver nitrate | AgNO ₃ | Aldrich | ≥99.0 |
| 3-Aminopropyltriethoxysilane (APTES) | H ₂ N(CH ₂) ₃ Si(OC ₂ H ₅) ₃ | Merck | ≥98.0 |
| Ethanol | CH ₃ CH ₂ OH | | 99.0 |
| Isophorone diisocyanate (IPDI) |  | Aldrich | 98.0 |
| n-Hexane |  | Lab- scan (A.R) | 99.0 |
| Sodium chloride | NaCl | - | - |
| Calcium chloride (anhydrous) | CaCl ₂ | Fluka | ≥93.0 |
| Gasoline, Kerosene | - | - | - |
| Furnace oil, Diesel | - | - | - |

2.2. Intercalation of Montmorillonite

For organic modification of montmorillonite, long chain alkyl amine was used as intercalating agent. The intercalation reaction was accomplished in aqueous medium through ion exchange method (Figure 2.1). Organic cations act as vertical support to keep the aluminosilicate layers separate, thereby increasing the d-spacing. In a typical procedure, the ammonium salt of intercalating agent was prepared by slow addition of concentrated hydrochloric acid to dodecylamine and then water was added; the resulting solution was heated at 80°C. In a separate beaker, montmorillonite was dispersed in water at 80°C. The suspension of layered

silicates was added to the solution of ammonium salt of intercalating agent with vigorous stirring for 3 hours at 60°C. The precipitates of organoclay were isolated and washed with water several times to ensure the removal of residual ammonium salt. The complete removal of chloride ion was determined by titration of filtrate with AgNO₃ after each washing, until there were no AgCl precipitates. Finally the product was dried in vacuum oven for 24 hours at 60°C. The dried cake was grounded to powder and abbreviated as OMMT.

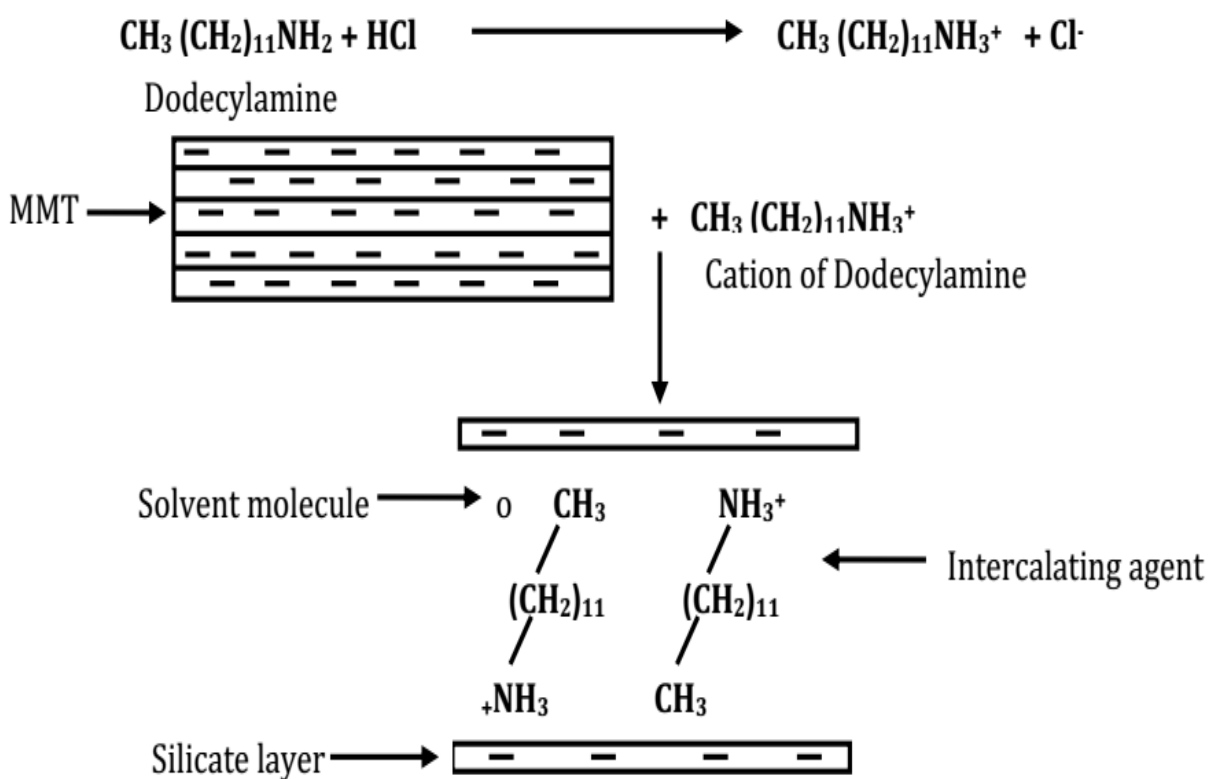


Figure 2.1: Scheme for organic modification of Montmorillonite

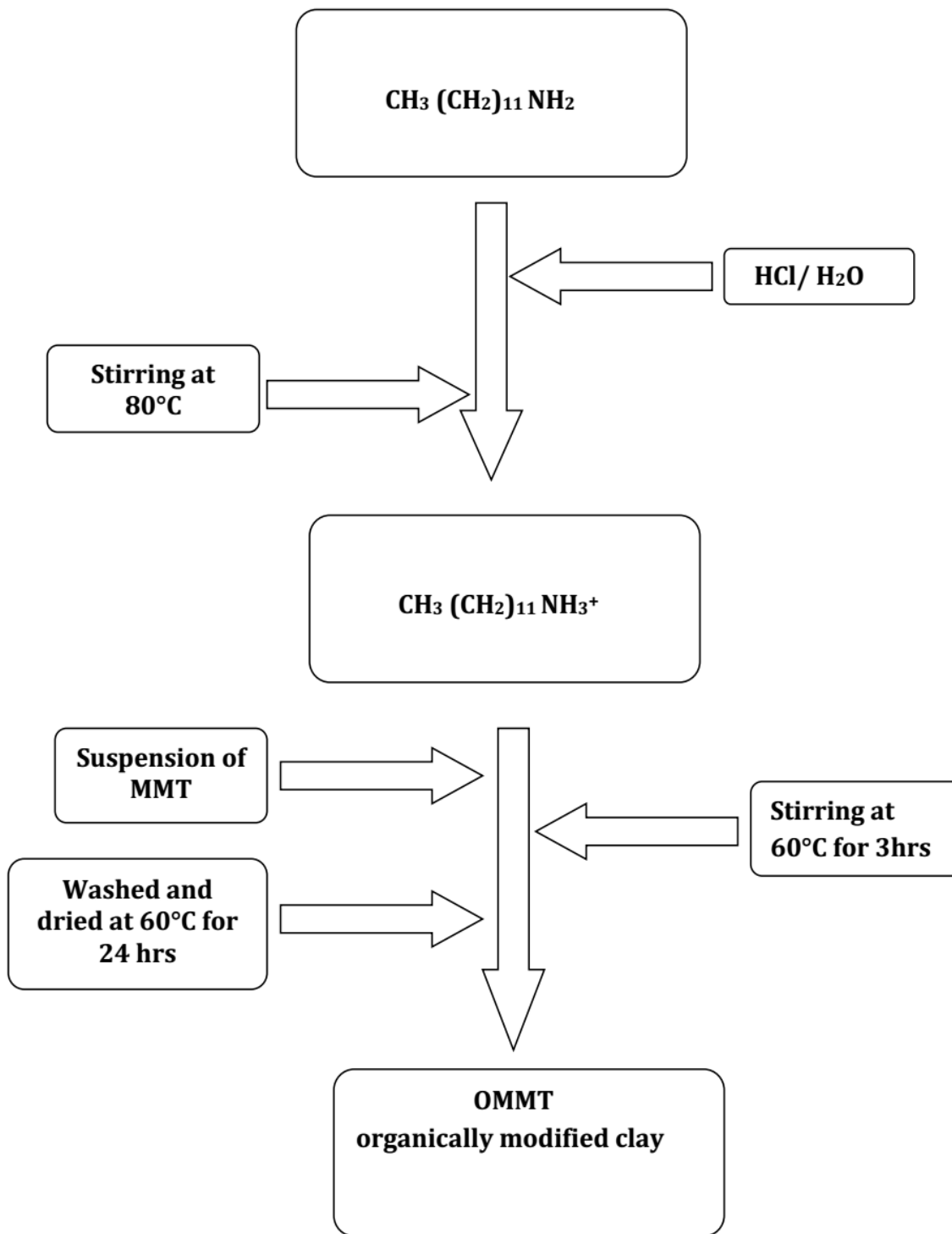


Figure 2.2: Scheme for synthesis of organically modified montmorillonite

2.3. Silane functionalization of Organo-Clay

Hydroxyl groups present on the surface and edges of montmorillonite have been utilized for silane grafting. During grafting reaction, 2.5g of O-MMT was added in a flask followed by addition of ethanol/water solution mixture under stirring. 2.0g of APTES was introduced after complete dispersion of O-MMT. The mixture was stirred for 8hrs at 80°C. Resultant product was washed with mixture of ethanol and water a number of times to remove the unreacted silane, dried at 60°C in a vacuum oven for 24 hrs. Silane functionalized organoclay is abbreviated as OS-MMT. The scheme for the reaction is given in figure 2.3.

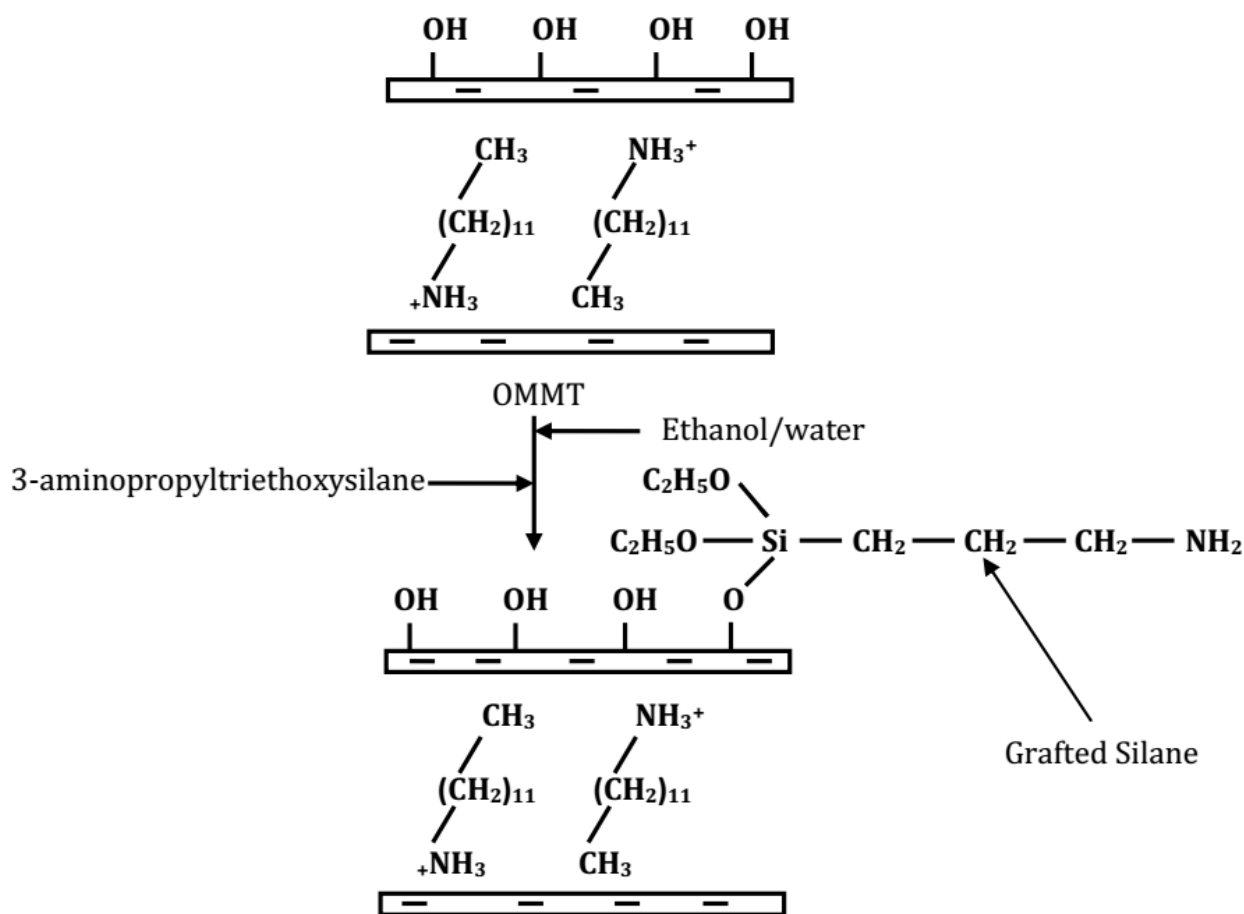


Figure 2.3: Scheme for chemical functionalization of O-MMT

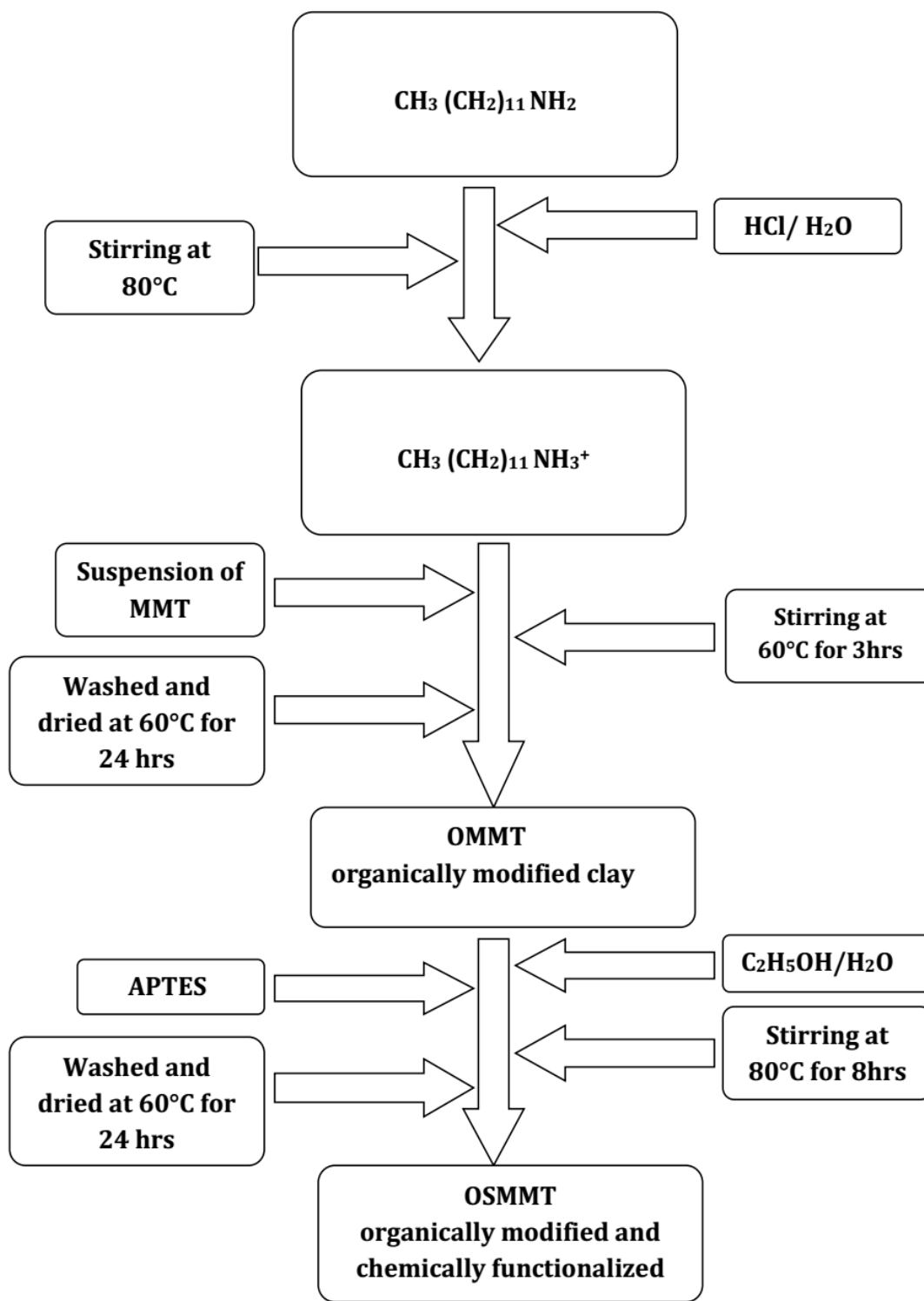


Figure 2.4: Scheme for synthesis of organically modified and chemically functionalized montmorillonite

2.4. Synthesis of Polymer-Clay nanocomposites

Polymer-clay nanocomposites were synthesized by adding pre-calculated amount of OSMMT in 30mL of n-hexane to reaction flask. A calculated amount of isophorone diisocyanate (IPDI) was added drop wise to reaction mixture as polyurea precursor. The dispersion of clay platelets in the matrix was carried out with constant high speed stirring for 72 hrs at room temperature. Nanocomposites of different compositions were prepared with varying amount of nanoclay and monomer as given in the table 2.2 using the same procedure. The reaction mixture was then poured into Petri dish and the solvent was allowed to evaporate at room temperature. Finally, the products were left to dry at room temperature for 2-3 days. Possible interaction between the two phases is given in figure 2.5.

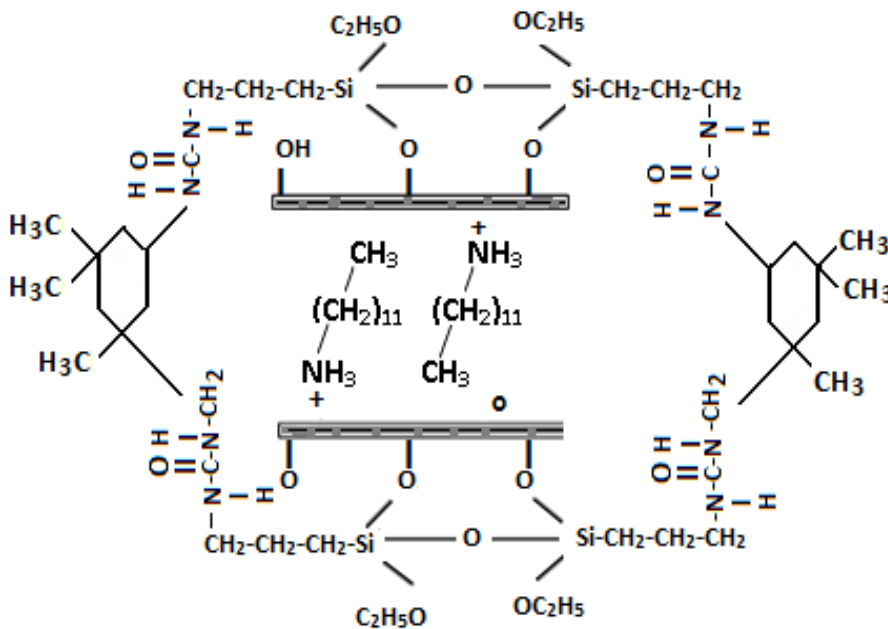


Figure 2.5: Scheme for possible interaction between polyurea matrix and organoclay reinforcement

Table 2.2: Compositions of Polyurea/organoclay nanocomposites

| Nanocomposite system | Sample ID or Code | Organoclay content | | Monomer content | |
|----------------------|-------------------|--------------------|------------|-----------------|------------|
| | | Wt% | Amount (g) | Wt% | Amount (g) |
| Nanocomposite A | PCN-10% | 10 | 0.1 | 90 | 0.9 |
| Nanocomposite B | PCN-30% | 30 | 0.3 | 70 | 0.7 |
| Nanocomposite C | PCN-50% | 50 | 0.5 | 50 | 0.5 |
| Nanocomposite D | PCN-70% | 70 | 0.7 | 30 | 0.3 |
| Nanocomposite E | PCN-90% | 90 | 0.9 | 10 | 0.1 |

PCN (Polymer-clay nanocomposite)

2.5. Characterization Techniques

Characterization of polymer clay nanocomposites has been performed to study their compositions, structure, surface and internal morphology, thermal properties and wetting behavior. Brief description on each technique employed is given below.

2.5.1 X-Ray Diffraction

Materials are composed of atoms. The arrangement of these atoms into crystal structure and the microstructure provides the foundations for understanding the synthesis, structure and properties of materials [124]. For qualitative and quantitative analysis of crystalline materials, X-ray diffraction is an important non-destructive technique which reveals information about phase identification, crystallinity, crystallite size, molecular orientation, order and structure etc. of materials [125,126]. Since the X-ray diffraction pattern is like fingerprint for a substance, it is possible to unambiguously identify a material by obtaining its diffraction pattern. According to A.W. Hull, "every crystalline material gives a pattern; the same substance always gives same pattern, while in a mixture of substances each produces pattern characteristic of it" [127].

X-rays are electromagnetic radiations of high energy (ranging from around 100eV to 10MeV) or shorter wavelength (10 to 10^{-3} nm), X-rays with their wavelength comparable to interplanar distance are diffracted by the regular planes of atoms and are called short wavelength or hard X-rays [128-129]. The essential components of X-ray diffractometer are: X-ray tube, optics, goniometer, sample holder and detector. In an X-ray tube, high voltage is applied between two electrodes. Cathode produces electrons with sufficient kinetic energies by thermionic effect. The accelerated electrons collide with the anode (metallic target) and X-rays are produced. While interacting with the target material, the deceleration of every electron is not in the same way, some of the incident electrons lose fractions of their total kinetic energy gradually until it is all spent. This process results in Bremsstrahlung or continuous spectrum. On the other hand, some of the electrons are capable of dislodging one of the inner shell electrons, creating a vacancy through impact ionization. An electron from outer shell fills the vacancy and produces X-rays. Since their wavelengths are characteristics of the target material they are called characteristic lines, being superimposed on continuous spectrum [130-131].

Thomson scattering is basically elastic scattering of incoming X-rays by electrons. The oscillating electric field of incident X-rays gives the electrons a sinusoidal change. Due to periodic acceleration and deceleration of electrons, there is generation of a new X-ray with the same wavelength as that of incident one. Thomson scattering of X-rays serves the basis for structural investigation by X-ray diffraction. The nucleus of an atom is relatively heavy and cannot be accelerated or decelerated by the X-ray beam. The scattering ability of an atom depends only on electrons, their number and distribution. The electrons around the atom start to oscillate with the same frequency as the incoming X-rays beam. In almost all

directions, there will be destructive interference as the diffracted waves are out of phase and there will be no resulting energy leaving the solid sample. While in case of crystals, there is regular arrangement of atoms, there will be constructive interference of scattered waves in few directions. The diffracted X-ray beam leaving the sample is considered as a beam composed of scattered rays that are in phase and hence reinforce each other [132]. Instead of considering the diffraction of a single electron, Bragg assumed the scattering of x-rays from the adjacent planes of atoms in a perfect crystal.

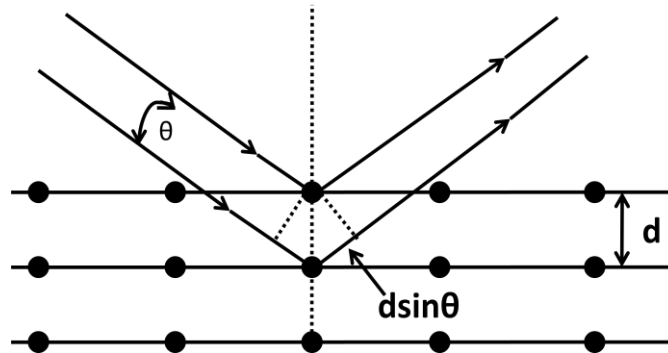


Figure 2.6: Diffraction of X-rays by crystal

The planes of atom in a crystal are separated by a distance **d**. When monochromatic x-rays having wavelength λ encounter the atoms in adjacent layers, constructive interference will take place in the directions where the path difference between the scattered waves is multiple integer of λ thus satisfying

$$n\lambda = 2d \sin \theta \quad (\text{eq.2.1})$$

Where n is the integer and θ is the diffraction angle that can be defined as the angle between the incident beam and plane of the crystal while the angle between incident and diffracted beam is 2θ [133, 134].

There is overwhelming geometrical relationship between the direction of constructively interfering waves (forming diffraction pattern) and the crystal structure. The regular arrangement of atoms over long repeat distance causes X-ray diffraction at small angle, on the other hand, short repeat distances cause diffraction at high angles. Similarly the perfect crystals with long range order give sharp and clear diffraction peaks. While the defects like impurities, planar faults and strains etc in the crystal structure make less precise atomic arrangements. They have distinct but broad, distorted and weak diffraction peaks. The diffraction pattern of amorphous materials lacks sharp peaks.

Three essential components of diffractometer are X-ray tube, sample holder and detector lying on the perimeter of a circle. X-ray source is fixed in its position while the detector is attached to the 2θ axis. Flat powder sample is usually placed on the ω axis parallel to X-ray Source. While taking the measurements, 2θ axis rotates twice of the ω axis therefore generally referred as two-theta scan.

There are five basic parameters that associated with the X-ray diffraction peak including peak position, peak shape, full width half maxima, maxim intensity and symmetry each with different physical meanings. According to Bragg's equation, when the wavelength of X-ray beam is fixed, the peak position corresponds to the distance (d) between the reflection planes (hkl). To resolve the peak positions following methods are used a) direct determination of peak position from diffraction angle at maximum b) determination of peak position from

diffraction angle at maximum after smoothing c) fitting of measured line using mathematic functions. Scherrer formula explains the broadening of diffraction peak of crystalline material.

$$D = K \lambda / \beta \cos \theta \quad (\text{eq. 2.2})$$

A broadening peak can be used to calculate the particle size. The **K** (Shape factor) depends on the crystal form and index **hkl**. Full width at half maximum (FWHM) allows us to evaluate the crystallite size more precisely as it contains the meaning of average dimension of crystalline material. The shape of peak indicates the contribution from crystallite size and strain because it is the function of domain size and lattice strain [135]. The anatomy of a XRD pattern is given in the Fig 2.7.

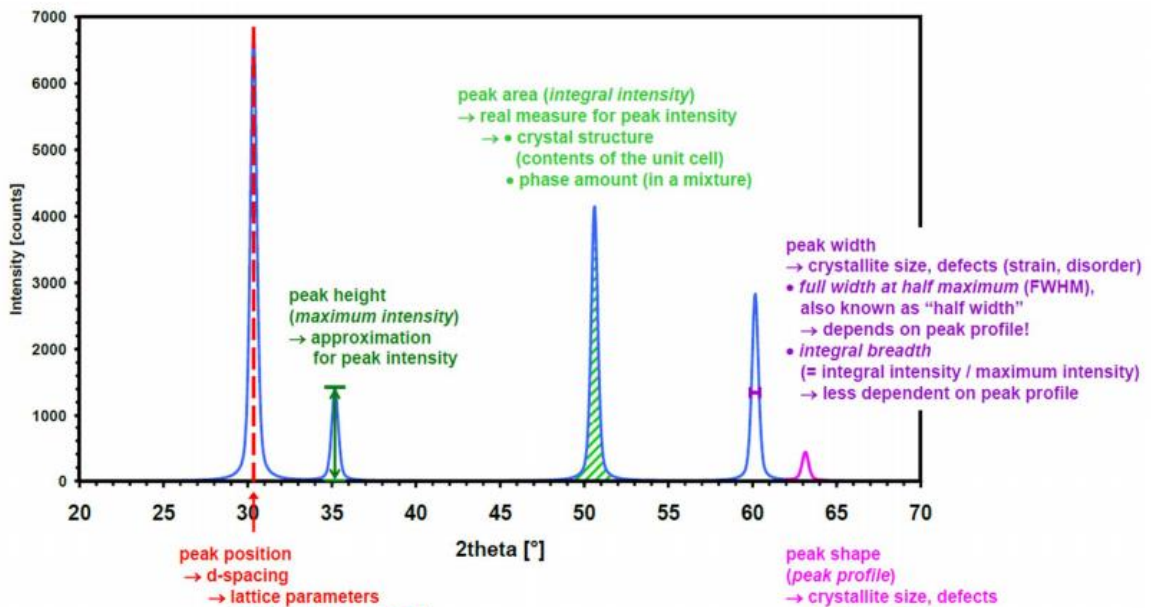


Figure 2.7: Graphical representation of an XRD pattern showing its basic features with their physical meanings

To determine the unit cell parameters from the peak positions miller indices **hkl** are assigned to each peak. This is called indexing process and is always the first step in analysis. Without

performing the indexing, it is not possible to analyze the diffraction pattern. For high symmetry structures indexing can be done manually, however, for low symmetry structures it becomes impossible to index the diffraction pattern by hand and auto indexing is carried out through computer algorithm. For indexing the peaks, θ values corresponding to each peak are obtained and then interplanar distance is calculated using Bragg's equation. For cubic system it is easy to convert the d-spacing into lattice parameter while in case of non cubic systems number of unknown parameters increases [124].

2.5.2 Scanning electron microscope

The optical microscope was used initially which provide the resolutions of specimen around 0.2 μm . For high resolutions, an electron source is used instead of light for illumination.

The advantage of using electrons over light source is not only the better resolution but as a result of interaction between electron beam and specimen variety of signals are generated, providing information characteristic of the specimen [136, 137]. Scanning electron microscope is the most common form of electron microscope pioneered by Charles Oatley and co-workers in late 1980s. The ease of interpretation of micrographs, diversity of information generated, two and three dimensional quantitative analysis of microstructure, crystallography, chemistry and the electronic properties makes it the most versatile and widely used characterization technique worldwide [138].

A thermionic or field emission cathode accelerates the electrons between electrodes by a voltage of 1-50 kV. The smallest beam cross section is demagnified by a series of electron lenses system that acts to control the diameter of the beam and focus it on the specimen. As a result, a small and focused electron probe is used to scan the surface of the specimen with the aid of scanning coils. Signals in the form of electromagnetic radiations are emitted from each

point that is struck by the accelerated electrons. Detectors are used to collect the selected portions of electromagnetic radiations usually secondary and back scattered electrons. Resulting signal is amplified and displayed. Image obtained is used to interpret topographic information of the objects [139]. The following fig. 2.8 shows the main components as well as the working principle of a typical SEM.

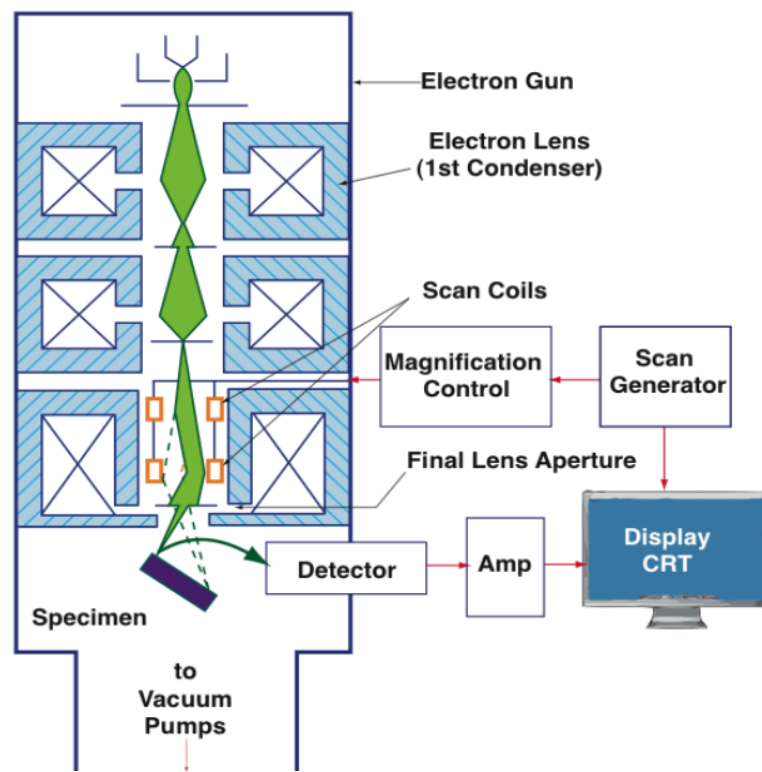


Figure 2.8: Main components and working principle of a typical SEM instrument

The main components of a typical SEM include an electron optical system (electron column) to produce an electron probe, stage to place the specimen, a secondary detector, a display unit and for performing various operations, an operating system is required. The electron optical system is further comprised of an electron gun, condenser and objective lens and to scan the

electron probe on the specimen surface scanning coils are also present with other components. Vacuum system is used to keep the optical system and the space surrounding the sample at vacuum. The detail of each component is given in following sections.

a) Electron gun

Electron gun is used to produce a stable electron beam having adjustable energy. There are three types of electron gun used in the electron column: tungsten hairpin & lanthanum hexaboride (LaB_6) filaments also called thermionic emission guns and field emission gun. When a filament (cathode) made of thin tungsten wire is heated at high temperature about 2800K, thermoelectrons are emitted from its tip and form an electron beam. Single crystal LaB_6 can be used as cathode, also work by thermionic emission. It offers several advantages such as larger maximum beam current and greater lifetime than tungsten filaments. However these filaments are expensive and requires high vacuum because of their high activity.

Cold cathode or field emission guns consist of a sharp metal tip which produces the brightest beam. A potential difference is applied between the tip and first anode. An electric field being concentrated at the tip facilitates the emission of electrons [140- 141].

b) Electromagnetic Lenses

For SEM analysis, a fine electron beam is required. Therefore, two stage magnetic lenses (condenser and objective lenses) are used, located below the electron gun for adjusting the diameter and current of electron beam. A thin metal plate “aperture” with a small hole is placed before and after the objective and condenser lens respectively. The electron beam after passing through the condenser lens illuminates the aperture which allows a fraction of

electron beam to reach the objective lens. The best performance of objective is vital as it is used for focusing and determining the final diameter of electron probe [142].

c) Specimen Stage

A specimen stage enables the placing of sample for analysis. It is responsible to support and move the sample smoothly. It offers various movements for specimen such as horizontal (X), vertical (Y), tilting and rotation.

d) Secondary electron detector and display unit

For detection of secondary electrons emitted from specimen, secondary electron detector is used. A fluorescent material is coated on the detector tip and a voltage is applied to it. When the secondary electrons from the specimen hit the scintillator light is generated. This light is converted to electrons which are amplified as electric signal. Most of the time, this detector is incorporated in the specimen chamber of SEM.

When the incident electron beam strikes the specimen, the accelerating electrons interact either elastically or inelastically with the electric field of both the nucleus and electrons of the specimen. The three dimensional region of interaction between the specimen and incident electron beam is responsible for diversity of signals emerging from it such as backscattered electrons (BSE), secondary electrons (SE), characteristics and continuous X-rays, auger electrons and cathodoluminescence etc [143] given in fig.2.9.

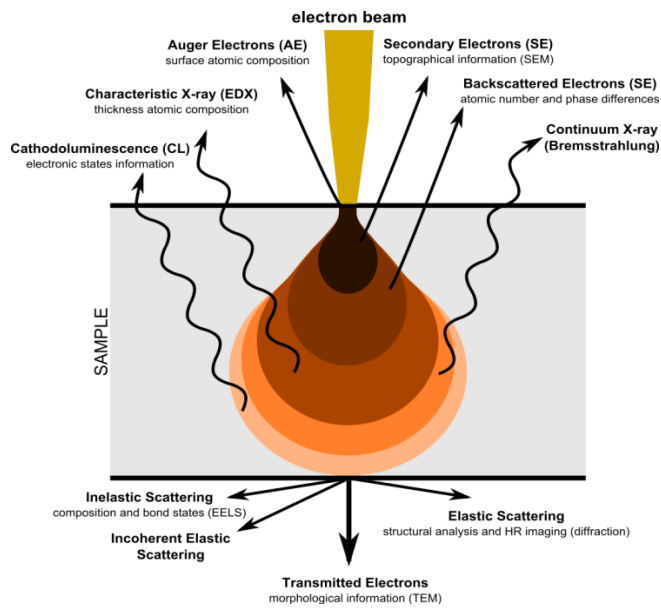


Figure 2.9: Interaction of incident electron beam with the specimen

For visual inspection of the material, two types of signals are utilized: secondary electrons and backscattered electrons. Both types of electrons are constantly produced from the surface of sample but they have distinct interaction. Secondary electrons are produced as a result of inelastic collision, usually knocked out from the orbits by incident electron beam. They give topographic information about the specimen surface with a resolution of $\sim 10\text{nm}$. Those incident electrons after approaching the nucleus are scattered through a large angle and re-emerge from the surface; these are called back scattered electrons (BSE). BSE are generated further from the surface of the material thus revealing the compositional, crystallographic information etc. Among the various other types of signals generated as a result of interaction between specimen and incident electron beam X-ray signals is used for SEM. Elemental composition of the specimen can be exposed by the measurement of the energies of characteristic X-rays detected by energy dispersive or wavelength dispersive spectrometer.

Energy dispersive X-ray spectroscopy EDX or EDS simultaneously analyze the X-rays from a wide range of elements and provides the qualitative analysis about the specimen [140, 144].

2.5.3 Infrared Spectroscopy

Infrared spectroscopy is one of the most important structural analysis techniques, based on the vibrational modes of the atoms of a molecule. If the vibration causes change in the electric dipole moment of the vibrating molecule, infrared energy will be absorbed at a frequency corresponding to the frequency of bond in the molecule. The spectral range of IR is divided into three regions: near IR ranging from 1 to 2.5 μm is used for quantitative analysis because it is poor in specific absorptions. Mid IR region (2.5 to 50 μm) it provides much information about the structures of compounds and is used for identification of functional groups. Far IR region (beyond 25 μm) requires specialized optics and sources [145-146].

Infrared spectrum is recorded in the form of wavenumber vs. absorbance or transmittance when a beam of infrared light from the source irradiates the sample. If the frequency of incident IR matches the vibrational frequency of bond, the electrons in the vibrational energy levels get excited. Upon de-excitation, emission of photons of characteristic wavelengths takes place. The energy of these photons is calculated and the spectrum is recorded, showing the IR wavelength where the sample absorbs. The interpretation of spectrum is easy because the bands appearing can be assigned to particular group frequencies [147].

Fourier transform infrared spectrometer is commonly used to perform the infrared spectroscopy. The interference of radiation between two beams yields an interferogram. Interferogram is the signal produced due to change of path length between two beams. Fourier transformation (mathematical method) is used to convert the domains of distance and

frequency to one another. Double beam dispersive spectrum can be obtained by producing an interferogram with and without the sample placed in the path of beam. The interferogram is then converted to spectra with and without sample absorptions. The ratio of both corresponds to double beam dispersive spectrum [148].

2.5.4 UV-Visible Spectroscopy

UV-visible spectroscopy is a quantitative technique which deals with the absorption of electromagnetic radiations by the sample in the ultraviolet and visible region ranging from 190nm to 380nm of spectrum. UV-visible radiations absorb by a molecule cause transitions in electronic energy levels, that's why this technique is also termed as electronic spectroscopy [149]. As molecule absorbs UV-visible radiations, an electron from HOMO (bonding σ or π) gain energy and promote to LUMO (antibonding π^* or σ^*) [150]. In case of highest occupied molecular orbital, sigma electrons are at low energy level as compared to π , non-bonding and antibonding LUMO which are at high energy level. In UV-visible Spectrum one or more well defined peaks appear, correspond to electronic transition from one level to another level and all these transitions require a fix amount of energy [151].

The working principle of UV-visible spectroscopy is based on Beer's Lambert law which relates the absorption of radiations with the concentration of absorbing molecules and path length of radiation. If there are large number of molecules greater will be the absorption of incoming radiation and greater will be the intensity of peak. The amount of radiations absorb by solute molecules in solution is an exponent function of concentration of solute and path length over which the absorption takes place. Therefore,

$$\log \frac{I}{I_0} = \epsilon cl \quad (\text{eq. 2.3})$$

Where I_0 is the intensity of incident radiations, I is the transmitted radiations, c is the concentration of solute, l is the path length and ϵ is the molar absorptivity coefficient. Where as $\log \frac{I}{I_0} = \text{absorption}$ so equation 2.3 becomes

$$A = \epsilon cl \quad \text{(eq. 2.4)}$$

Major components of UV-visible spectrophotometer include: light source, monochromator, sample holder and detector. The light source is deuterium or hydrogen lamp for UV-region (190-380nm) and tungsten lamp for visible region. Light of different source then passed through monochromator to select light of single wavelength by prism or diffracting grating. The essential parts of monochromator are entrance slit, collimating device (to produce parallel light), a wavelength selector, a focusing lens or mirror and an exit slit. The monochromator beam is then pass through cuvette made up of quartz or a glass. Quartz is normally used in UV region and is transparent to all regions. Glass cuvette can be used in visible region. The reference and sample beam then pass to photocell to detect transmitted radiations and recorded by spectrometer to observe the difference between the reference and sample beam and gives spectrum between wavelength and absorption[152].

Chapter 3

Results and Discussions

The polyurea/clay nanocomposites were synthesized for selective removal of oil from water during an oil spill cleanup process. The polyurea matrix was reinforced with organoclay to form nanocomposites. The nature of interactions between the two phases was confirmed with various characterization techniques including Fourier Transform Infrared (FTIR) Spectroscopy, X-ray diffraction (XRD), Scanning electron microscopy (SEM) and Thermal gravimetric analysis (TGA). While the adsorption capacities of clay based polymeric composites were evaluated with the help of UV-Visible spectroscopy and various expansion tests.

3.1 X-Ray Diffraction Analysis

The diffraction behavior of various types of clay and synthesized nanocomposite materials was studied with the help of x-ray diffraction technique using Rigaku X-ray diffractometer with Cu K α radiation source (wavelength of radiation, $\lambda=0.514\text{nm}$) equipped with graphite Monochromator. The diffraction data was recorded in a 2θ range of 2° to 80° with a step size of 0.04° at a step time of 1 second. Diffraction analysis was carried out at room temperature and under constant set of conditions.

In clay/polymer nanocomposites, low 2θ values in X-ray diffraction pattern facilitate the assessment of change in the d-spacing of the intercalated structures. Three possibilities are there; 1) non dispersion of reinforcement or formation of microstructure indicated by no change in characteristic peak, 2) shifting of peak towards low 2θ values signify the

intercalated structure present in the nanocomposite and 3) disorder or amorphous portion/structure in nanocomposites results in a broad peak or no characteristic peak.

3.1.1 X-Ray diffraction of various clay types

X-ray diffraction pattern for all types of clay including both modified and unmodified silicate layers is given in the following fig. 3.1. The diffraction peak at $2\theta = 8.84^\circ$ is assigned to (001) reflections, the basal or d-spacing of unmodified montmorillonite (MMT) come out to be **1.00nm** which is calculated using Bragg's equation [153]. After chemical functionalization of layered silicate with silane coupling agent, the significant increase in the interlayer space is observed. SMMT showed a peak at $2\theta = 6.75^\circ$ corresponding to d-spacing of **1.31nm**, this value is in agreement with the values already reported [154]. Peak attributed to d_{001} spacing shifted to left towards lower theta values provide evidence for incorporation of silane molecules between the clay stacking [155].

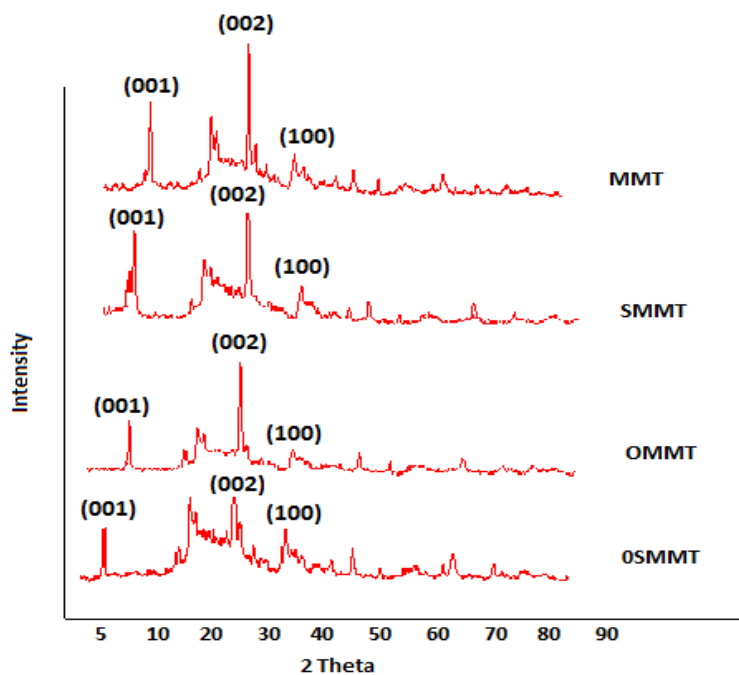


Figure 3.1: X-ray diffraction pattern for montmorillonite (MMT), silane functionalized montmorillonite (SMMT), chemically modified montmorillonite (OMMT) and organically modified and chemically functionalized montmorillonite (OSMMT).

The organic modification of montmorillonite with dodecylamine result in shifting of its diffraction peak to a new position at $2\theta=5.94^\circ$ corresponding to greater d-spacing i.e. **1.49nm**. Shifting of 001 reflection towards lower angle value confirmed the intercalation or organic modification of montmorillonite because large sized organic cations replaced the small sodium ions Na^+ present between the layers of clay minerals.

In case of organically modified and chemically functionalized montmorillonite (OSMMT), both the modifications acted in a collective way and result in an intense peak corresponding to 001 reflection at $2\theta= 5.3^\circ$. The d-spacing of OS-MMT is calculated as **1.67nm**. This showed grafting of aminosilane and intercalation of organic cations in the inter galleries of layered silicates offer low attractive forces between the montmorillonite layers which result in increase of distance between them. Table 3.1 shows the X-ray diffraction data for all types of clay at 001 reflection.

Table 3.1: XRD data for clays at (001) reflection

| Type of clay | 2θ (degree) | d-spacing (nm) |
|---------------------|--------------------------------------|-----------------------|
| MMT | 8.84° | 1.00 |
| SMMT | 6.75° | 1.31 |
| OMMT | 5.94° | 1.49 |
| OSMMT | 5.3° | 1.67 |

3.1.2 X-ray diffraction analysis of nanocomposites

X-ray diffraction patterns of nanocomposite systems contain the characteristic peaks of both the reinforcement and matrix phase. The diffraction patterns for different nanocomposite systems are given in the fig. 3.2.

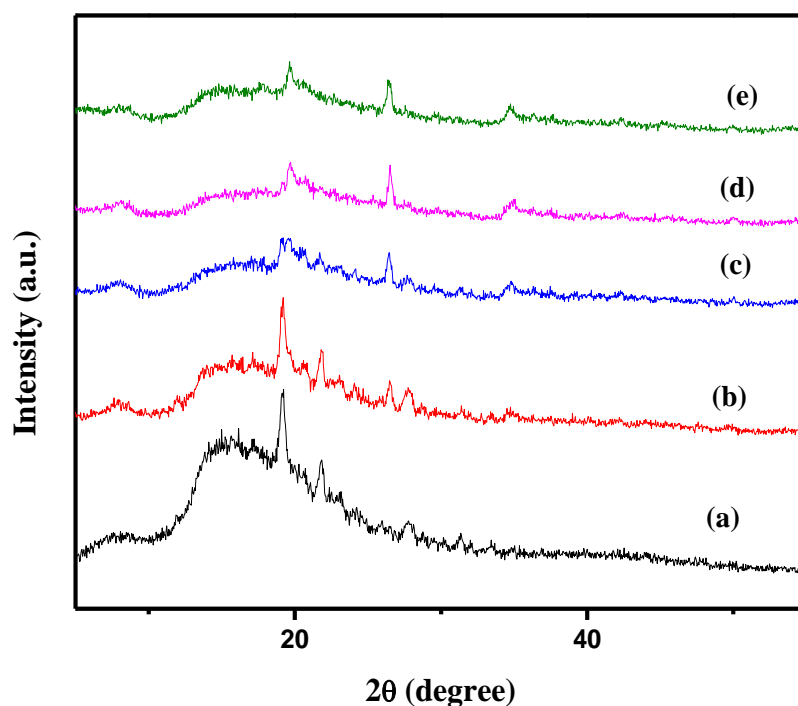


Figure 3.2: X-ray diffraction patterns for polymer/clay nanocomposites; a) PCN-90%, b) PCN-70%, c) PCN-50%, d) PCN-30% and e) PCN-10%.

The x-ray diffraction patterns of clay/polymer nanocomposites exhibit inadequacy of sharp peaks indicating the amorphous nature of polyurea matrix. Nanocomposite system PCN-70% and PCN-90%, exhibit relatively an intense peak at around $2\theta=20^\circ$, attributed to presence of modified montmorillonite which constitute 70 and 90% of the total weight of these

composites respectively. There is no peak at higher angle exhibited by other three nanocomposite systems because the hump of polymeric matrix overlapped the characteristic peaks of layered silicates.

For all nanocomposite system, there is no diffraction peak for 001 reflection plane below $2\theta=10^\circ$ which inferred that matrix phase get inserted into nanolayers of clay, whose interplanar distance was already increased through modification. Hence, it is evident from these observations that intercalated and exfoliated nanocomposites of polyurea/OS-MMT have been synthesized.

3.2 FT-IR Spectroscopic Analysis

For structural elucidation of various types of clay and resulting nanocomposites, FT-IR analysis was carried out using Alpha (BRUKER) spectrophotometer over the range of 4000-600 cm^{-1} at room temperature. No sample preparation was required as the instrument was equipped with ATR technique.

3.2.1 Pristine Montmorillonite (MMT)

The FT-IR spectra of unmodified clay exhibited several characteristic bands in different regions as shown in Fig. 3.3.

Montmorillonite gave a very intensive band at 1030 cm^{-1} attributed to in-plane stretching of Si-O of silicate layers. Bands at 3631 cm^{-1} and 797 cm^{-1} correspond to stretching and bending vibration of structural OH groups respectively. These bands affirmed the existence of hydroxyl groups on surface and edges of clay layers.

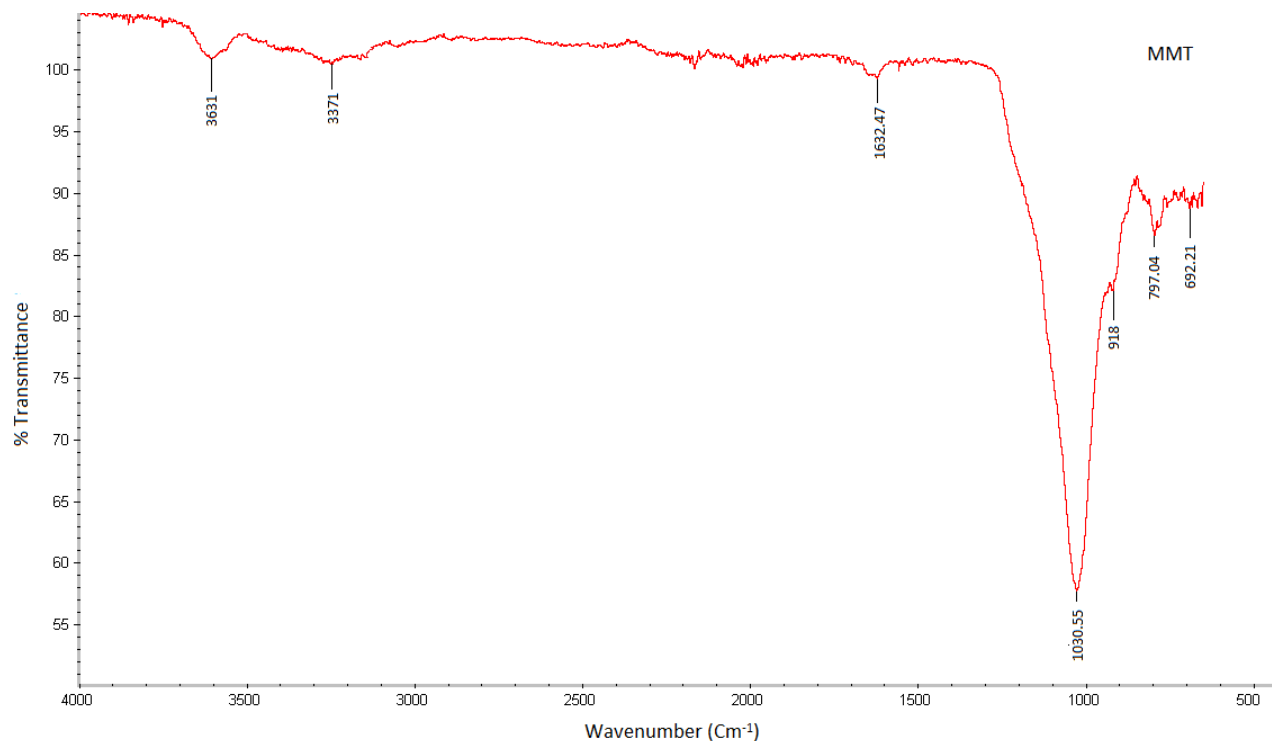


Figure 3.3: FT-IR spectrum of pristine Montmorillonite (MMT)

A relatively broad band at 3371 cm^{-1} show the stretching vibration of OH whereas a band at 1623 cm^{-1} indicate the bending vibration of OH of water molecules adsorbed in clay interlayer galleries. While a band corresponding to octahedral layers of aluminum silicate Al-O-Si appeared at about 918 cm^{-1} . The obtained results are in agreement with literature [156-158].

3.2.2 Organophilic Montmorillonite (OMMT)

The organic modification of montmorillonite was carried using alkyl ammonium salt. The FTIR Spectrum of organically modified montmorillonite (OMMT) is given in Fig. 3.4.

Organophilic clay exhibited two characteristic and closely placed bands at 2925 and 2851 cm^{-1} corresponding to aliphatic C-H asymmetric and symmetric stretching. The bending vibration of aliphatic C-H appeared at 1460 cm^{-1} . These bands provide the strong evidence for

successful intercalation of quaternary ammonium cations between the silicate layers [156,159].

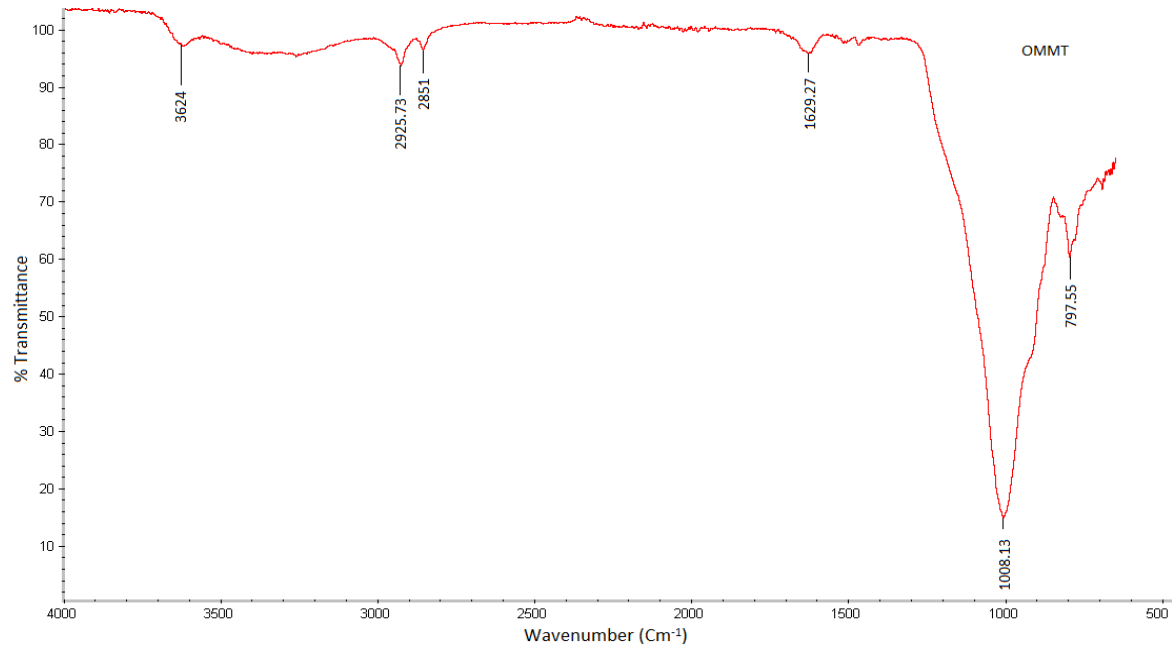


Figure 3.4: FT-IR spectrum of organically modified montmorillonite (OMMT)

A broad but less intense stretching band at 3286cm⁻¹ and a bending vibration at 1629cm⁻¹ are due to OH groups of water absorbed on clay. The decrease in intensity of stretching band of water's hydroxyl groups exhibited the weak or poor affinity of organo modified montmorillonite for water. Whereas the stretching vibration of structural OH groups appeared at 3624cm⁻¹ along with bending vibration at 797cm⁻¹. The most intense band at 1008cm⁻¹ is assigned to Si-O stretching of silicate layers. This band showed broadness and slight shift in its position as compared to that of unmodified clay. Organic modification might be the reason for this change where the small inorganic cations are replaced by bulky or large organic cations, resulting in an increase of basal spacing separating the silicate layers.

3.2.3 Silylated Montmorillonite (SMMT)

Hydroxyl groups present on the surface of montmorillonite have been exploited for silane grafting. The reaction was carried out in ethanol/water mixture with 3-aminopropyltriethoxysilane (APTES) employed as coupling agent. FT-IR spectrum of silane functionalized montmorillonite (SMMT) is given in Fig. 3.5.

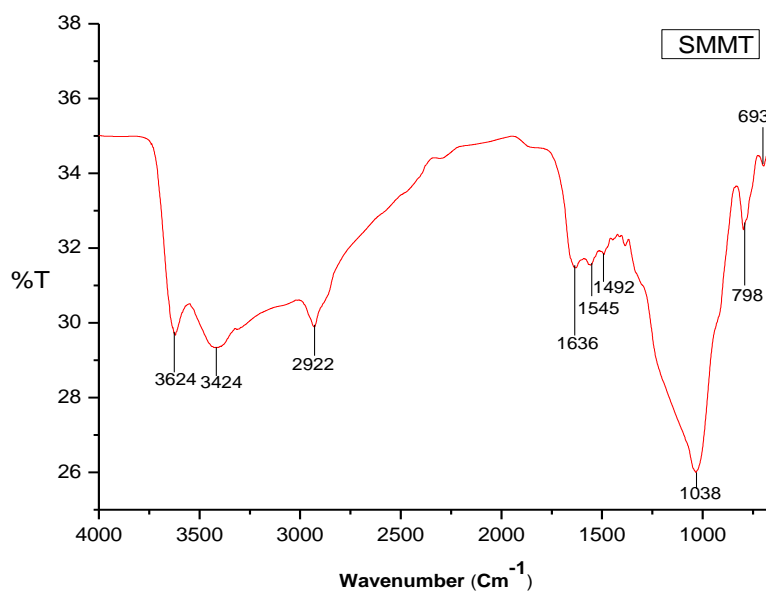


Figure 3.5: FT-IR spectrum for silane functionalized montmorillonite (SMMT)

The presence of APTES in the silylated product is evident with the band at 2922 cm⁻¹ which correspond to asymmetric stretching of -CH₂ of Propyl group present in the coupling agent. This was further confirmed with the appearance of band at 693 cm⁻¹ that indicate out of plane deformation for -CH [160]. The band appeared at 1545cm⁻¹ is assigned to bending vibration of N-H of amino group of APTES. The change in the shape and width of Si-O stretching was also observed together with frequency shift from 1030 cm⁻¹(unmodified clay) to 1038 cm⁻¹(silylated clay). All these bands provide strong evidence regarding the intercalation and

fruitful grafting of APTES on clay layers [160-161]. Again the stretching vibrations of structural hydroxyl groups were observed at 3624 cm^{-1} . However the change in shape and intensity of band can also be observed, indicating the grafting of silane with these groups. The band at 798 cm^{-1} is due to bending vibration of surface OH groups.

The absorption bands at 3424 cm^{-1} and 1636 cm^{-1} correspond to stretching and bending vibrations of OH group of absorbed water molecules, respectively.

3.2.4 Organo-modified and chemically functionalized Montmorillonite (OSMMT)

Organic modification with quaternary ammonium salt and chemical functionalization with silane coupling agent were carried out simultaneously to synthesized organically modified and silane functionalized MMT prior to use for nanocomposite synthesis. The following Fig. 3.6 shows the FTIR spectrum of OSMMT.

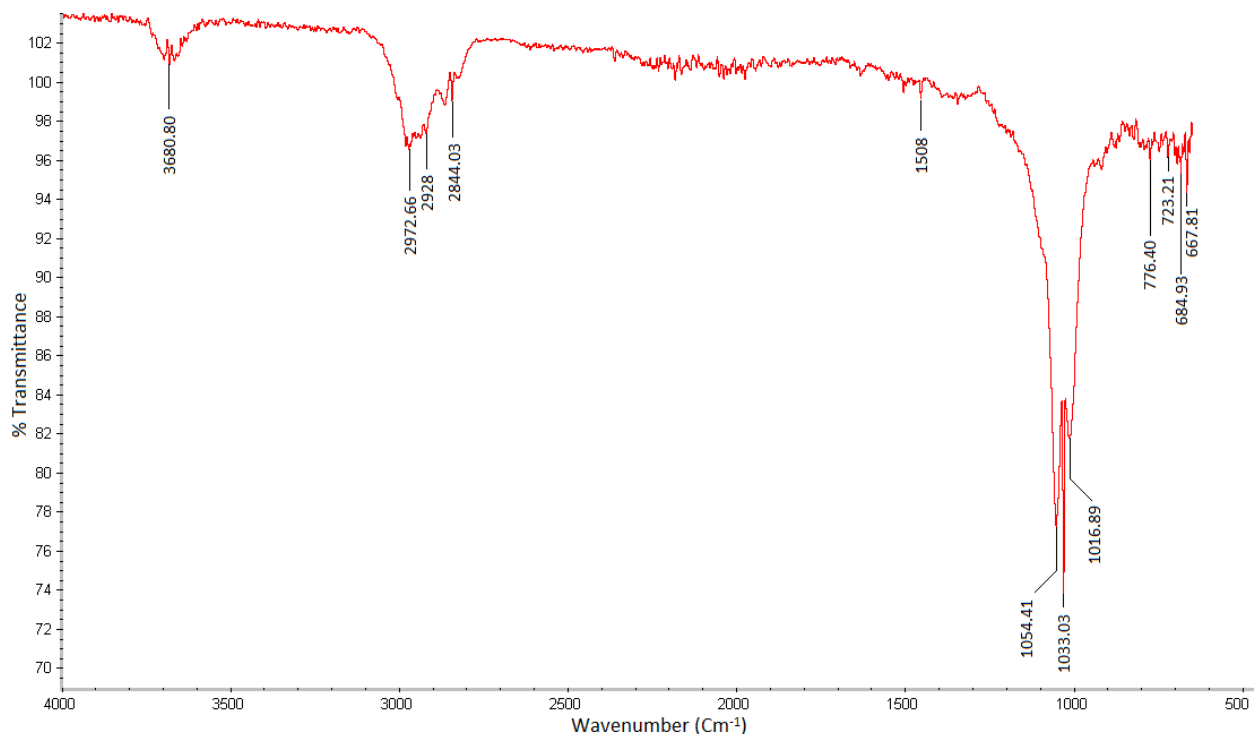


Figure 3.6: FT-IR spectrum of organically modified and silane functionalized montmorillonite

The presence of amino groups in the silicate network is confirmed with the appearance of weak band at 684cm^{-1} which indicate the bending of N-H bonds, whereas the symmetrical absorption at 1508cm^{-1} inferred the existence of $-\text{NH}_3^+$ of organic modifier in the interlayer galleries [162]. The band at 3680cm^{-1} is due to asymmetric stretching vibration of Si-OH indicating the penetration of hydrolyzed APTES solution in the layers, as the reaction was carried out in ethanol/water mixture [163]. Whereas bending vibration of the same group appeared at 776 cm^{-1} , the shift in band position showed the grafting of silane group. An intense band at 1033cm^{-1} attributed to Si-O stretching of silicate layer.

Organic modification with quaternary ammonium salt is evident with the appearance of asymmetric stretching vibrations at 2972 cm^{-1} and 2936 cm^{-1} for C-H₃ (terminal CH₃) and C-H₂ respectively. These two asymmetric stretching vibrations are followed by another band at 2844 cm^{-1} which correspond to symmetric stretching of C-H₂ [164]. Unreacted terminal $-\text{Si}-\text{OCH}_2\text{CH}_3$ gave a band at 1054 cm^{-1} but in most of the cases apt to be obscured by strong Si-O stretching vibration [165].

According to a previous study, the Si-O-Si vibrations at $1016, 1033, 1054\text{cm}^{-1}$ gradually merge into broad vibration band thus revealed that the skeletal Si-O bands perturbed by the grafting of APTES on the silicate layers [164]. The FTIR data for various clay types is given in the tabular form as shown in Table 3.2

Table 3.2: *Fourier Transform Infrared data for different clays*

| Functional groups | Observed Frequency (cm ⁻¹) | | | |
|---------------------------------------|----------------------------------------|------|----------|-------------------------------------|
| | MMT | OMMT | SMMT | OS-MMT |
| OH Stretching | 3631 | 3624 | 3624 | 3680 |
| OH bending | 797 | 797 | 798 | 776 |
| OH stretching (H ₂ O) | 3371 | 3286 | 3424 | - |
| OH bending (H ₂ O) | 1623 | 1629 | 1636 | - |
| Aliphatic C-H stretching | - | - | - | 2972 |
| CH ₂ asymmetric stretching | - | 2925 | 2922 | 2936 |
| CH ₂ symmetric stretching | - | 2851 | - | 2844 |
| C-H bending | - | 1460 | - | - |
| N-H bending | - | - | 1545 | 1508(NH ₃ ⁺) |
| Si-O stretching | 1030 | 1008 | 1038 | 1033 |
| Al-O-Si | 918 | - | - | - |
| -CH and NH deformation | - | - | 693 (CH) | 684 (NH) |
| -Si-O-R (unreacted) | - | - | - | 1054 |

3.2.5 FT-IR analysis for nanocomposite systems

Polymer clay nanocomposites with varying concentrations (10-90wt %) were prepared with the uniform dispersion of different amounts of organically modified and chemically functionalized clay (OSMMT) as reinforcement in polyurea matrix. FTIR spectrum of these composites exhibited feature bands of both matrix and reinforcement as shown by the Fig. 3.7.

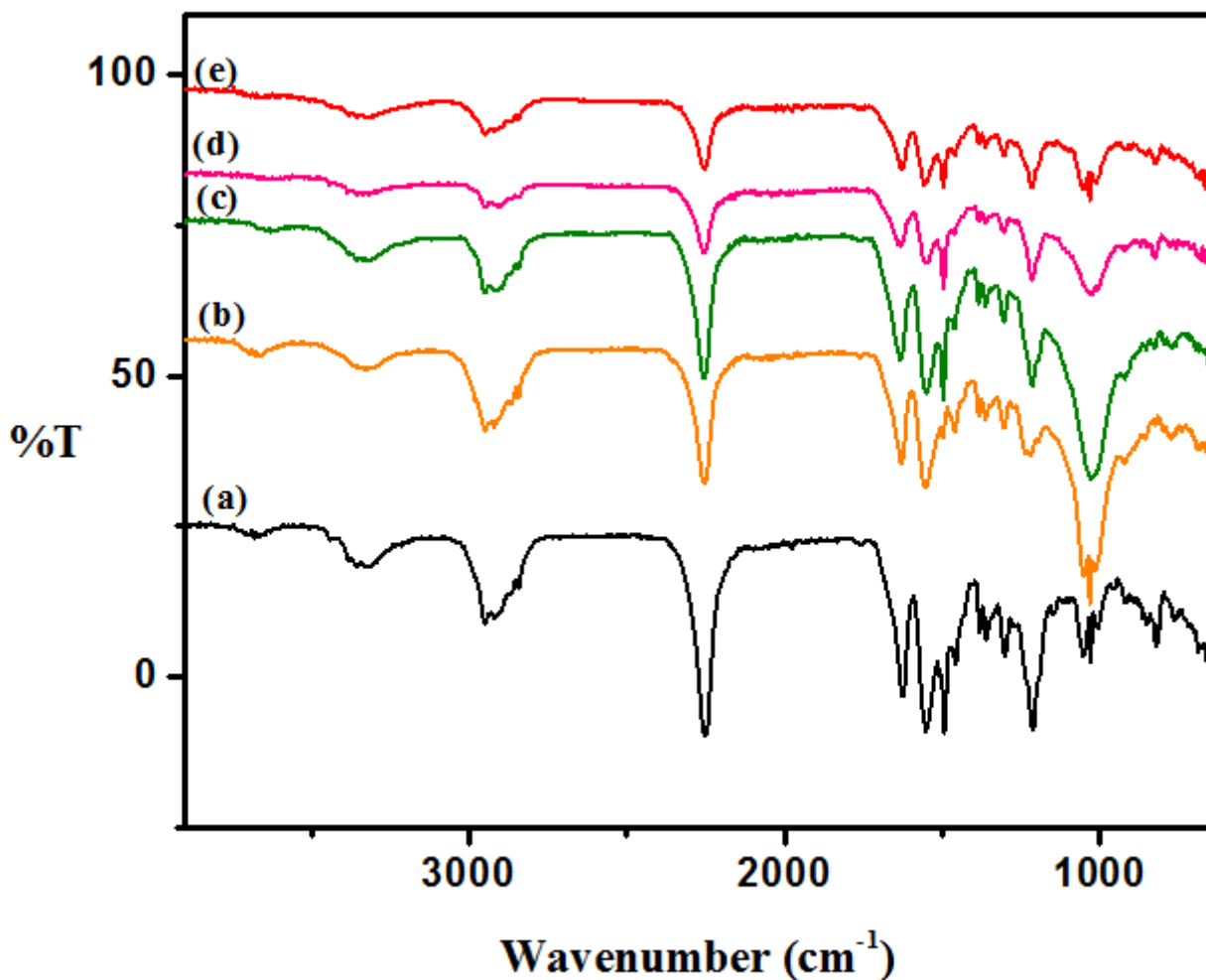


Figure 3.7: Merged FT-IR spectrum of nanocomposite systems a) PCN-10%, b) PCN-30%, c) PCN-50%, d) PCN-70% and e) PCN-90%

The single band centered at $\sim 3300\text{ cm}^{-1}$ correspond to stretching vibration of hydrogen bonded N-H and no band for free N-H is appeared showing that almost all the N-H groups are completely hydrogen bonded in the resultant material, whereas the asymmetric and symmetric stretching vibrational bands at 2950 to 2840 cm^{-1} are attributed to C-H stretching of $-\text{CH}_3$ methyl group and $-\text{CH}_2$ methylene group respectively derived from Propyl group of silane coupling agent mounted on layered silicate (reinforcing phase).

The strong stretching vibrations near 1629 cm^{-1} seem to be caused by stretching of carbonyl group (-CO-) followed by a second N-H band at about 1555 cm^{-1} indicate that the urea linkage has been formed [174]. The C-N stretching of amide group (-CONH) appeared at around 1215 to 1219 cm^{-1} also confirmed the formation of urea linkage in the given nanocomposite systems. The band at 2254 cm^{-1} correspond to stretching vibration of unreacted -NCO groups of diisocyanate of polyurea matrix. However the intensity of this band exhibited significant variations among all nanocomposites depending upon the amount of matrix phase present in each system and the extent of reaction between isocyanate and amine group of matrix and reinforcing phase respectively. For example the isocyanate group gave very intense peak in nanocomposite system PCN-10% where matrix phase constitute 90% of the total weight of composite material. Then it start becoming less intense with decrease in matrix amount and increase in reinforcing phase i.e. OSMMT which provide more amine groups to be reacted with -NCO group to form urea linkage [167-168].

The bands at 1461 or 1462 and 1387 cm^{-1} are assigned to the asymmetric and symmetric vibrations of the methyl groups present in reinforcing phase [169]. The band at $\sim 1033\text{ cm}^{-1}$ attributed to Si-O stretching of silicate layers. This band also exhibited the intensity variations but opposite to that of -NCO group, with every increase in amount of reinforcing phase the intensity of Si-O stretching band increased. The nanocomposite system PCN-90% (with 90wt% reinforcement) gave more intense band for Si-O as compared to other nanocomposite systems. The FTIR data for all the nanocomposite system is tabulated in Table 3.3.

Table 3.3: *A comparative analysis of FT-IR data for different nanocomposites*

| Functional groups | System A (PCN10%) | System B (PCN30%) | System C (PCN50%) | System D (PCN70%) | System E (PCN90%) |
|---------------------------------------|-----------------------------|-----------------------------|-----------------------------|-----------------------------|-----------------------------|
| N-H stretching (H-bonded) | 3318 | 3331 | 3360 | 3311 | 3322 |
| Aliphatic C-H stretching | 2950 | 2951 | 2951 | 2951 | 2950 |
| CH ₂ asymmetric stretching | 2923 | 2921 | 2919 | 2912 | 2922 |
| CH ₂ symmetric stretching | 2844 | 2844 | 2844 | 2839 | 2844 |
| N-H (amide group) | 1556 | 1558 | 1554 | 1551 | 1556 |
| CO (carbonyl group) | 1629 | 1628 | 1632 | 1633 | 1629 |
| C-N (amide group) stretching | 1215 | 1217 | 1215 | 1215 | 1219 |
| Isocyanate group -NCO | 2253 | 2254 | 2259 | 2254 | 2253 |
| Si-O stretching | 1033 | 1032 | 1027 | 1031 | 1033 |
| CH ₃ asymmetric bending | 1461 | 1462 | - | 1462 | 1461 |
| CH ₃ symmetric bending | 1385 | 1385 | 1386 | 1385 | 1385 |
| Si-OH | 3680 | - | - | 3624 | 3680 |
| Unreacted Si-O-R groups | 1056 | 1051 | - | - | 1053 |

Where weight percent (wt %) represents the amount of reinforcement present in each composite system.

3.3 Performance profile of synthesized material for oil removal

3.3.1 Preparation of synthetic saline oil-water

To mimic the real situation, synthetic saline oily water was prepared through addition of petroleum hydrocarbons in saline solution of NaCl and CaCl₂ (10:1) with total salts of

55000ppm, the mixture was kept to a high speed stirring for 10minutes. The average concentration of oil in prepared solution was 300ppm.

3.3.2 Oil-water separation test

Initially 0.5g of synthesized sorbent material was dispersed in 30mL of saline solution containing oil/water emulsion. The mixture was kept for 240 minutes at room temperature to ensure the equilibrium of system. After oil-water separation process, the sorbent material was removed through scooping method. UV-Visible spectrophotometer (UV-Spectrophotometer/ Specord200 plus Analytikjena Germany) was used to determine the unknown concentration of oil present in the water phase by analyzing the absorbance of oil at a particular wavelength. For this purpose, calibration curves of absorbance Vs concentrations using different concentrations (ranging from 0 to 100ppm) of different oils (Diesel, gasoline, kerosene) were constructed. For the extraction of oil from water chloroform was used as solvent. The absorbance at λ_{max} gave the estimation of oil concentration present in water samples [156].

Evaluation of oil absorption:

The percentage of oil removal (% Removal) and removal capacity at equilibrium is calculated using following equations 1 and 2.

$$\% \text{ Removal} = (C_o - C_{eq})/C_o \times 100 \quad (1)$$

Where C_o is the initial concentration of oil in oil-water emulsion (solution) in ppm (mg/L), C_{eq} represents the final concentration of oil in oil-water emulsion (solution).

$$Q_{eq} = \frac{V}{m} (C_o - C_{eq}) \quad (2)$$

Where Q_{eq} is the amount of oil in mg/g of sorbent material, V represents the volume of adsorbate (mL) and m is the mass of sorbent in grams. C_o and C_{eq} is the initial and final concentration of oil present in solution (O/W emulsion). Percentage removal and removal capacity is calculated for all five systems of nanocomposite materials and three types of petroleum hydrocarbons.

a) Diesel oil

Figure 3.8 shows the calibration curve of diesel oil built with coefficient of determination (R^2) equal to 0.9961 whereas the table 3.4 represents the results of percentage removal and removal capacity at equilibrium for all nanocomposite materials.

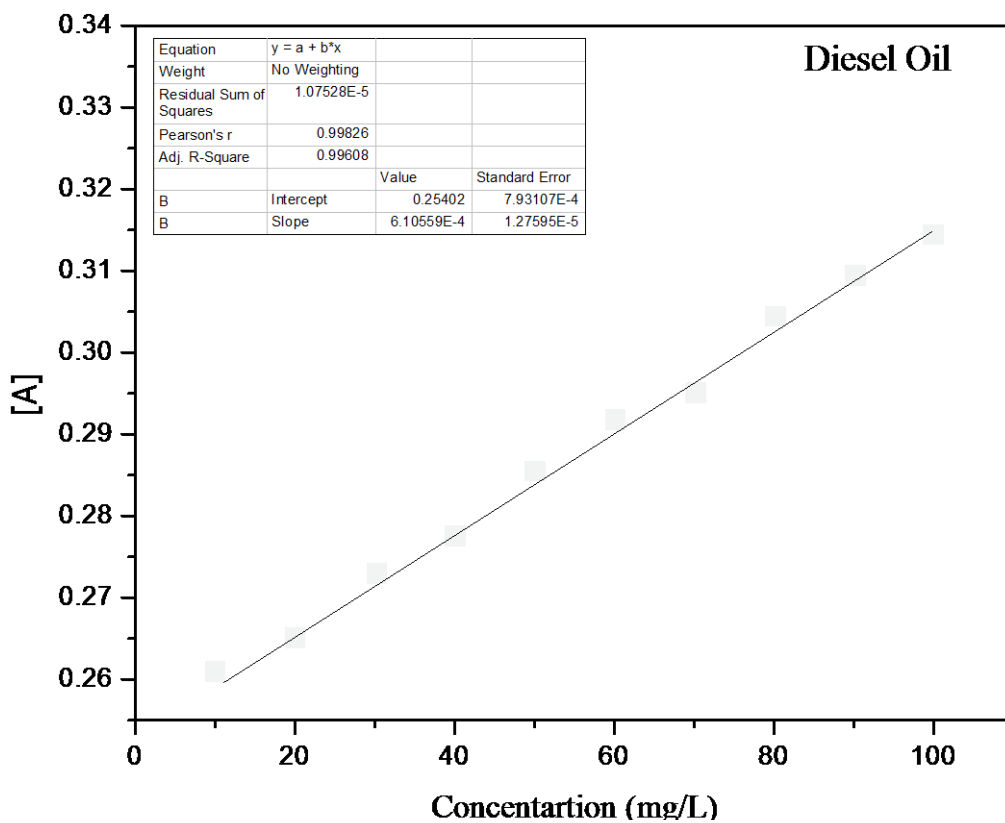


Figure 3.8: Calibration curve for estimation of unknown concentration of diesel oil in water after oil-water separation test

Table 3.4: Results of percent removal (%Rem) and removal capacity (Q_{eq}) for diesel oil

| Sorbent material | C_o (mg/L) | C_{eq} (mg/L) | % Removal | Removal capacity (mg/g) |
|-------------------------|--------------------------------|-----------------------------------|------------------|--------------------------------|
| Nanocomposite A | 300 | 97.28 | 67.57 | 20.27 |
| Nanocomposite B | 300 | 72.44 | 75.85 | 22.42 |
| Nanocomposite C | 300 | 39.46 | 86.84 | 21.31 |
| Nanocomposite D | 300 | 55.87 | 81.37 | 24.43 |
| Nanocomposite E | 300 | 59.65 | 80.11 | 24.03 |

b) Gasoline

Calibration curve of absorbance versus various concentrations of gasoline was built with coefficient of determination (R^2) 0.99847 to find out the unknown concentration of gasoline present in oil-water emulsion after selective removal of oil from water.

Removal efficiency of nanocomposite sorbent materials is calculated for gasoline using equation 1 and 2.

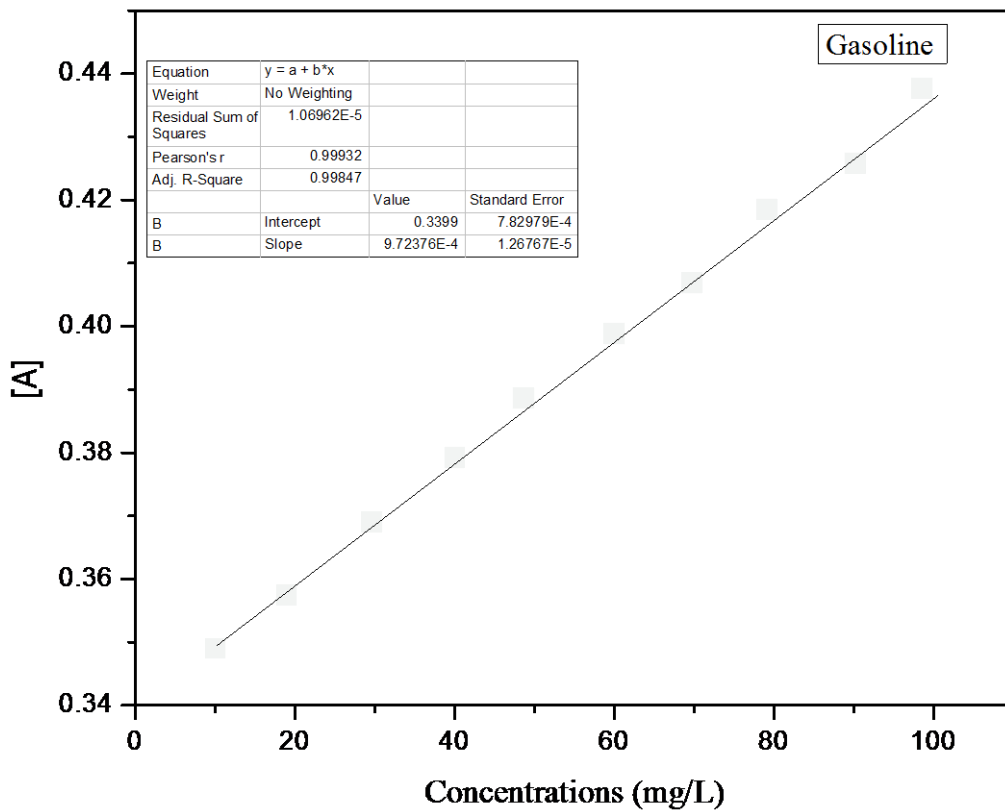


Figure 3.9: Calibration curve for estimation of unknown concentration of gasoline in water after oil-water separation test

Table 3.5: Results of percent removal (%Rem) and removal capacity (Q_{eq}) for gasoline

| Sorbent material | C_o (mg/L) | C_{eq} (mg/L) | % Removal | Removal capacity (mg/g) |
|------------------|--------------|-----------------|-----------|-------------------------|
| Nanocomposite A | 300 | 81.52 | 72.83 | 21.85 |
| Nanocomposite B | 300 | 65.97 | 78.01 | 23.40 |
| Nanocomposite C | 300 | 28.77 | 90.41 | 27.123 |
| Nanocomposite D | 300 | 45.09 | 84.97 | 25.491 |
| Nanocomposite E | 300 | 57.84 | 80.72 | 24.216 |

c) Kerosene oil

To determine the concentration of kerosene oil in oil-water emulsion, calibration curve was built with coefficient of determination (R^2) equal to 0.9928 as shown in fig 3.10. The data for % removal and removal efficiency for kerosene oil is arranged in table 3.6.

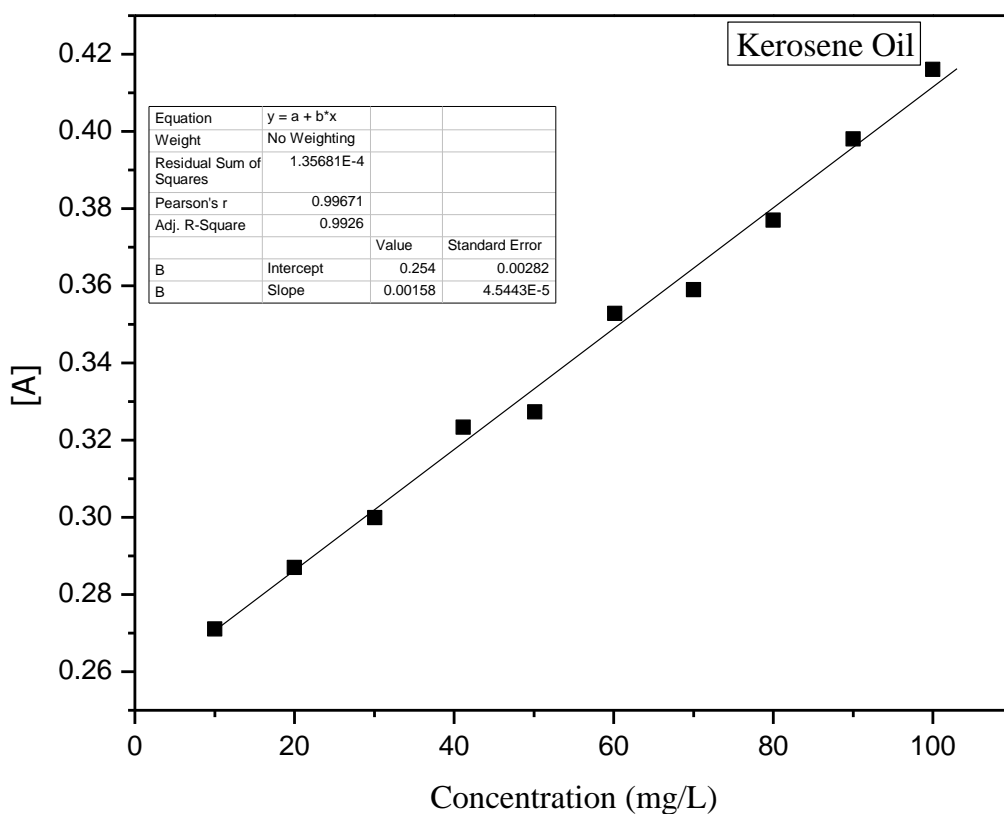


Figure 3.10: Calibration curve for estimation of unknown concentration of kerosene in water after oil-water separation test

Table 3.6: Results of percent removal (%Rem) and removal capacity (Q_{eq}) for kerosene

| Sorbent material | C_o (mg/L) | C_{eq} (mg/L) | % Removal | Removal capacity (mg/g) |
|------------------|--------------|-----------------|-----------|-------------------------|
| Nanocomposite A | 300 | 85.23 | 71.59 | 21.48 |

| | | | | |
|-----------------|-----|-------|-------|-------|
| Nanocomposite B | 300 | 69.95 | 76.68 | 23.00 |
| Nanocomposite C | 300 | 33.19 | 88.93 | 26.68 |
| Nanocomposite D | 300 | 47.51 | 84.16 | 25.24 |
| Nanocomposite E | 300 | 58.04 | 80.65 | 24.20 |

According to results given in Table 3.4, 3.5 and 3.6, the absorption capacity of sorbent materials increase with increasing clay content in resultant nanocomposites from 10 to 50 wt% and then start decreasing. Although the absorption capacity of PCN-70% and PCN-90% nanocomposites is higher than 10 and 30 wt% composites but they possess less absorption capacity than 50wt%. This might be attributed to structure of nanocomposite material because when the modified clay content constitute more than 50 wt% of the total weight of composites there are greater chances for agglomeration of layered silicates because the polymeric matrix is present in an amount, not sufficient for causing the complete exfoliation of layered silicates to give exfoliated polymer/clay nanocomposites. As a result the adsorption sites of modified clay are not well exposed to petroleum hydrocarbons (gasoline, kerosene and diesel oil) and hence the absorption capacity decreases. Among all sorbent materials, nanocomposite with 50% modified clay present as reinforcement possesses maximum swelling capacity for all types of oil. Figure 3.11 a) and b) summarize the results of oil absorption capacities for all types of sorbent materials.

It can also be seen from fig 3.11 a) and b) that synthesized sorbent materials exhibited greater affinity for gasoline and kerosene oil as depicted by their high sorption capacity whereas the low sorption capacity express poor affinity of sorbent materials towards diesel oil.

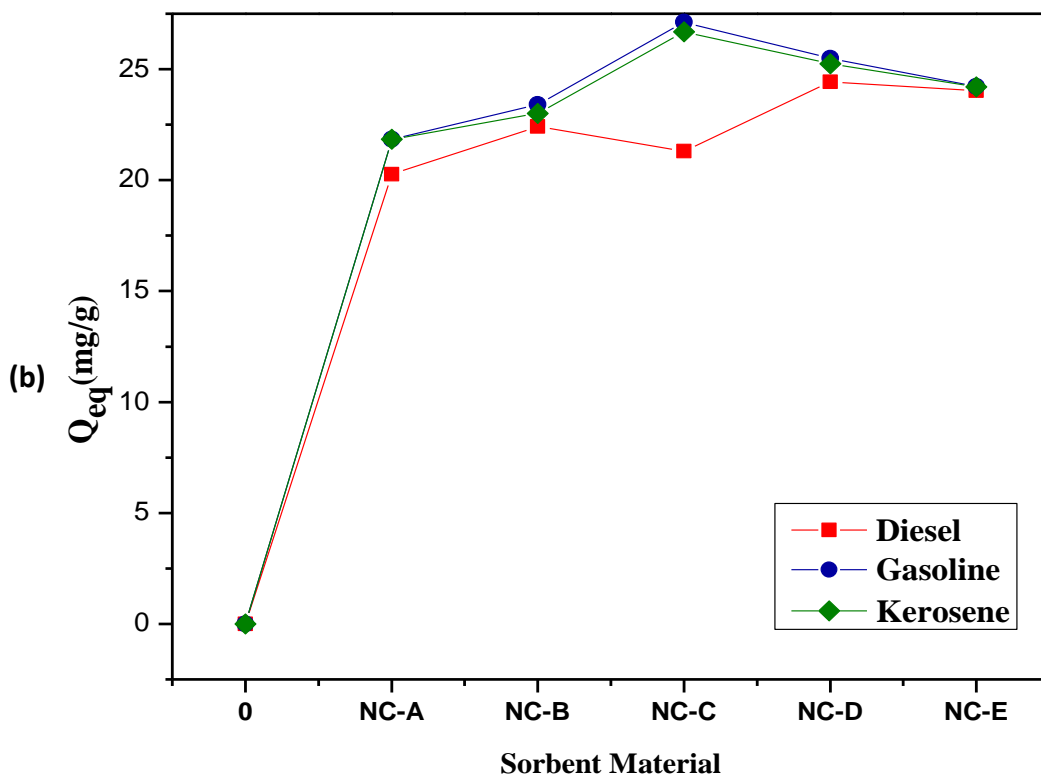
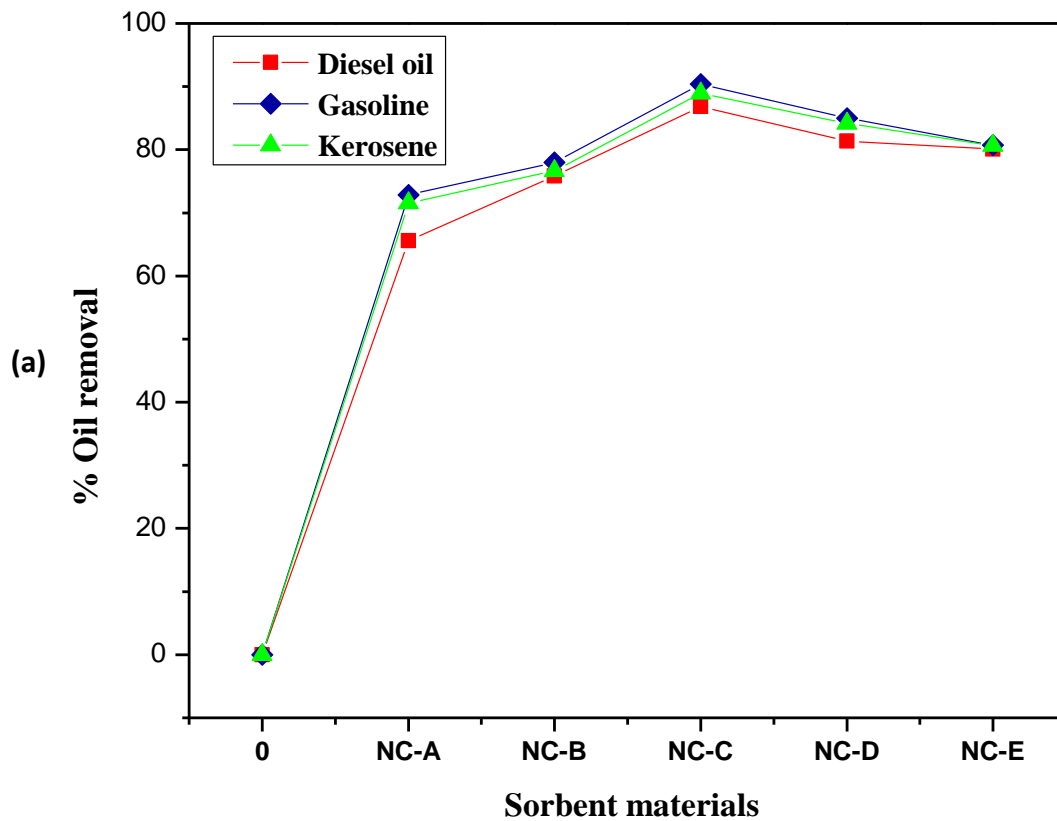


Figure 3.11: A) Oil removal efficiency (% Oil removal) **B)** removal capacity at equilibrium with synthesized sorbent materials using petroleum hydrocarbons

3.3.3 Adsorption capacity test

Adsorption capacities of three nanocomposite materials: B-30 wt%, C-50wt% and D-70wt% for diesel oil, kerosene and gasoline was measured in a method based on “Standard Methods of Testing Sorbent Performance of Adsorbents (ASTM F716-82 and ASTM F726-99)”. In a typical procedure, about 1g of sorbent was weighed which is then lowered into the test tube containing an initial layer of test sample (petroleum hydrocarbons). The sorbent material was allowed to float freely in test liquid for 15 minutes and then removed through scooping method. After that sorbent was allowed to drain for at least 15 minutes and then weighed using weighing balance. The ratio of sorbed oil to dry sorbent mass ratio is used to calculate the amount of sorbed oil. The formula for adsorption capacity is given in eq. 3.

$$Ad = (M_2 - M_1)/M_1 \times 100 \quad (3)$$

Where M_1 and M_2 are the masses of sorbent materials before and after sorption of oil respectively, expressed in grams and Ad is the adsorption capacity expressed in g/g; grams of oil adsorbed per gram of dry sorbent material. The results for adsorption capacity are shown in fig 3.12 indicating that sorbent material based on nanocomposite system C in which 50% modified clay is used as reinforcement possess maximum adsorption capacity for all oil types, especially it is much higher for gasoline than kerosene and diesel oil. The ability of nanocomposite system C to adsorb maximum oil exhibit highly oleophilic character which comes through homogenous dispersion of modified layered silicates in polymeric matrix resulting in exfoliated nanocomposite material in which maximum adsorption sites are exposed to adsorb oil.

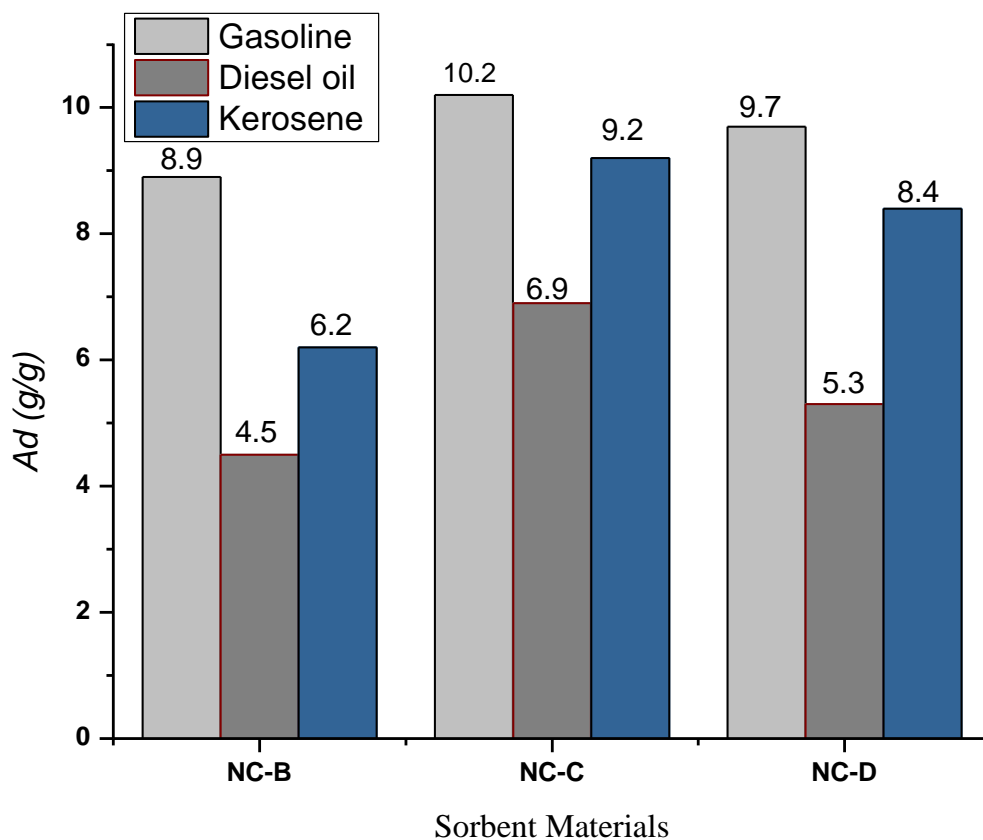


Figure 3.12: Adsorption capacity (Ad (g/g)) of Nanocomposite sorbents in petroleum hydrocarbons

3.3.4 Sorption capacity, selectivity and buoyancy tests

Oil sorption capacity, selectivity and buoyancy test were performed for PCN-50% polymer clay nanocomposites which exhibited excellent performance for removing oil from water. The following fig 3.13 shows the oil sorption capacity with different masses of sorbent (PCN-50%) from which it is clear that initially the sorption capacity of sorbent material increases with increase in its amount and attain a maximum value i.e. it shows maximum sorption capacity when 1g of sorbent material was used, then it start decreasing because a high amount of

sorbent is present in a limited area with fixed volume of oil and the contact between oil and sorbent decreases hence the sorption capacity [170].

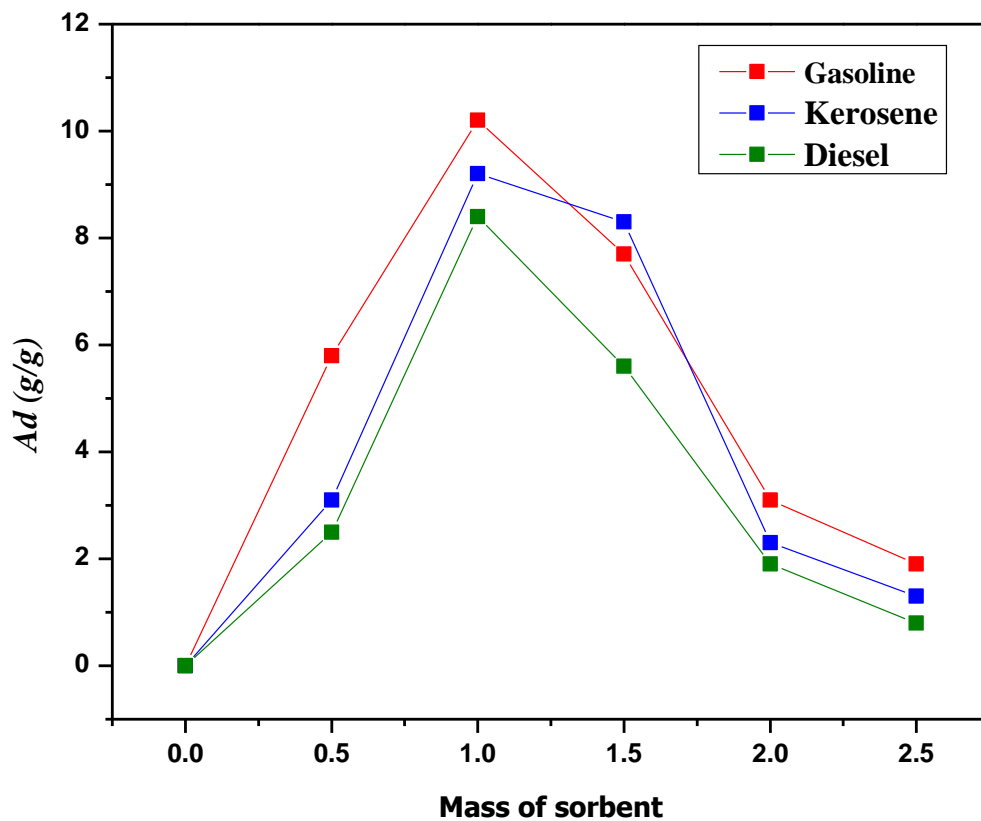


Figure 3.13: Evaluation of oil sorption capacity of PCN-50% nanocomposites with different masses

The selective and buoyant nature of sorbent material (PCN-50%) is demonstrated in fig 3.14, where the sorbent powder was added to oil-water solution. The sorbent float on the surface of water and selectively remove oil from water.

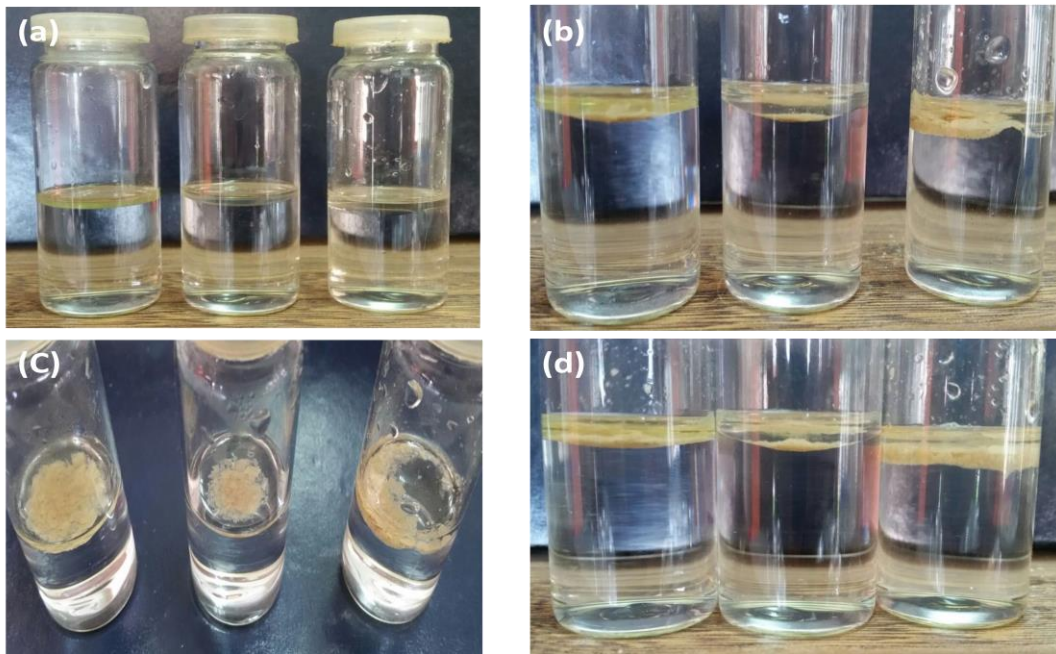


Figure 3.14: Demonstration of oil-water separation process a) oil-water emulsion b) addition of sorbent material, c) and d) selectivity and buoyancy of sorbent materials

3.4 Conclusion and Outlook

In this research work, polymer/clay nanocomposites were prepared as novel candidate sorbent materials for oil spill remediation. Na⁺- Montmorillonite was used as reinforcing phase whereas the hydrophobic polyurea was employed as matrix phase. The hydrophilic nature of clay was changed to hydrophobic or oleophilic nature through the modification of interlayer space and surface to make it compatible with polymer as well as with the organic solvents. The large chain containing organic cations open the aluminosilicates layers and fix the petroleum hydrocarbons via columbic forces whereas silane groups provide functional group (-NH₂) that react with the -NCO group of polymer matrix and result in intercalated and exfoliated nanocomposites. Five nanocomposite systems with different concentration of clay (10-90wt %) were prepared and characterized using XRD and FTIR analysis. The XRD analysis for all types of clay exhibited the change in 2θ (001 reflection) position relative to pristine clay which showed that the clay minerals have been modified. The XRD pattern of nanocomposites lack sharp peaks due to amorphous nature of polymer which overlapped the characteristic peaks of reinforcement phase thus confirmed that highly intercalated or exfoliated nanocomposites materials have been synthesized. FTIR analysis also confirmed the organic and silane modification of silicate layers as well as the possible interaction between polymer and organophilic montmorillonite to form nanocomposites. Oil water separation test showed that the synthesized materials possess maximum oil absorption capacity for organic solvents (diesel, kerosene and gasoline). The best oil sorption capacity was reported with PCN-50% polymer/clay nanocomposites i.e. 90.41 % for gasoline. Further tests such as adsorption capacity evaluation, selectivity and buoyancy tests also confirmed the superhydrophobic property of sorbent material. In addition to this, high uptake capacity,

selectivity, buoyancy, ease of fabrication are significant characteristics of this material that encourage its application as sorbent material in oil spill clean-up process.

Oil recoverability and reusability of material has not been studied yet in present research work. In future, experiments will be executed to establish the oil recoverability from sorbed material as well as to make it reusable for multiple time. Super magnetic iron nanoparticles have been used for the preparation of sorbent material used for oil spill removal. To use the full potential of iron magnetic nanoparticles their incorporation will be carried out in synthesized sorbent materials.

Bibliography

- [1] D.R. Askeland, P.P. Fulay and D.K. Bhattacharya, *Essentials of Materials and Engineering*, 2nd edition, Cengage Learning Inc. Stamford, USA, 2010.
- [2] Y. W. Chung, *An introduction to material science and engineering*, CRC press by Taylor & Francis LLC, Boca Raton, Florida, 2007.
- [3] G. Murray, C.V. White and W. Weise, *Introduction to Engineering materials*, 2nd edition, Taylor & Francis, 2007.
- [4] V. Raghavan, *Material Science and engineering: A first course*, 6th edition, PHI Learning private limited, 2015.
- [5] C.M. Gilmore, *Material science and engineering properties*, Cengage Learning Inc. Stanford, USA, 2015.
- [6] M. Ohring, *Engineering material science*, Academic press, San Diego, California, 1995.
- [7] N. Karak, *Fundamentals of polymers; Raw Materials to Finished Products*, PHI Learning Pvt. Ltd, 2009.
- [8] J.W. Nicholson, *The Chemistry of Polymers*, 3rd edition, The Royal society of Chemistry, Cambridge, UK, 2006.
- [9] D.I. Bower, *An Introduction to Polymer Physics*, Cambridge University Press, New York, USA, 2002.
- [10] G.S. Misra, *Introductory Polymer Chemistry*, 1st edition, New Age International Publisher Ltd, New Delhi, India, 1993.
- [11] R.O. Ebewele, *Polymer Science and Technology*, CRC Press by Taylor & Francis Group LLC, Boca Raton, Florida, 2000.
- [12] C. Painter, C. Paul and M. Michael, *Fundamentals of Polymer Science* 1st edition, Technomic Publisher, Lancaster, 1997.

- [13] N. McCrum, G. Buckely and C.P. Bucknall, *Principles of Polymer Engineering*, 1st edition, Oxford University Press, Oxford, 1997.
- [14] A. K. Kaw, *Mechanics of composite Matrerials*, 2nd edition, CRC Press by Taylor & Francis Group LLC, Boca Raton, Florida, 2006.
- [15] R.M. Jones, *Mechanics of Composite materials*, 2nd edition, CRC Press by Taylor & Francis Group, USA, 1998.
- [16] K.K. Chawla, *Composite Materials: Science and Engineering*, 3rd edition, Springer Science and Buisness Media, 2012.
- [17] D. Hull and T.W. Clyne, *An Introduction to Composite Materials*, 2nd edition, Cambridge University Press, New York, USA, 1996.
- [18] M.K.S. Sai, *Review of Composite Materials and Applications*, International Journal of Latest Trends in Engineering and Technology, 6(3), 129-135, 2016.
- [19] G. Gupta, A. Kumar, R. Tyagi and S. Kumar, *Application and Future of Composite Materials: A Review*, Int. J. Innov. Res. Sci. Eng. Technol. 5(5), 6907-6911, 2016.
- [20] F.L. Matthews and R.D. Rawlings, *Composite Materials: Engineering and Science*, Elsevier, 1999.
- [21] W.D. Callister, *Materials Science and Engineering: An Introduction*, 7th edition, John Wiley & Sons, Inc. 2007
- [22] M. Kutz, *Mechanical Engineer's Handbook*, 4th edition, John Wiley & Sons, Inc. 2015.
- [23] J.R. Vinson and R.L. Sierakowski, *The Behavior of Structures Composed of Composite Materials*, Springer Science and Buisness Media, 2012.
- [24] L.J. Broutman and R. H. Krock, *Composite Materials; Interfaces in Polymer Matrix Composites*, Vol. 6, Academic Press, Inc. 1974.
- [25] R. V. Kurahatti, A.O. Surendranathan, S.A. Kori, N. Singh, A.V. R. Kumar and S. Srivastava, *Defence Applications of Polymer Nanocomposites*, Defence Science Journal, 60(5), 551-563, 2010.

- [26] P.K. Mallick, *Fiber-Reinforced Composites: Materials, Manufacturing, and Design*, 3rd edition, CRC Press by Taylor & Francis Group, LLC, Boca Raton, 2008.
- [27] J. Feng, S. R. Venna, D. P. Hopkinson, *Interactions at the Interface of Polymer Matrix-Filler Particle Composites*, *Polymer*, 103, 189-195, 2016.
- [28] D.D. L. Chung, *Carbon Fiber Composites*, Butterworth-Heinemann, 1994.
- [29] F.C. Campbell, *Structural Composite Materials*, ASM International, 2010.
- [30] M. J. Wilson, *Rock Forming Minerals; Sheet Silicates Clay Minerals*, 2nd edition, Geological Society of London, 1978.
- [31] H. H. Murray, *Overview-Clay Mineral Applications*, *Applied Clay Science*, 5, 379-395, 1991.
- [32] J.T. Klopogge, *Synthesis of Smectites and Porous Pillared Clay catalysts: a review*, *Journal of Porous Materials*, 5, 5-41, 1998.
- [33] J. C. Miranda- Trevino and C.A. Coles, *Kaolinite Properties, Structure and Influence of Metal Retention on pH*, *Applied Clay Science*, 23, 133-139, 2003.
- [34] S. M. Auerbach, K. A. Carrado and P. k. Dutta, *Handbook of Layered Materials*, CRC Press, 2004.
- [35] M. Alexandre and P. Dubios, *Polymer- Layered Silicate Nanocomposites: Preparation, Properties and Uses of a New Class of Materials*, *Materials Science and Engineering*, 28, 1-63, 2000.
- [36] M. Kotal and A. K. Bhowmick, *Polymer Nanocomposites from Modified Clays: Recent Advances and Challenges*, *Progress in Polymer Science*, 51, 127-187, 2015.
- [37] C. D. Barton, *Clay Minerals: Encyclopedia of Soil Science*, Marcel Dekkar, Inc. 2002.
- [38] J.C.A.A. Roelofs and P.H. Berben, *Preparation and Performance of Synthetic Organoclays*, *Applied Clay Science*, 33, 13-20, 2006.
- [39] D. M. Moore and R. C. Reynolds, *X-ray Diffraction and the Identification and Analysis of Clay Minerals*, Oxford University Press, New York, USA, 1997.

- [40] S. Lee and M. D. Tiwari, *Organo and Inorgano-Organic Modified Clays in the Remediation of Aqueous Solutions: An Overview*, Applied Clay Science, 59-60, 84-102, 2012.
- [41] R. Liu, R. L. Frosta, W. N. Martens and Y. Yuan, *Synthesis, Characterization of Mono, di, tri Alkyl Surfactant Intercalated Wyoming Montmorillonite for the Removal of Phenol from Aqueous Systems*, Journal of Colloid Interface Science, 327, 287-294, 2008.
- [42] X. Meng, X. Du, Z. Wang, W. Bi and T. Tang, *The Investigation of Exfoliation Process of Organic Modified Montmorillonite in the Thermoplastic Polyurethane with Different Molecular Weights*, Composites Science and Technology, 68, 1815-1821, 2008.
- [43] S.S. Ray and M. Okamoto, *Polymer/layered Silicate Nanocomposites: A Review from Preparation to Processing*, Progress in Polymer Science, 28, 1539-1641, 2003.
- [44] M. Zanetti, S. Lomakin and G. Camino, *Polymer Layered Silicate Nanocomposites*, Macromolecular Materials and Engineering, 279, 1-9, 2000.
- [45] X. Kornmann, H. Lindberg and L. A. Berglund, *Synthesis of Epoxy-Clay Nanocomposites: influence of the nature of the clay on structure*, Polymer, 42, 1303-1310, 2001.
- [46] Z. Z. Yu, M. Yang, Q. Zhang, C. Zhao and Y. W. Mai, *Dispersion and Distribution of Organically Modified Montmorillonite in Nylon-6,6 Matrix*, Journal of Polymer Science Polymer Physics, 41, 1234-1243, 2003.
- [47] I.J. Chin, T. Thurn-Albrecht, H.C. Kim, T.P. Russell and J. Wang, *On Exfoliation of Montmorillonite in Epoxy*, Polymer, 42, 5947-5952, 2001.
- [48] S. Xu and S.A. Boyd, *Cationic Surfactant Adsorption by Swelling and Non Swelling Layer Silicates*, Langmuir, 11, 2508-2514, 1996.
- [49] J. A. Smith, P. R. Jaffe and C.T. Chiou, *Effect of Ten Quaternary Ammonium Cations on Tetrachloromethane Sorption to clay from water*, Environmental Science and Technology, 24(8), 1167-1172, 1990.
- [50] P. G. Slade and W. P. Gates, *The Swelling of HDTMA Smectites as Influenced by Their Preparation and Layer Charges*, Applied Clay Science, 25, 93-101, 2004.

- [51] P. C. LeBaron, Z. Wang and T. J. Pinnavaia, *Polymer-layered Silicate Nanocomposites: An Overview*, Applied Clay Science, 15, 11-19, 1999.
- [52] G. Lagaly, *Inorganic Layer Compounds, Phenomena of Interface Reactions with Organic Compounds*, Naturwissenschaften, 68, 82-88, 1981.
- [53] L. B. de Paiva, A. R. Morales, R. Francisco and V. Diaz, *Organoclays: Properties, Preparation and Applications*, Applied Clay Science, 42, 8-24, 2008.
- [54] S. Ek, E. I. Liskola and L. Niinisto, *Atomic Layer Deposition of Aminofunctionalized Silica Surfaces using 3-Aminopropyltriethoxysilane as a Silylating Agent*. Journal of Physical Chemistry B, 108(28), 9650-9655, 2004.
- [55] M. Huskic, M. Zigon and M. Ivankovic, *Comparison of the Properties of Clay Polymer Nanocomposites Prepared by Montmorillonite Modified by Silane and by Quaternary Ammonium Salts*, Applied Clay Science, 85, 109-115, 2013.
- [56] D. Romanzini, V. Piroli, A. Frache, A. J. Zattera and S. C. Amico, *Sodium Montmorillonite Modified with Methacryloxy and Vinylsilanes: Influence of Silylation on the Morphology of Clay/unsaturated Polyester Nanocomposites*, Applied Clay Science, 114, 550-557, 2015.
- [57] A. A. Silva, K. Dahmouche and B. G. Soares, *Nanostructure and Dynamic Mechanical Properties of Silane-Functionalized Montmorillonite/Epoxy Nanocomposites*. Applied Clay Science, 54, 151-158, 2011.
- [58] A. Gianni, E. Amerio, O. Monticelli and R. Bongiovanni, *Preparation of Polymer/clay Mineral Nanocomposites Via Dispersion of Silylated Montmorillonite in a UV Curable Epoxy Matrix*, Applied Clay Science, 42, 116-124, 2008.
- [59] W. Shen, H. P. He, J. X. Zhu, P. Yuan and R. I. Frost, *Grafting of Montmorillonite with Different Functional Silanes via Two Different Reaction Systems*, Journal of Colloid and Interface Science, 313, 268-273, 2007.
- [60] H.P. He, J. Duchet, J. Galy and J. Gerard, *Grafting of Swelling Clay Materials with 3-aminopropyltriethoxysilane*, Journal of Colloid and Interface Science, 288, 171-176, 2005.

- [61] H. He, Q. Tao, J. Zhu, P. Yuan, W. Shen and S. Yang, *Silylation of Clay Mineral Surfaces*, Applied Clay Science, 71, 15-20, 2013.
- [62] F. Pistcitelli, P. Posocco, R. Toth, M. Fermeglia, S. Pricl, G. Mensitieri and M. Lavorgna, *Sodium Montmorillonite Silylation: Unexpected effect of the aminosilane chain length*, Journal of Colloid and Interface Science, 351, 108-115, 2010.
- [63] L.M. Daniel, R. L. Frost and H. Z. Zhu, *Edge-modification of Laponite with Dimethyloctylmethoxysilane*, Journal of Colloid and Interface Science, 321(2), 302-309, 2008.
- [64] L. Su, Q. Tao, H. He, J. Zhu, P. Yuan and R. Zhu, *Silylation of Montmorillonite Surfaces: dependence on Solvent Nature*, Journal of Colloid and Interface Science, 391, 16-20, 2013.
- [65] P. Anadao, *Polymer/Clay Nanocomposites: Concepts, Researches, Applications, and Trends for the Future*, F. Ebrahimi (Ed), Nanocomposites-New Trends and Developments, Intech, Croatia, 2012.
- [66] G. W. Beall and C. E. Powell, *Fundamentals of Polymer-Clay Nanocomposites*, Cambridge University Press, New York, USA, 2011.
- [67] P. Kiliaris and C. D. Papaspyrides, *Polymer/layered Silicate (Clay) Nanocomposites: An Overview of Flame Retardancy*, Progress in Polymer Science, 35, 902-958, 2010.
- [68] Q. T. Nguyen and D. G. Baird, *Preparation of Polymer-Clay Nanocomposites and Their Properties*, Advances in Polymer Technology, 25(4), 270-285, 2007.
- [69] H. Akat, M.A. Tasdelen, F. D. Prez and Y. Yagci, *Synthesis and Characterization of Polymer/Clay Nanocomposites by Intercalated Chain Transfer Agent*, European Polymer Journal, 44, 1949-1954, 2008.
- [70] E. P. Giannelis, *Polymer-Layered Silicate Nanocomposites: Synthesis, Properties and Applications*, Applied Organometallic Chemistry, 12, 675-680, 1998.
- [71] G. Lagaly, *Introduction: from Clay Mineral-Polymer Interactions to Clay Mineral-Polymer Nanocomposites*, Applied Clay Science, 15, 1-9, 1999.

- [72]G. Beyer, *Nanocomposites: A New Class of Flame Retardants for Polymers*, *Plastics, Additives & Compounding*, 4(10), 22-27, 2002.
- [73]M.J. Solomon, A. S. Almusallam, K.F. Seefeldt, A. Somwangthanaroj and P. Varadan, *Rheology of Polypropylene/clay Hybrid Materials*, *Macromolecules*, 34, 1864-1872, 2001.
- [74] A. Rehab and N. Salahuddin, *Nanocomposite Materilas based on Polyurethane Intercalated into Montmorillonite Clay*, *Materials Science and Engineering A*, 399(1), 368-376.
- [75]K. Yano, A. Usuki, A. Okada, T. Kurauchi and O. Kamigaito, *Synthesis and Properties of Polyimide-Clay Hybrid*, *Journal of Polymer Science A*, 31, 2493-2498, 1993.
- [76] S. Sadhu and A.K. Bhowmick, *Preparation and Properties of nanocomposites based on acrylonitrile- butadiene rubber, styrene rubber and polybutadiene rubber*, *Journal of Polymer Science B: polymer Physics*, 42, 1573-1585, 2004.
- [77]D.G. Lopez, I.G. Mitre, J. F. Fernandez, J. C . Merino and J. M. Pastor, *Influence of clay Modification process in PA6-layered Silicate Nanocomposite Properties*, *Polymer*, 46, 2758-2765, 2012.
- [78]R. P. Moraes, T. S. Valera, A.M.C. Pereira, N. R. Demarquette and A.M. Santos, *Influence of the type of Quaternary Ammonium Salt Used in the Organic Treatment of Montmorillonite on the Properties of Poly(Styrene-co-butyl acrylate)/layered silicate nanocomposites prepared by In-Situ miniemulsion Polymerization*, *Journal of Applied Polymer Science*, 119, 3658-3669, 2011.
- [79] J.W. Gilman, T. Kashiwagi, M. Nyden,, E. Manias, *Flammability Studies of Polymer Layered Silicate Nanocomposites: Polyolefin, Epoxy and Vinyl ester resins*, *Chemistry and Technology of Polymer Additives*, Blackwell Scientific, London, 249-265, 1998.
- [80] S. Sadhu and A.K. Bhowinck, *Effect of Chain Length of Amine and Nature and Loading of Clay on Styrene-Butadiene rubber- clay nanocomposites*, *Rubber Chemistry and Technology*, 76, 860-875.
- [81] J. Morawiec, A. Pawlak, M. Slouf, A. Galeski, E. Piorowska and N. Krasnikowa, *Preparation and Properties of Compatibilized LDPE/ Organo-modified Montmorillonite Nanocomposites*, *European Polymer Journal*, 41, 1115-1122, 2005.

- [82] A. Ganguly, M. Maiti and A.K. Bhowmick, *Structure- Property Relationship of Specialty Elastomer-Clay Nanocomposites*, Bulletin of Material Science, 31, 455-459, 2008.
- [83] M. Maiti, S. Sadhu and A.K. Bhowmick, *Ethylene- Octene Copolymer(engage)-Clay Nanocomposites: Preparation and Characterization*, Journal of Applied Polymer Science, 101, 601-610, 2006.
- [84] P.I. Xidas and K.S. Triantafyllidis, *Effect of the type of Alkyl ammonium on Clay Modifier on the Structure and thermal/Mechanical properties of Glassy and Rubbery Epoxy-clay nanocomposites*, European Polymer Journal, 46, 404-417, 2010.
- [85] M. Modesti, S. Besco, A. Lorenzetti, V. Causin, C. Marega, J. W. Gilman,.....,M. Zammaranno, *ABS/ clay Nanocomposites obtained by a solution Technique: Influence of Clay Organic Modifier*, Polymer Degradation and Stability, 92, 2206-2213, 2007.
- [86] Y. Someya and M. Shibata, *Morphology, Thermal and Viscoelastic Properties of Poly (glycidyl methacrylate-co-methyl methacrylate) based Nanocomposites with Various Organo-modified Clays*, Polymer, 46, 4891-4898, 2005.
- [87] M. Pramanik, S.K. Srivastava, B. K. Samantaray and A.K. Bhowmick, *Rubber-Clay Nanocomposites by Solution Blending*, Journal of Applied Polymer Science, 87, 2216-2220, 2003.
- [88] M.S. Rama, S. Swaminathan, *Polycarbonate/Clay Nanocomposites via In-situ Melt polycondensation*, Industrial & Engineering Chemistry Research, 49, 2217-2227, 2010.
- [89] S.R. Ha and K.Y. Rhee, *Effect of Surface Modification of Clay using 3-aminopropyltriethoxysilane on the Wear Behavior of Clay/ Epoxy Nanocomposites*, Colloids and Surfaces A, 322, 1-5, 2008.
- [90] M.U. Alvi, S. Zulfiqar, C.T. Yavuz, H.S. Kweon and M.I. Sarwar, *Influence of Aminosilane Coupling Agent on Aromatic Polyamide/Intercalated Clay Nanocomposites*, Ind. Eng. chem.Res, 52, 6908-6915, 2013.

- [91] A.A. Silva, K. Dahmouche and B.G. Soares, *Nanostructure and Dynamic Mechanical Properties of Silane Functionalized Montmorillonite/Epoxy Nanocomposites*, Applied Clay Science, 54, 151-158, 2011.
- [92] A. Usuki, M. Kawasumi, A. Okada, Y. Fukushima, T. Kurauchi and O. Kamigaito, *Synthesis of Nylon 6-Clay Hybrid*, Journal of Materials Research, 8(5), 1179-1184, 1993.
- [93] P. Liu, Q. Cai, W. Lin, B. Chen and B. Zhang, *Offshore Oil Spill Response Practices and Emerging Challenges*, Marine Pollution Bulletin, 110(1), 6-27, 2016.
- [94] S. Anisuddin, N. Al-Hashar and S. Tahseen, *Prevention of Oil Spill in Seawater Using Locally Available Materials*, Arabian Journal of Science and Engineering, 30, 2005.
- [95] A.K. Mishra, G. S. Kumar, *Weathering of Oil Spill, Modeling and Analysis*, Aquatic Procedia, 4, 435-442, 2015.
- [96] X. Liu and K.W. Wirtz, *Total Oil Spill Costs and Compensations*, Maritime Policy & Management, 33(1), 49-60, 2006.
- [97] D.S. Etkin, *Worldwide Analysis of Marine Oil Spill Cleanup Cost Factors*, Arctic and Marine Oil Spill Program Technical Seminar, Environment Canada, 2000.
- [98] C. Robertson and C. Krauss, *Gulf Spill is the Largest of its Kind; Scientists Say*. New York Time, 2010.
- [99] C. I. Hagerty and J.I. Ramseur, *Deepwater Horizon Oil Spill*, Selected Issues for Congress, DIANE Publishing, 2010.
- [100] A.A. Allen, *In-Situ Burning: a New Technique for Oil Spill Response*, Spiltec, Woodinville, WA, 1998.
- [101] A.A. Al-Majed, A.R. Adebayo and M.E. Hossain, *A Sustainable Approach to controlling Oil Spills*, Journal of Environmental Management, 113, 213-227, 2012.
- [102] C. Cojocar, M. Macoveanu and M. Cretescu, *Peat-based Sorbents for the Removal of Oil Spills from Water Surface: application of artificial neural network modeling*, Colloid and Surfaces A, 384(1-3), 675-684, 2011.

- [103] M. Zhang, J. Chen, B. Chen, J. Cao, M. Hong and C. Zhou, *Fabrication of Polystyrene Fibers with Tunable Co-Axial Hollow Tubing Structure for Oil Spill Cleanup*, Applied Surface Science, 367, 126-133, 2016.
- [104] A.O. Ifelebuegu, T. V. A. Nguyen, P. Ukotije-Ikwut and Z. Momoh, *Liquid-Phase Sorption Characteristics of Human Hair as a Natural Oil Spill Sorbent*, Journal of Environmental Chemical Engineering, 3, 938-943, 2015.
- [105] S. A. Sayed and A.M. Zayed, *Investigation of the Effectiveness of Some Adsorbent Materials in Oil Spill Clean-Ups*, Desalination, 194, 90-100, 2006.
- [106] D. Wu, L. Fang, Y. qin, W. Wu, C. Mao and H. Zhu, *Oil Sorbents with High Sorption Capacity, Oil/Water Selectivity and Reusability for Oil Spill Cleanup*, Marine Pollution Bulletin, 84, 263-267, 2014.
- [107] G. O. Aydin and H. B. Sonmez, *Hydrophobic Poly(alkoxysilane) Organogels as Sorbent Material for Oil Spill Cleanup*, Marine Pollution Bulletin, 96, 155-164, 2015.
- [108] L. Yu, G. Hao, J. Gu, S. Zhu, N. Zhang and W. Jiang, *Fe₃O₄/PS Magnetic Nanoparticles: Synthesis, Characterization and Their Application as Sorbents of Oil from Waste Water*, Journal of Magnetism and Magnetic Materials, 394, 14-21, 2015.
- [109] S. Kizil, K. Karadag, G. O. Aydin and H. B. Sonmez, *Poly(alkoxysilane) Reusable Organogels for Removal of oil/organic Solvents from Water Surface*, Journal of Environmental Management, 149, 57-64, 2015.
- [110] M. Patowary, R. Ananthakrishnan and K. Pathak, *Chemical Modification of Hygroscopic Magnesium Carbonate into Superhydrophobic and Oleophilic Sorbent Suitable for Removal of Oil Spill in water*, Applied Surface Science, 320, 294-300, 2014.
- [111] J. Lin, Y. Shang, B. Ding, J. Yang, J. Yu and S.S. Al-Deyab, *Nanoporous Polystyrene Fibers for Oil Spill Cleanup*, Marine Pollution Bulletin, 64, 347-352, 2012.
- [112] A. Siddiqa, A. Shahid and R. Gill, *Silica Decorated CNTs Sponges for Selective Removal of Toxic Contaminants and Oil Spills from Water*, Journal of Environmental Chemical Engineering, 3, 892-897, 2015.

[113] M. Khosravi and A. Azizian, *Synthesis of a Novel Highly Oleophilic and Highly Hydrophobic Sponge for Rapid Oil Spill Cleanup*, Applied Materials & Interfaces, 7, 25326-25333, 2015.

[114] K. G. Raj and P. A. Joy, *Coconut Shell based Activated Carbon-iron Oxide Magnetic Nanocomposite for Fast and Efficient Removal of oil Spills*. Journal of Environmental Chemical Engineering, 3, 2068-2075, 2015.

[115] P.M. Reddy, C. Chang, J. Chen, M. Wu and C. Wang, *Robust Polymer Grafted Fe₃O₄ Nanospheres for Benign Removal of Oil from Water*, Applied Surface Science, 368, 27-35, 2016.

[116] M.F. Mota, M. G. F. Rodrigues and F. Machado, *Oil-Water Separation Process with Organoclays: A Comparative Analysis*, Applied Clay Science, 99, 237-245, 2014.

[117] S.C.G. Rodrigues, M.B. Queiroz, K.R.O. Pereira, M.G.F. Rodrigues and F.R. Valenzuela-Diaz, *Comparative Study of Organophilic Clays to be Used in the Gas & Petrol Industry*, Material Science Forum, 660-661, 1037-1042, 2010.

[118] M.B. Queiroz, S. C. G. Rodrigues, H.M. Laborde and M.G. F. Rodrigues, *Swelling of Brazilian Organoclays in Some Solvents with Application in the Petroleum Industry*, Material Science Forum, 660-661, 1031-1036, 2010.

[119] M.F. Mota, J. A. Silva, M.B. Queiroz, H.M. Laborde and M.G. F. Rodrigues, *Organophilic clay for Oil/Water Separation Process by Finite Bath Tests*, Brazilian Journal of Petroleum and Gas, 5(2), 097-107, 2011.

[120] C. Bertagnolli and M.G. C. da Silva, *Characterization of Brazilian Bentonite Organoclays as Sorbents of Petroleum-derived Fuels*, Materials Research, 15(2), 253-259, 2012.

[121] K.R. O. Pereria, R.D. Hanna, M. M. G. R. Vianna, C. A. Pinto, M. G. F. Rodrigues and F. R. V. Diaz, *Brazilian Organoclays as Nanostructured Sorbents of Petroleum-Derived Hydrocarbons*, Materials Research, 8(1), 77-80, 2005.

[122] H. Moazed and T. Virarghavan, *Removal of Oil from Water by Bentonite Organoclay*, Practice Periodical of Hazardous, Toxic and Radioactive Waste Management, 9(2), 130-134, 2005.

- [123] A.C. Gonzaga, B.V. Sousa, L.N.L. Santana, G.A. Neves and M. G. F. Rodrigues, *Study of Different Methods in the Preparation of Organoclays from the Bentonite with Application in the Petroleum Industry*, Brazilian Journal of Petroleum and Gas, 1(1), 16-25, 2007.
- [124] B. Fultz, J. Howe, *Transmission Electron Microscopy and Diffractometry of Materials*, Graduate Texts in Physics, 4th edition, Springer-Verlag Berlin Heidelberg, 2013 .
- [125] R. Das, M.E. Ali and S.B.A. Hamid, *Current Applications of X-ray powder diffraction*, Rev. Adv. Mater. Sci, 38, 95-109, 2014.
- [126] Linda C. Sawyer and David T. Grub, *Polymer Microscopy*, 1st edition, Chapman and Hall Ltd. 1987.
- [127] A. W. Hull, *A New Method of Chemical Analysis*, J. Am. Chem. Soc, 41(8), 1168-1175, 1919.
- [128] B. Beckhoff, B. Kamgiefer, N. Langhoff, R. wedell and H. Wolff (Eds.), *Handbook of Practical X-Ray Fluorescence Analysis*, Springer-Verlag Berlin Heidelberg, 2006.
- [129] Y. Waseda, E. Matsubara and K. Shinoda, *X-Ray Diffraction Crystallography*, Springer-Verlag Berlin Heidelberg, 2011.
- [130] R. DE Wolf, *Implementation, Analytical Characterization and Application of a Novel Portable XRF/XRD Instrument* [dissertation]. Ghent: Ghent University; 2011-2012.
- [131] B.D. Cullity, *Elements of X-ray Diffraction*, Addison Wesley Publishing Company, 1956.
- [132] M. Birkholz, *Thin Film Analysis by X-ray Scattering*, Wiley-VCH Verlag GmbH & Co. KGaA, Weinheim, 2006.
- [133] T. K.S. Wong, *Semiconductor Strain Metrology: Principles and Applications*, Bentham Science Publisher, 2012.
- [134] C. Hammond, *The basics of Crystallography and diffraction*, 4th edition, Oxford University Press, Oxford, 2015.
- [135] Z. Jian and W. Hejing, *The physical Meanings of 5 Basic Parameters for an X-ray Diffraction Peak and Their Application*, Chin. J. Geo. Chem, 22(1), 38-44, 2003.

- [136] R. F. Egerton, *Physical Principles of Electron Microscopy: An introduction to TEM, SEM and AEM*, 1st edition, Springer US, 2005.
- [137] B. Cheney, *Introduction to scanning electron microscopy*, Materials Engineering Department of San Jose State University, 2007.
- [138] D.C. Joy, *Scanning Electron Microscopy for Materials Characterization*, Current Opinion in Solid State and Material Science, 2, 465-468, 1997.
- [139] L. Reimer, *Scanning Electron Microscopy: Physics of Image Formation and Microanalysis*, 1st edition, Springer-Verlag Berlin Heidelberg, 1985.
- [140] K. D. Vernon-Parry, *Scanning electron Microscopy: An Introduction*, III-Vs Review, 13(4), 40-44, 2000.
- [141] J.I. Goldstein, C.E. Lyman, D.E. Newbury, E. Lifshin, P. Echlin, L. Sawyer, ... J. R. Michael, *Scanning Electron microscopy and X-ray Microanalysis*, 3rd edition, Springer-New York, 2003.
- [142] M.T. Postek, K.S. Howard, A.H. Johnson and K.L. McMichael, *Scanning Electron Microscopy: A Student's Handbook*. Ladd Research Industries. Inc, Williston, VT.1980.
- [143] B. Hafner, *Scanning Electron Microscopy Primer*, Characterization Facility, University of Minnesota-Twin Cities, 1-29, 2007.
- [144] G. Dhem, J. M. Howe and J. Zweck, *In-Situ electron Microscopy: Applications in Physics, Chemistry and Materials Science*. John Wiley & Sons, 2012.
- [145] H. Gunzler and H. U. Gremlich, *IR Spectroscopy: An Introduction*, Wiley-VCH, Weinheim, Germany, 2002.
- [146] F. Rouessac and A. Rouessac, *Chemical Analysis: Modern Instrumentation Methods and Techniques*, 2nd edition, John Wiley & Sons, Ltd, 2013.
- [147] B. Stuart, *Infrared Spectroscopy*, Kirk-Othmer Encyclopedia of chemical Technology, John Wiley & Sons, 2005.
- [148] B. Stuart, *Infrared Spectroscopy: Fundamentals and Applications*, John Wiley & Sons, Ltd, 2004.

- [149] T. Owen, *Fundamentals of UV-visible spectroscopy*, Agilent Technologies, California, USA, 2000.
- [150] Challa S.S.R. Kumar, *UV-VIS and Photoluminescence Spectroscopy for Nanomaterials characterization*, Springer Science and Business Media, 2013.
- [151] R. J. Anderson, D.J. Bendell and P.W. Groundwater, *Organic Spectroscopic Analysis*, Royal Society of Chemistry, Great Britain, 2004.
- [152] B.J. Clark, T. Frost and M.A. Russell, *UV Spectroscopy: Techniques, Instrumentation and Data handling*, Springer Science & Business Media, 1993.
- [153] M.U. Alvi, S. Zulfiqar, C.T. Yavuz, H.S. Kweon and M.I. Sarwar, *Influence of Aminosilane Coupling Agent on Aromatic Polyamide/Intercalated Clay Nanocomposites*, Ind. Eng. chem.Res, 52, 6908-6915, 2013.
- [154] A.M. Shanmugaraj, K.Y. Rhee and S.H. Ryu, *Influence of Dispersing Medium on Grafting of Aminopropyltriethoxysilane in Swelling Clay Materials*, J. Colloid InterfaceSci, 298, 854-859.
- [155] P.T. Bertuoli, D. Piazza, L.C. Scienza and A.J. Zattera, *Preparation and Characterization of Montmorillonite Modified with 3-Aminopropyltriethoxysilane*. Applied Clay Science, 87, 46-51, 2014.
- [156] M.F. Mota, M. G. F. Rodrigues and F. Machado, *Oil-Water Separation Process: A Comparative Analysis*, Applied clay Science, 99, 237-245, 2014.
- [157] J.D. Russel and A.R. Fraser, *Infrared Methods: Clay Mineralogy, Spectroscopic and Chemical Determinative Methods*, 1st edition, Springer Netherlands, London, pp.11-67, 1994.
- [158] K.R. Pereira, R.A. Hanna, M.M. Vianna, C.A. Pinto, M.G. Rodrigues and F.R. Valenzulea-Diaz, *Brazilian Organoclays as Nanostructured Sorbents of Petroleum-derived Hydrocarbons*, Materials Research, 8(1), 77-80, 2005.
- [159] S. Zulfiqar, Z. Ahmad and M.I. Sarwar, *Probing the Properties of Nanocomposites Synthesized from Aramid and Surface Modified Clay*, Australian Journal of Chemistry, 62, 441-447, 2009.

- [160] L. Su, Q. Tao, H. He, J. Zhu, P. Yuan and R. Zhu, *Silylation of Montmorillonite Surfaces: Dependence on Solvent Nature*, Journal of Colloid and Interface Science, 391, 16-20, 2013.
- [161] Q. Tao, Y. Fang, T. Li, D. Zhang, M. Chen, S. Ji, H. He, S. Komarneni, H. Zhang, Y. Dhong and Y. D. Noh, *Silylation of Saponite with 3-Aminopropyltriethoxy Silane*, Applied Clay Science, 132, 133-139, 2016.
- [162] A.S.M. Chong and X.S. Zhao, *Functionalization of SBA-15 with APTES and Characterization of Functionalized Materials*, The Journal of Physical Chemistry B, 107(46), 12650-12657, 2003.
- [163] N. Majoul, S. Aouida and B. Bessals, *Progress of Porous Silicon APTES-functionalization by FTIR Investigation*, Applied Surface Sciences, 331, 388-391, 2015.
- [164] S.Q. Yang, P. Yuan, H.P. He, Z. H. Qin, Q. Zhou, J.X. Zhu and D. Liu, *Effect of Reaction Temperature on grafting of γ -aminopropyltriethoxy silane (APTES) on Kalonite*, Applied Clay Science, 62, 8-14, 2012.
- [165] M. Asgari, A. Abouelmaged and U. Sundararaj, *Silane Functionalization of Sodium Montmorillonite and its Effect on Rheological and Mechanical Properties of HDPE/Clay Nanocomposites*, Applied Clay Science, 146, 439-448, 2017.
- [166] Y. Ma, X. Chu, G. Tang and Y. Yao, *The Effect of Soft Segment on the Formation and Properties of Binary Core Microencapsulated Phase Change Materials with Polyurea/Polyurethane Double Shell*, Journal of Colloid and Interface Science, 392, 407-414, 2013.
- [167] S.S. Dhumal and A.K. Suresh, *Understanding Interfacial Polycondensation: Experiments on Polyurea System and Comparison with Theory*, Polymer, 51, 1176-1190, 2010.
- [168] S. Zhan, S. Chen, L. Chen and W. Hou, *Preparation and Characterization of Polyurea Microencapsulated Phase Change Material by Interfacial Polycondensation Method*, Powder Technology, 292, 217-222, 2016.
- [169] Z. Ying, C. Zhang, S. Jiang, Q. Wu, B. Zhang, Y. Yu, M. Lan, H. Cheng and F. Zhao, *Synthesis of Novel Hydrophobic Polyurea Gel from CO₂ and Amino-modified Polysiloxane*, Journal of CO₂ Utilization, 15, 131-135, 2016.

[170] M. Patoway, R. Ananthakrishnan and K. Pathak, *Chemical Modification of Hygroscopic Magnesium Carbonate into Superhydrophobic Sorbent Suitable for Removal of Oil Spill in water*. *Applied Surface Science*, 320, 294-300, 2014.

